

VIDEO BASED MONITORING OF TORSIONAL EYE MOVEMENTS

by

ELAZER REUVEN EDELMAN

S.B. Electrical Engineering, Massachusetts Institute of Technology (1978)

S.B. Life Sciences, Massachusetts Institute of Technology (1978)

Submitted in partial fulfillment of the  
requirements for the degree of

MASTER OF SCIENCE

at the

MASSACHUSETTS INSTITUTE OF TECHNOLOGY

June, 1979

© Elazer Reuven Edelman, 1979

Signature of Author \_\_\_\_\_

Department of Electrical Engineering and Computer  
Science, June 25, 1979

Certified by \_\_\_\_\_

Charles M. Oman, Thesis Supervisor

Certified by \_\_\_\_\_

P.S. Schluter, Thesis Co-Supervisor

Accepted by \_\_\_\_\_

Chairman, Department Committee

## VIDEO BASED MONITORING OF TORSIONAL EYE MOVEMENTS

by

ELAZER REUVEN EDELMAN

Submitted in partial fulfillment of the requirements for the degree of Master of Science in the Department of Electrical Engineering and Computer Science, on June 25, 1979.

## ABSTRACT

A prototype version of a video based eye movement monitor has been developed and used to perform experiments with human subjects. While primarily intended for monitoring torsional eye movements, it could also be adapted to measure other types of ocular motion. A contact lens mounted feature provides a stable and distinct image for a low light level video camera. The video output signal is filtered, processed, and the results are then transmitted to a computer. There, they are reconstructed and stored for later analysis, including trigonometric comparisons which yield a total angle of rotation of the feature and, thus, the eye.

Existing torsional eye movement monitors are cumbersome, time consuming and somewhat hazardous. The lens used in this research is rendered totally adherent to a subject's eye with little discomfort and no potential danger. Furthermore, resolution of better than 6 minutes of arc has been achieved, matching that reported by these other methods. Electronic processing and computer analysis allow for repetitive evaluation of a large number of video fields. In addition, preliminary evidence indicates that this scheme may be implemented to provide a real time assessment of eye position and orientation.

## Thesis Supervisor

Charles M. Oman  
Helmholtz Associate Professor  
of Health Sciences and Technology

## Thesis Co-Supervisor:

Paul S. Schluter  
Project Engineer  
Biomedical Engineering Center

To my father and mother and  
my brothers, Teddy, Raphael and Daniel.

## ACKNOWLEDGEMENTS

I will be forever amazed at the selflessness of the MIT community. In the course of this research I have been assisted by numerous people, all of whom eagerly made available suggestions and equipment, displaying surprising interest in my work and generosity with their time and patience. I would have liked to thank them all here, but could not possibly do so properly. I do, however, wish to mention those without whose sustained efforts "this work could never have been completed".

My advisors, Dr. Charles Oman and Paul Schluter, provided valuable insights during the course of this work and especially in the writing of this thesis. I have learned from their persistence and rigor and look forward to continued association with them. Dr. Laurence Young has been a continuing source of inspiration. He gave often from the boundless treasure within, and on top of, his head.

Kerry Campbell and Sherry Modestino expended tremendous efforts in the preparation of this document. Their enthusiasm was contagious and their concern and confidence deeply appreciated. Dr. Anthony Cavallerano sacrificed much of his valuable time towards the development of the contact lens sandwich. His expertise and good humor made the work, not only successful, but enjoyable. Bob Hoffman was always available for consultation and a much needed hand. His work on the initial system design and subsequent support was indispensable. Bill Morrison and Bob Renshaw gave unhesitatingly of their time and



could always be counted on. Anthony Arrott and Jehuda Ish-Shalom listened on occasion, but more often than not talked and tutored. Their cajoling and scrutiny led to significant advances in this work. Dr. Byron Lichtenberg was a much called upon and appreciated colleague in the area of OCR research.

I would also like to thank: Dr. Alan Natapoff for his guidance and encouragement and for all his efforts on my behalf; Al Shaw and Fred Merlis, who gave freely of their time and equipment; Dr. David Sheena for the facilities he made available to me; Neil Novich for his help in the data analysis; and all the members of the Man Vehicle Laboratory and MIT community from whom I have learned and benefitted.

This work was supported by NASA Grant NSG 2032.

יג' אב' 57

## TABLE OF CONTENTS

	PAGE
CHAPTER 1 INTRODUCTION	13
1.1 Objectives, Methods, Results	13
1.2 Thesis Organization	17
CHAPTER 2 INNER EAR AND OCR: DYNAMIC AND STATIC	18
CHAPTER 3 PREVIOUS ATTEMPTS	24
3.1 Afterimages	24
3.2 Photographic OCR Determination	26
3.3 Contact Lenses	27
CHAPTER 4 CONTACT LENS MOUNTED FEATURE, VISUALLY INDUCED OCR, AND EXPERIMENTAL SETUP	35
4.1 Dark Feature on Bright Pupil	35
4.2 Inducing OCR	38
4.3 Experimental Apparatus	43
4.3.1 Low Light Level Video Camera	43
4.3.2 Camera Lens	44
4.3.3 Video Tape Recorder	46
CHAPTER 5 VIDEO SIGNAL PROCESSOR	47
5.1 DC Restoration	49
5.2 Signal Enhancement	49
5.3 Highlighting	50
5.4 Data Transfer	52

	PAGE	
CHAPTER 6	VSP DATA TRANSACTIONS	60
6.1	Data Transfer	62
6.2	Data Analysis	70
6.2.1	Vertical Window	73
6.2.2	Data Rejection	73
6.2.3	Scaling	75
6.2.4	Statistics	75
CHAPTER 7	RESULTS, DISCUSSION AND CONCLUSIONS	81
7.1	Theoretical Resolution	81
7.2	Empirical Resolution	84
7.3	Fixed Straight Line	84
7.4	Rotating Straight Line	85
7.5	Subject Contact Lens Mounted Feature	87
7.6	Summary of System Performance	92
7.7	Contact Lens	94
7.8	Comparison of Techniques	95
CHAPTER 8	SUGGESTIONS FOR FUTURE INVESTIGATIONS	97
8.1	Monitoring Other Eye Movements	97
8.2	Enhancing Feature Extraction	99
8.3	Real Time	100
8.4	Contact Lens Implementation	101
8.5	Higher Order Fit	103
8.5.1	Regression Coefficients and Statistical Parameters	103
8.5.2	Slope Determination	105

	PAGE
8.6 Polan Mapping	105
8.7 Further Rejection	106
8.8 Phase Lock Loop on Horizontal Clock	106
8.9 Increased Optical Magnification	106
APPENDIX A USER'S GUIDE	107
I. Experimental Setup	107
I.1 Video Signal Processor	107
I.1.1 Video Input, Output, Highlighted Video	110
II. Computer Data Collection	111
III. Data Preview	114
IV. Data Analysis	117
V. Analysis Evaluation	122
APPENDIX B COMPUTER PROGRAM LISTINGS	130
APPENDIX C MEMORY BUFFER SIZE	154
APPENDIX D CONTACT LENS 'SANDWICH': DEVELOPMENT AND THEORY	156
APPENDIX E VIDEO	171
REFERENCES	177

## TABLE OF FIGURES

		PAGE
Figure 2.1A	The vestibular system	20
Figure 2.1B	Relationship of the two sets of semicircular canals	20
Figure 2.2	Compensatory movements of the eyes	22
Figure 2.3	Effects of head tilting on eyes	22
Figure 4.1	Bright pupil arrangement	37
Figure 4.2	Newvicon tube, spectral sensitivity curve	44
Figure 5.1	Block diagram of the VSP	48
Figure 5.2	Generation of horizontal register WRITE ENABLE pulse	53
Figure 5.3	Generation of active line pulse	55
Figure 5.4	Video Scanning Processor circuit diagram I	57
Figure 5.5	Video Scanning Processor circuit diagram II	58
Figure 5.6	VSP digital component layout	59
Figure 6.1	System options	61
Figure 6.2	VSP register definitions: Digital output buffer	65
Figure 6.3	VSP register definitions: Digital input buffer options	66
Figure 6.4	Data collection flow diagram	72
Figure 6.5	Computation of $\epsilon_{\theta}$ by method 1	79
Figure 7.1	Minimum resolvable angle, rotation about one end point	82
Figure 7.2	Minimum resolvable angle, center of rotation on feature	83
Figure 7.3	Regressed line overlaid on actual data of abstract target	86

		PAGE
Figure 7.4	Fitted line-data overlay: two contact lens mounted features	90
Figure A.1	System options	108
Figure A.2	Overlay: feature in bottom half of pupil	124
Figure A.3	Overlay: two features adjacent to pupil-iris border	125
Figure D.1	Poly-HEMA segment	159
Figure E.1	Interlaced raster scan	172
Figure E.2	RMA T-111 sync signal	174
Figure E.3	Modulation level of video, blanking and synchronization signals	176

## LIST OF TABLES

		PAGE
Table 2.1	Summary of torsional nystagmus reported in the literature	23
Table 3.1	Summary of representative methods of measuring torsional eye movements	33
Table 6.1	LPSDR input/output pin assignments	64
Table 7.1	System performance summary	93

## TABLE OF PHOTOGRAPHS

PHOTOGRAPH	PAGE
3.1 Video image presented to the VSP of black hair sandwiched between two soft lenses mounted on 'bright pupiled' subject's eye.	32
4.1 Plastic hemispherical dome mounted on rotating hub. Light source in dome center projects random pattern of dots onto a wide white screen.	39
4.2 Experimental setup; dome dots are projected on the white screen in the background.	41
4.3 Subject in test position, normally room lights are out with dome source providing sole illumination.	41
4.4 Closeup of subject, head restraint and bite board. Hooded cable is fiber optics bundle with IR filter mounted on its end.	42
5.1 Subject mounted Soflens-hair 'sandwich at VSP video output (directly connected to video input).	51
5.2 VSP highlighted video output version of photograph 5.1.	51
7.1 Orientation angle versus time, plot for a line rotating at $15^{\circ}/\text{sec}$	88
7.2 Eye angle versus time plot of what may be OCR or torsional saccades.	89
A.1 User, computer, plotter, etc.	109
A.2 Front view of setup.	109
A.3 Highlighted video displayed on video monitor.	112
A.4 Cable and jacks of VSP panel.	112
A.5 Light pen window definition.	119
A.6 Eye angle versus time plot generated by PLTHTA.FOR.	129



CHAPTER 1  
INTRODUCTION

This thesis involves the development of a video eye monitor that is designed to track eye movements, especially torsional ones. This research was stimulated by an interest in understanding visual-vestibular interactions, and to observe the phenomenon of ocular counterrolling (OCR) which is considered to be the only completely acceptable measurement of otolith function. Ocular counterrolling or counter torsion is the involuntary conjugate movement of the eyes about their lines of gaze opposite to the lateral inclination of the head with respect to gravity. Counterrolling reflexes have evolved in all animals and man to help keep a stable image on the retina. Head movements in one direction are countered by proportional eye movements in the opposite direction, so that objects in the visual field are stabilized. Accepted measurements of ocular countertorsion, however, are difficult to perform and time consuming. The most widely used method is that of E.A. Miller, who, in 1962, described a photographic technique where a 35 mm slide of a counterrolled eye is rotated through a dove prism until it is aligned with a reference position slide. The angle the prism is rotated determines the estimated angle of ocular counterrolling. Because of the limitations of the few existing techniques, a new technique has been developed for observing this motion. A video

television camera and scanner track the rotation of a pattern placed on a soft contact lens. The lens can be marked in such a manner as to provide distinct images to the device. Furthermore, the lens can be rendered totally adherent to the surface of a subject's eye.

The video method is appropriate for use in dynamic, visually noisy environments and is well suited for use in viewing a line against the background of the human eye. An image of the eye with the contact lens is focussed on the camera tube and the resulting video output filtered, processed, condensed and read into a computer. There, it is reconstructed and stored for eventual handling, including trigonometric comparisons which extract a total angle of rotation of the contact lens image and thus the eye.

A minimum resolvable angle of less than 6 minutes of arc was achieved from measurements of an abstract target. A standard error of estimate about the computed angle of less than a minute was found for evaluation of fixed straight line targets, 2 to 4 minutes for moving lines and 7 to 10 minutes of arc for contact lens mounted features. Miller reported a resolution of 5.3 minutes. At the same time, versions of his technique extended to dynamic measurements that have a sampling rate limited by the time required to recharge the photoflash. Furthermore, tedious hours of frame by frame analysis are required. With the present video method, analysis is automatic at a sampling rate of 60 fields per second. In addition, field-by-field review of the raw and analyzed data is also possible.

This new technique should prove to be of some interest to a variety of people. A fast, automatic and simple to use external indication of otolith function would be of invaluable clinical assistance in evaluating the otolithic vestibulo-ocular reflex. In addition, other types of eye motion can also be detected with slight, if any, modification. Vertical and horizontal nystagmus are two important measures of vestibular function which could then also be measured. Further, if a compact, precise device of this nature were to be used for 'in-space' observation of counterrolling, it would be possible to assess the effects of weightlessness on otolith information usage. It has been proposed that these very effects contribute heavily to disorientation and motion sickness, problems that still pose operational barriers to manned space flight.

The development of the basic concept behind this work was discussed in my Bachelor's thesis. There, a voltage comparator was used to analyze a video signal of a white line against a black background. Nothing more sophisticated than a large stationary line could be evaluated. The possibility of using a sandwich of soft contact lenses to hold a trackable object was discussed, but an acceptable feature had not yet been developed.

This thesis describes four major areas of research. First, the development of a contact lens mounted feature which not only adheres to the eye, presenting a well defined tracking object, but which also does not interfere with the subject's vision or pose safety hazards.

Second, improvement of the video signal processor so that it can extract the coordinates of a moving feature from the background noise of the eye. This required an extensive amount of noise elimination, signal filtering, as well as image enhancement and processing. Third, the interfacing of the signal processor to a digital computer, enabling data storage at the video field refresh rate.

The final phase of this thesis consists of data analysis, including determination of eye angle with respect to time, and evaluating the performance of the system as a whole. Abstract targets such as black lines on white backgrounds are processed in the same manner as data from real eyes for determination of the system resolution.

In summary, this prototype version of a video based eye movement monitor is capable of tracking a contact lens mounted feature with accuracy and resolution matching existing techniques. At the same time, it does so at a significantly increased sampling rate. The lens is safe and sanitary and may be adapted for use in other monitoring systems. Further, electronic digital processing and computer data analysis permit sophisticated analysis of many points per field. Lastly, it has been shown that this scheme is suitable for implementation as a real time system for evaluation of many types of eye movements.

## 1.2 Thesis Organization

Chapter 2 presents a brief review of the role of the inner ear in refining eye movements, especially ocular counterrolling. Chapter 3 details and compares some representative attempts at measuring torsional eye movements with this work. A summary table is provided as well. Chapters 4, 5, and 6 describe the methods employed in this research including descriptions of the experimental equipment and data recording and analysis techniques. Chapter 7 presents and discusses the results of this work, including theoretical and empirical evaluations of minimum resolvable angle for estimation of eye rotation, accuracy determinations, and certain other key observations. This work is then contrasted to the techniques mentioned in Chapter 3. Chapter 8 provides suggestions for further investigation and some conclusions.

A series of appendices are included as well. Appendix A is a "User's Guide" suggesting step by step operation of the prototype system from experiment to data analysis. Program output, photographs or computer generated plots of the monitor display are provided. Appendix B contains listing of the computer programs used in this work. Appendix C details the considerations that must be made in determining and perhaps altering the size of the buffers used in data writes to the disk. Appendix D is an updated summary of a theoretical explanation for the lens adherence properties. The bulk of this investigation is reported in my Bachelor's thesis. Some background information on these lenses is also provided. Appendix E describes certain video signals and defines video terminology necessary for understanding this thesis.

## CHAPTER 2

## INNER EAR AND OCR: DYNAMIC AND STATIC

The eyeball, supported in the orbit by fascia and ligaments, is rotated by the ocular muscles around a centroid of rotation whose locus is within the globe. No fixed center of rotation can be found due to translatory globe movements and for this reason some feel that no analysis of eye movements can be made in exact quantitative terms [Adler, 1965]. Nonetheless, for almost as long as man has been using his eyes to examine the world about him, those on the outside have been peering in through his eyes trying to understand the body within.

From a mechanical point of view, one may consider rotations about three separate axes: the vertical (z) axis, which produces horizontal movement; the horizontal (x) axis, leading to elevation or depression of the globe, and the anteroposterior (y) axis, producing torsion, clockwise or counterclockwise. Movements about the first two of these axes can be voluntarily elicited, but it will be one of the involuntary reflexes of the third axis that will be concern of this thesis.

The vestibular apparatus of the inner ear coordinates and modifies all voluntary eye movements according to the position of the head in

in space. These refining influences attempt to provide a stable and clear image to the retina by repositioning the visual axis.

The inner ear, or labyrinth, consists of two parts: the utricular and saccular otoliths, and also the semicircular canals. Figure 2.1 shows their apparent position with respect to the auditory portion of the ear. The maculae in each utricle and saccule are receptor organs connected to the brain by the vestibular nerve. They consist of sensory epithelium consisting of hair cells and supporting cells and overlaid with a gelatinous membrane in which are embedded calcium carbonate crystals called otoconia. These crystals have a higher specific gravity than their surroundings and thus are displaced by changes in the direction and magnitude in gravity or inertial forces relative to the macular plates. Though the precise mode of stimulation is still contested, it may be said that sensory cell cilia embedded within the gelatinous layer are bent by slight relative displacement of the otolithic membrane. The hair cell acts as a transducer converting mechanical energy to neural impulses in the afferent neuron. The frequency pattern of nerve impulses traveling over the eighth nerve to the brain depends upon the anatomical spatial arrangement of the two pairs of otolith organs and their orientation with respect to the acting gravito-inertial force.

These impulses produce changes in muscular tonus causing postural changes which persist as long as the head position is maintained. Tonic impulses also reach extraocular muscles producing compensatory eye rotations that maintain the vertical meridians of the cornea

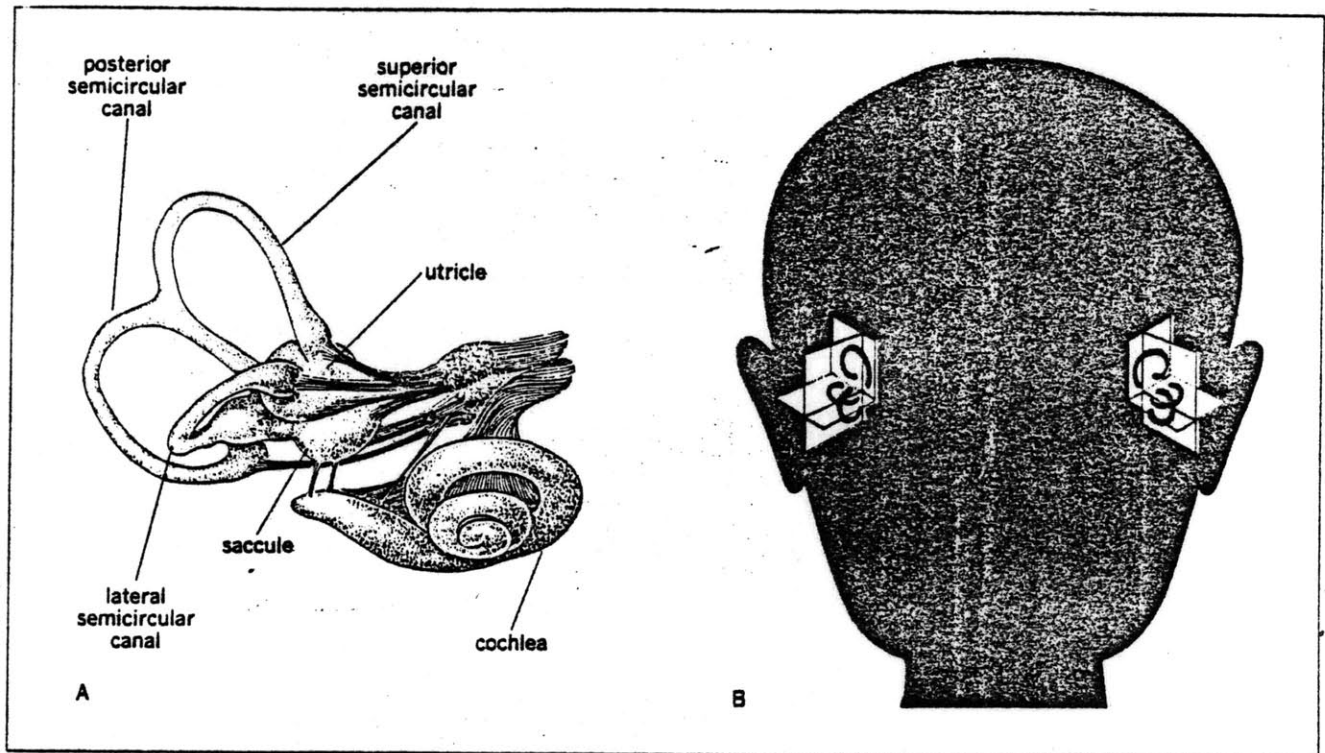


Figure 2.1

- (A) The vestibular system.
- (B) Relationship of the two sets of semicircular canals (from Vander, Sherman and Luciano, 1973).



in their original primary position, vertical and parallel to each other.

When the head is tilted, the eyes execute these torsional movements about their anteroposterior axes, so that as the head tilts, the vertical meridians of the corneas tend to stay erect. This compensatory torsional movement, known as ocular counterrolling (OCR), is illustrated in the figures below from Duke-Elder [1973] and Adler [1965]. In Figure 3a, right shoulder head tilt requires levocycloverision, or conjugate ocular torsion to the left, be produced by increasing the tone to the right superior oblique and right superior rectus muscles (intorsion) and to the left oblique and the left inferior rectus muscles (extorsion).

A distinction must be made between static and dynamic OCR. The former, as illustrated in Figures 2 and 3, is a long-term static or DC component of rotation that is thought to be otolithic in nature. While the latter contains additional movements such as rotatory jitter or torsional nystagmus, perhaps as a result of information relayed by the semicircular canals. Most early investigations were concerned with the static phenomenon since measurement techniques available lack the bandwidth or analysis capability to handle dynamic information. Miller could only report that he observed variations of up to a degree. Robinson irrigated the ear with 42°C water to calorically induce up to 1 degree of torsional nystagmus at 0.5° per second. Melvill Jones (1964) found 2 Hz roll nystagmus of, at maximum, 10 degrees in magnitude, by recording eye movements of subjects in aerodynamic spin. Galoygan et al (1973, 1976) working with tilt and

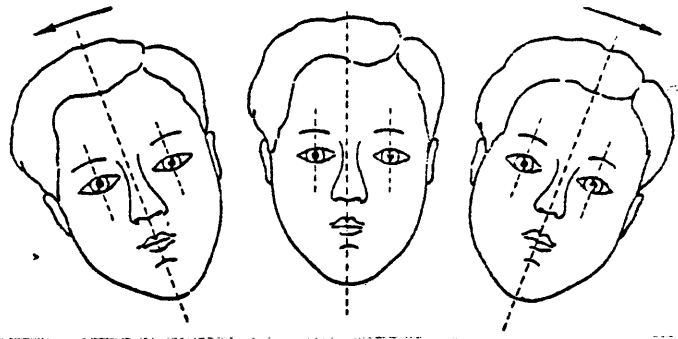


Figure 2.2 Compensatory movements of the eyes on inclination of the head.

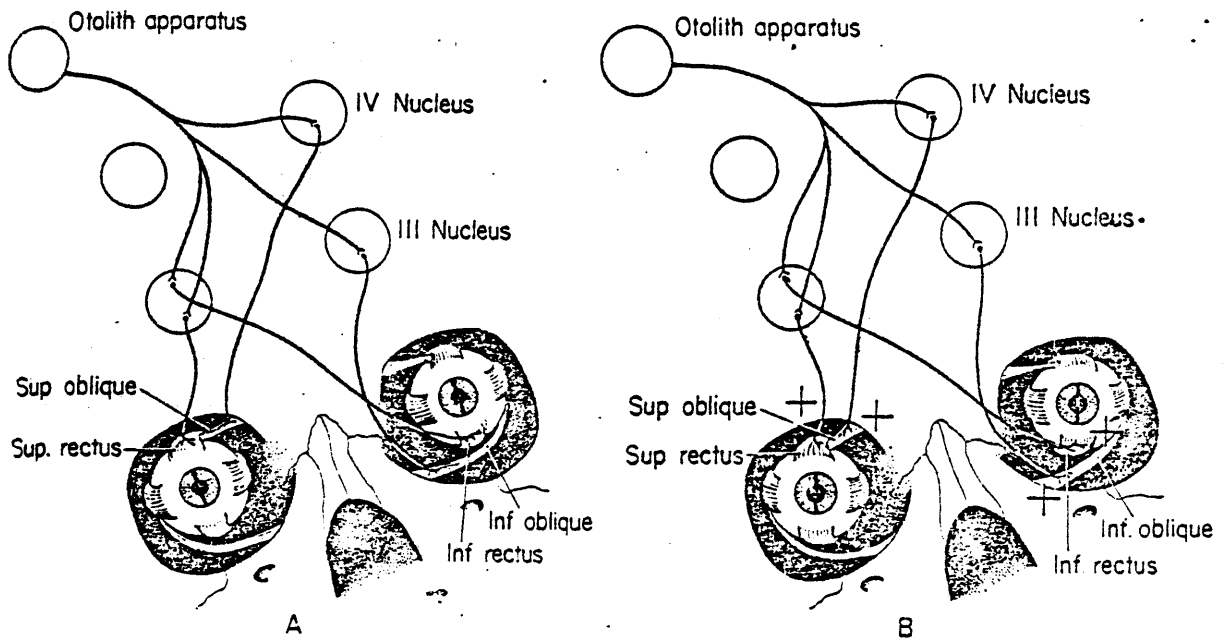


Figure 2.3 The effects of head tilting. A, the head is tilted toward the right shoulder. In the absence of any compensating mechanism, the vertical meridians of the corneas are tilted to the right. B, the otolith apparatus compensates for this and keeps the vertical meridians perpendicular. Plus marks; increased tonus of muscles. (From Held, 1966).

galvanic vestibular stimulation as means of inducing OCR reported torsional saccades in the range of 0.5 to 8 degrees with velocities from 100 to 200 degrees/second. Finally, Matin (1964) photoelectrically measured 5 minutes of arc from calorically invoked torsional nystagmus occurring at about 3 Hz.

The following table summarizes these results and will be used in the discussion of my own results presented in Chapter 5.

AUTHOR	SACCADE MAGNITUDE	<u>FREQUENCY</u> VELOCITY	MODE OF OCR STIMULATION
Robinson (1963)	≈ 1°	velocity 0.5°/sec	caloric
Melville Jones (1964)	10 deg	2 Hz	aerodynamic spin
Matin (1964)	5 min	3 Hz	caloric
Galoygan (1973, 1976)	0.5 - 8 deg	velocities of 100-200 deg/sec	head tilt, galvanic

Table 2.1 Reported magnitudes and frequencies (or velocities) of torsional nystagmus

## CHAPTER 3

## PREVIOUS EFFORTS

Over the years, many methods have been developed for examination of eye movements. Few acceptable methods, however, exist for monitoring ocular counterrolling. Those that are used are primarily suitable for static OCR, possessing neither sufficient sampling rate to observe the dynamic movements nor the practical ability to analyze large amounts of data.

### 3.1 Afterimage

One of the earliest and most basic techniques prints a well-defined afterimage on a subject's retina by shining a bright source or flashing a bright light in a subject's eyes. Periodic flashes of the light will leave a trace of afterimages, whose density indicates fixation duration and the spacing of which indicates the velocity of eye movements.

Since the retinal afterimage moves with the eye, the subject may be asked to align an object with his afterimage, to achieve a subjective determination of eye movement. In the same manner, subjects have been asked to track their blind spots by keeping an object out of sight. The spot, 20 degrees off the axis of rotation, travels with the eye.

Though no elaborate apparatus or attachments to the eye are necessary, nor is the head restrained, these methods suffer from a number of drawbacks. Flashes of light produce a series of eye movements and

blinks, and intermittent illumination is required to maintain the effect. Blind spot tracking is difficult, unnatural and unreliable. Furthermore, there is some evidence that afterimages induce perceptual phenomenon (Aubert-Muller) which may cause faulty compensatory eye movements. In these subjective methods, the subject is interpreting his own visual impressions and Fluor (1974) has concluded that this leads to a large uncertainty. More reliable and more reproducible objective techniques have, therefore, been designed to allow an investigator to observe artificial or natural landmarks on the human eye.

Tracking of the iris-scleral boundary (the limbus), iral folds and pigment, scleral blood vessels, corneal reflections and the retina have all been demonstrated. However, there is a lack of uniformity from subject to subject and even for the same subject diurnally or for slightly varying experimental conditions. Furthermore, examination of the eye has shown that scleral and conjunctival blood vessels are nearly indistinguishable, though one is imbedded in the globe and the other riding over it; and that iral features contort with pupil contraction and dilation. To circumvent some of these problems, drugs have been applied or lights flashed in the subject's eye to maintain constant pupil diameter.

Fluor used a goniometer ocular attached to a Zeiss microscope to allow an observer to track these landmarks. This ocular has in its visual field a hair cross, which can be rotated about a circular protractor. The investigator attempts to keep track of one or two iral landmarks as the eye shifts. Fluor contrasted the 3 degree

variability in this method with 3 to 10 degrees he found in subjective afterimage indications of movement.

### 3.2 Photographic OCR Determination

The classic method for determining ocular counterrolling from photographic recordings of natural landmarks was developed by Miller in 1962. Magnified test images are successively superimposed upon a projected image of the subject's eye in a reference state. The comparison photograph is rotated until the landmarks on the two images of the iris are aligned. Miller [1963, 1965] reported a precision of  $\pm 5.3$  minutes of arc for determination of static OCR throughout 360 degrees of body roll. Difficulties arise due to required manual alignment and use of natural features. Yet, this technique has been implemented in many forms. Hannen et al (1966), Kellogg (1977), and Diamond et al (1979), among others, have used Miller's technique for evaluation of photographs taken at a maximum of once every 0.1 second as the subject was being rotated about his visual axis.

Melvill Jones (1963, 1965) described a cine-photographic method comprising a forward-facing cine camera with close-up lens mounted on one side of a helmet fixed to a subject's head by a dental bite board. This allowed a sampling of 16, 32, and 64 frames per second and provided an accuracy of  $\pm 1$  degree for torsional eye movements. Yet, as the others, it required frame by frame correlation for analysis, a task which is monumental and subject to error. Each frame must be manually correlated with a test frame and then, in some cases,

correlated a second time with a photographic record of body tilt. Nonetheless, this method is in use in many forms today and work in improving it is continuing. Lichtenberg (1979), for example, utilized fiduciary marks within each photograph as a means of assessing an eye angle independent of head movement.

### 3.3 Contact Lenses

According to Young and Sheena [1975], the most precise measurements are made with the use of a device attached to the eye with a contact lens. Methods utilizing eye attachments, started with work on animals and included tattoo marks on the cornea, sutures in the conjunctiva, and other depositions on the corneal surface. Later, investigations in this area were extended to humans where corneal deposition of various gelatinous mixtures or organic matter were made. These were followed by the placement of mirrors, sheets of plastic or metal in the eye. But for the most part, modern techniques have concentrated on the use of contact lenses.

Ditchburn cites Orchansky's attempt in 1889 as one of the earliest recorded attempts at using contact lens like material. In that case, a metal or glass shell was placed over the cornea. A mirror with a small hole for the pupil was then fastened to the shell. Light was reflected from the mirror onto a moving film. Many other investigators attached mirrors to contact lenses and, in 1956, Fender separated the mirror from the lens with a stalk which led to the mounting of a large number of objects on stalks attached to the contact lenses, including

polarized lenses, various grid materials, and line diagrams (e.g. Forgacs et al, 1973).

Such systems have been applied to OCR measurements as well. Kamada et al (1976) placed a number of different transducers on contact lenses to reflect light such that it impinged on cells in two charge coupled arrays. Phase differences in the positions of the two arrays are noted and used to determine the angle of rotation. They report 5 to 8 minutes of resolution for bandwidths of 200 to 1000 Hz.

Goloygan, Petrov and Zenkin (1973, 1976) studied dynamic cyclo-torsion in response to pendular motion, and caloric as well as galvanic stimulation of the inner ear. They reported a 0.1 degree accuracy with an apparatus consisting of a suction cup, affixed to the eye, which reflected light onto a slit photokymograph as it rotated with the eye,

Matin (1964) used the electrical outputs from photocells which measure deflections of beams from two plane mirrors embedded in a scleral contact lens to get a continuous recording of these orthogonal components of eye rotations. These outputs were fed into an array of operational amplifiers, permitting the on-line analog recording of a variety of mathematical fractions of eye movement. Though, he reports a resolution of two seconds of arc and flat frequency response from DC to 1.35 KHz, his use of contact lens mirrors is questionable and his optical alignment impractically crucial.

Robinson (1963) introduced the principal nonoptical contact lens measuring method. A special contact lens is made to adhere to the eye by applying a negative pressure to the back of the lens. Topical anesthesia (ornithine) is administered prior to lens insertion. Two small



wire coils perpendicularly oriented to each other are embedded in the contact lens and used to pick up an induced voltage from two large perpendicular electromagnetic coils surrounding the subject. The induced voltage, read through wires extending from the lens, varies only with the size of the eye angle relative to the magnetic field and is independent of head position with the uniform position of the field. He was able to note approximately 1 degree of torsional nystagmus and claimed resolution of 15 seconds of arc at a 1 Hz bandwidth. Collewijn et al (1975) attempted to improve on this method by devising a flexible ring which fits on the limbic area, concentric with the cornea. The ring is cast out of silicon rubber in a special mold. The eye is anesthetized, the ring wetted with Ringer's solution, placed on the limbus and pressed firmly upon the eye. Fluid between the eye and the ring is evacuated in this way and the elasticity of the ring causes an underpressure which keeps the ring firmly in place. This method is of great importance since it is free of head movement influences. Yet, the lens and wires may pose some potential safety hazard.

Both Ditchburn and Young and Sheena concur that there are important advantages to contact lens systems such as these. With methods of this sort, eye rotation may be measured at good, if not best, possible resolution. There are, however, serious drawbacks which are common to most of the lens techniques. Many do not adapt readily to observation of torsional motions and all cause discomfort or have certain associated physical hazards. Mirrors, wires and metal objects may tear or abrade the eye. Hard lenses of

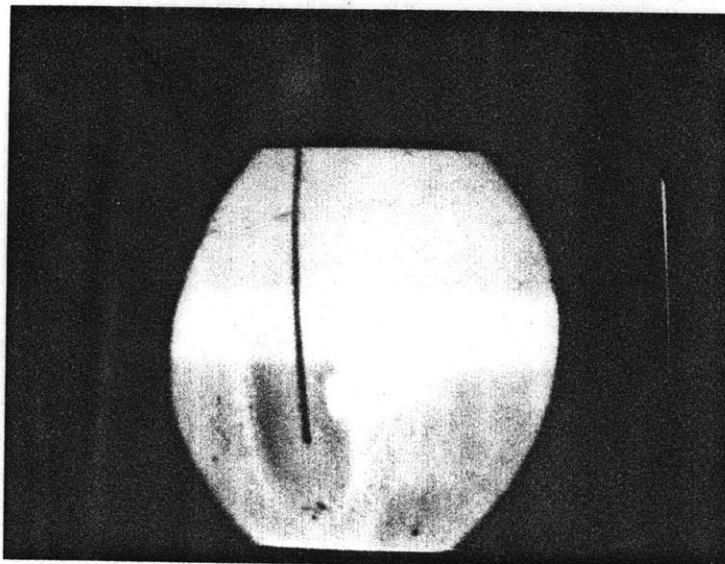
any material reshape the cornea. Those methods utilizing negative pressure for adherence pose considerable danger due to the possibilities of corneal drying, deformation, deoxygenation, or edema. Worse still, damage to the accommodation muscles may occur as a result of the pressure stress.

Some lenses are not firmly attached to the eye and thus slip and wander. Those that adhere rigidly are often painful and difficult to use with human beings. Subject's vision or experimental results may be impaired by such lenses as well as by the interference of the feature with transduction, vision, etc. Many require some form of topical anesthesia (e.g. ophthaine (Robinson), tetracaine (Forgacs et al, 1973), novesine (Collewijn et al, 1975)) which is undesirable as it may affect the eye movements under observation or the process of visual discrimination. Further, the body's first line of defense (pain) is inhibited by this shut down of the early warning system and effects such as abrasion may continue unnoticed and may eventually lead to serious damage. In addition, there is the expense of providing custom fit lenses for all subjects, which, when coupled with the discomfort and inconvenience for use, make hard contact lens systems inappropriate for use in widespread investigations of large populations.

It is obvious that standard techniques for detecting OCR not only cannot quantify the effect dynamically, but are also highly unacceptable for use with humans. Though an ideal monitor would be noninvasive, some sort of contact lens system is necessary to measure ocular counter-

rolling for the assessment of otolith function. The use of two "soft" contact lenses or a feature molded into a single soft lens coupled with the devised scanning system described in this thesis will allow measurement of this phenomenon without the attendant risks and expenses.

The sandwich of two soft contact lenses about a dark feature such as a black hair may be made to adhere to the eye surface under appropriate conditions. If the pupil is whitened through standard 'bright pupil' procedures the stable and safe hard lens embedded hair appears as a high contrast feature mounted to the eye. Current investigations are proceeding towards molding or casting of the hair into a single contact lens. Relevant characteristics of the lens material and certain chemical and physical phenomena associated with the mechanics of lens adherence are presented in Appendix D. Below, the objectives in developing these lenses and the most recent work that has been done with them is described.



Photograph 3.1 Video image presented to the VSP of black hair sandwiched between two soft lenses mounted on 'bright pupiled' subject's eye.

	AUTHOR	SCAN TECHNIQUE	ANALYSIS METHOD	SAMPLING RATE	BANDWIDTH
1	MILLER	photographic	frame by frame correlation		
2	HANNEN			10 Hz	
3	MELVILL JONES	cine	frame by frame correlation	64 Hz	
4	FLUUR	goniometer	investigator alignment		limited by human manual frequency response
5	FLUUR	afterimage	subject alignment		
6	MATIN	photoelectric	analog solution differential equations		500 Hz
7	YAMADA		optical correlation		200-1000 Hz
8	ROBINSON	search coil			1000 Hz
9	GALOYGAN	slit photokymograph			time precision 70 msec
10	EDELMAN	video	electronic	60 Hz	

Table 3.1a Summary of representative methods of measuring torsional eye movements

	ACCURACY	NOISE LEVEL	NATURAL LANDMARKS	CONTACT LENS MOUNTED OBJECT	TOPICAL ANESTHESIA	FLUID EVACUATION
1	5.3'		X			
2		> 5' - 30'	X			
3	60'		X			
4	3°		X			
5	3 - 10°					
6	3"			mirrors	X	X
7	5 - 8'			mirrors	X	X
8	15'			coil of wire	X	X
9	0.1°			light source	X	X
10	> 6'			soft lens-hair		

Table 3.1b

## CHAPTER 4

CONTACT LENS MOUNTED FEATURE, VISUALLY INDUCED OCR,  
AND EXPERIMENTAL SETUP4.1 Dark Feature on Bright Pupil

At the outset, it was hoped that a pattern could be placed in the "sandwich" which would not interfere with subject vision or eye movements and would be safe, comfortable, and easily discernable. Given the simplest detection scheme, such as a threshold detector, one would naturally attempt to utilize a straight high contrast transition. Though different materials, such as thread, plastics, paper, etc., were placed between the two lenses, concern for comfort and 'sandwich' integrity suggested that attention be directed towards small, thin objects. The bonding properties of the lenses appear (Appendix D) to be proportional to the surface area. Thus, line targets on a contrast background material that covered much of the lens were ruled out. Natural features of the eye were utilized to their fullest to provide the dark or light background.

The pupil, the eye's "black hole", provided the most promising contrast and fishing line, white thread, white hair, and light wire were placed in the lens as well as fine chemical tubing filled with ophthalmological fluorescent dye (sodium fluorescene) and dyed colored thread. The colored objects were viewed under different light conditions and through complementary filters, so that, for example, a blue thread was observed under a blue filter. The blue object appeared lighter

than the rest of the image and stood out against the background of the eye. Problems arose due to the width of certain materials. Objects appeared grossly large and interfered with the lens adherence as well.

Fine wire seemed to be the solution, yet drawn gold fibers initiated safety concerns for on occasion the wire broke through the thinner contact lens. Human hair, obviously biocompatible, was substituted. Attempts at using white hair against the black of the pupil, however, were not successful. Microscopic examination of the hair revealed it to be translucent and at times little different in appearance from the contact lens. A black hair against a white pupil was implemented by means of a 'bright pupil' arrangement. This involves the direction of a beam of light along the optical axis. Focussed as a point on the retina, it should return as a beam which entirely fills the pupil, making it appear white. A Dolan-Jenner Fiber Lite high intensity illuminator (Model 170-D) projected light through a hood at the end of which was mounted a near IR (89B Polaroid) gelatin filter, providing a nearly invisible (dim red) beam. The cable and small black hood are evident in Photographs 4.2 and 4.3. In a setup requiring television observation of the eye, the incident illumination is reflected on the eye by a beam splitter placed in the path between the subject and the camera (see Figure 4.1).



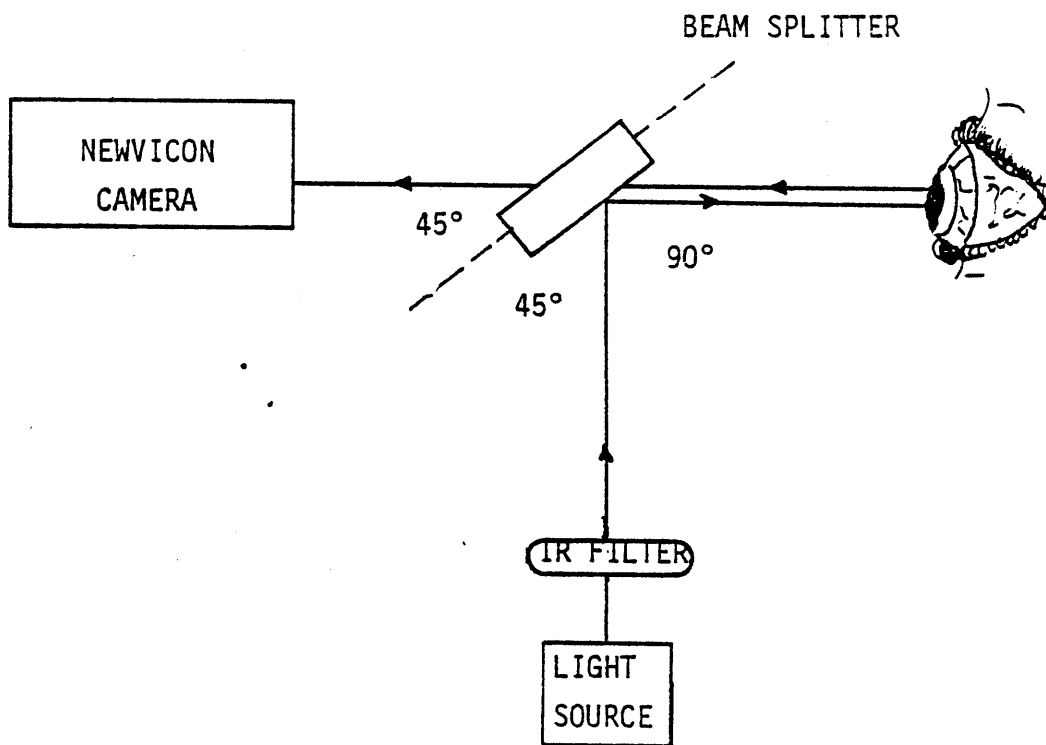


Figure 4.1 Bright Pupil Arrangement

## 4.2 Inducing OCR

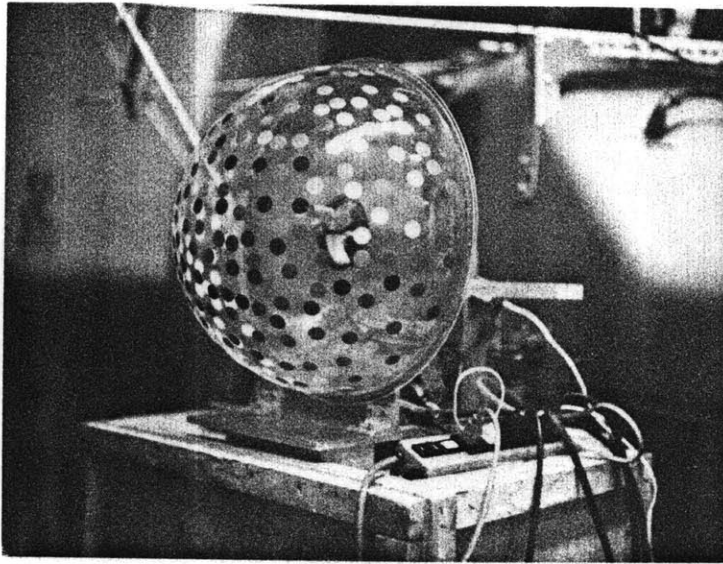
Though ocular counterrolling has traditionally been thought of as an otolithic reflex responding to changes in the gravito-inertial vector with respect to the head, there is some evidence it can be influenced by changes in perception of orientation. Thus, while OCR is often induced by utilizing the vestibular reflex through actual head or body tilt or through galvanic or caloric stimulation of the inner ear, it is also possible to produce OCR through use of moving visual displays.

Thus, a subject looking at the center of a large display rotating in a frontal plane about the line of sight experiences a number of perceptual, oculomotor, and postural phenomena. A clockwise field rotation will usually produce a counterclockwise sensation of self-motion known asvection. In addition, cyclotorsion of the observer's eyes in the same direction as that of the rotating field and a roll of the apparent horizontal in the opposite direction of the field are apparent. Numerous studies have dealt with these effects.

Visually induced eye torsion is typically on the order of  $1^\circ$  to  $2^\circ$  (Dichgans et al, 1972) while eye torsion produced by head tilt (true OCR) may be as large as  $6^\circ$  to  $8^\circ$  (Miller, 1961).

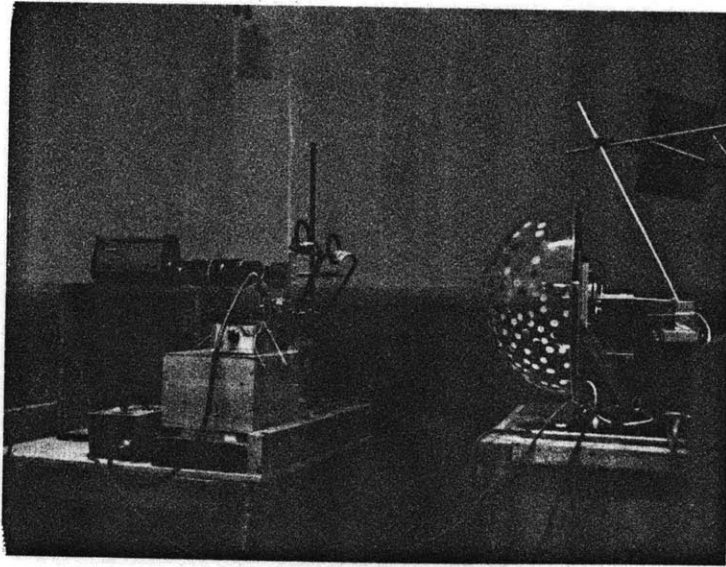
Finke and Held (1978) argue for the existence of relatively independent processes underlying induced tilt and ocular torsion during observation of rotating visual fields about the line of sight. Yet, induced tilt may still be used as an effective means of stimulating ocular torsion for testing.

A rotating pattern was projected on a wide white screen by placing

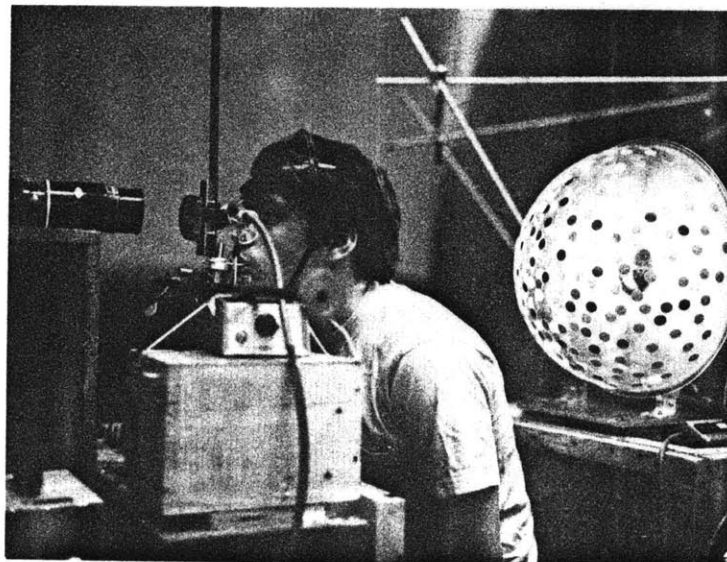


Photograph 4.1 Plastic hemispherical dome mounted on rotating hub. Light source in dome center projects random pattern of dots onto a wide white screen.

a light source inside a clear plastic hemisphere with randomly placed dots. The dome as shown in the photograph below, was mounted on a hub which could be variably rotated from 0 to 90 degrees per second. Brandt et al (1975) investigated the use of such patterns as stimulus displays. They concluded that the maximum induced tilt resulted when the ratio of dot area to total stimulus field area was between 15 and 70 percent; a 22 percent dot density appeared to work well. They also found that stationary contrasts inhibit visually induced self-motion and that the location in depth of these contrasts has a significant effect upon this inhibition. This effect is considerable when contrasts are located in the background or the moving stimuli, but weak when appearing in the foreground. For this reason, compelling circularvection was experienced whether the subject stood in front of the dome or in back of it, or whether a video camera was visible to the subject or not.



Photograph 4.2 Experimental setup; dome dots are projected on the white screen in the background.



Photograph 4.3 Subject in test position, normally room lights are out with dome source providing sole illumination.



Photograph 4.4 Closeup of subject, head restraint and bite board. Hooded cable is fiber optics bundle with IR filter mounted on its end.

### 4.3 Experimental Apparatus

The restraint setup evident in the above photographs limits head movements which often occurred at vection onset, perhaps as a form of compensation. An adjustable chin rest and movable temple pressure disks are used along with a dental bite board. The bite board is formed by softening Kerr Dental impression sticks about a piece of metal. Subjects bite into the compound leaving an impression of their teeth. The board is held in an adjustable clamp and the entire restraint setup aligned with the light source and video camera.

#### 4.3.1 Low Light Level Video Camera

The heart of any television camera is its pickup tube. Different tubes serve different needs. Minimum visual illumination is used to avoid providing the subject with spatial orientation cues. To achieve high resolution at such low light levels, a PANASONIC Newvicon tube was inserted inside a standard PANASONIC WV-200P television camera. As the spectral sensitivity graph below shows, the Newvicon has a much higher sensitivity over the visible and near infrared light range when compared to standard and silicon vidicon. It can, in fact, be used in complete visual darkness with invisible infrared illumination. This feature allows us to achieve an especially large bright pupil since infrared light shows very little in the visible region, causing little pupil contraction. The Newvicon has limited blooming of high brightness details and good picture quality due to high tube resolution, 550-650 TV lines at picture center and low dark current level (0.7 nA).

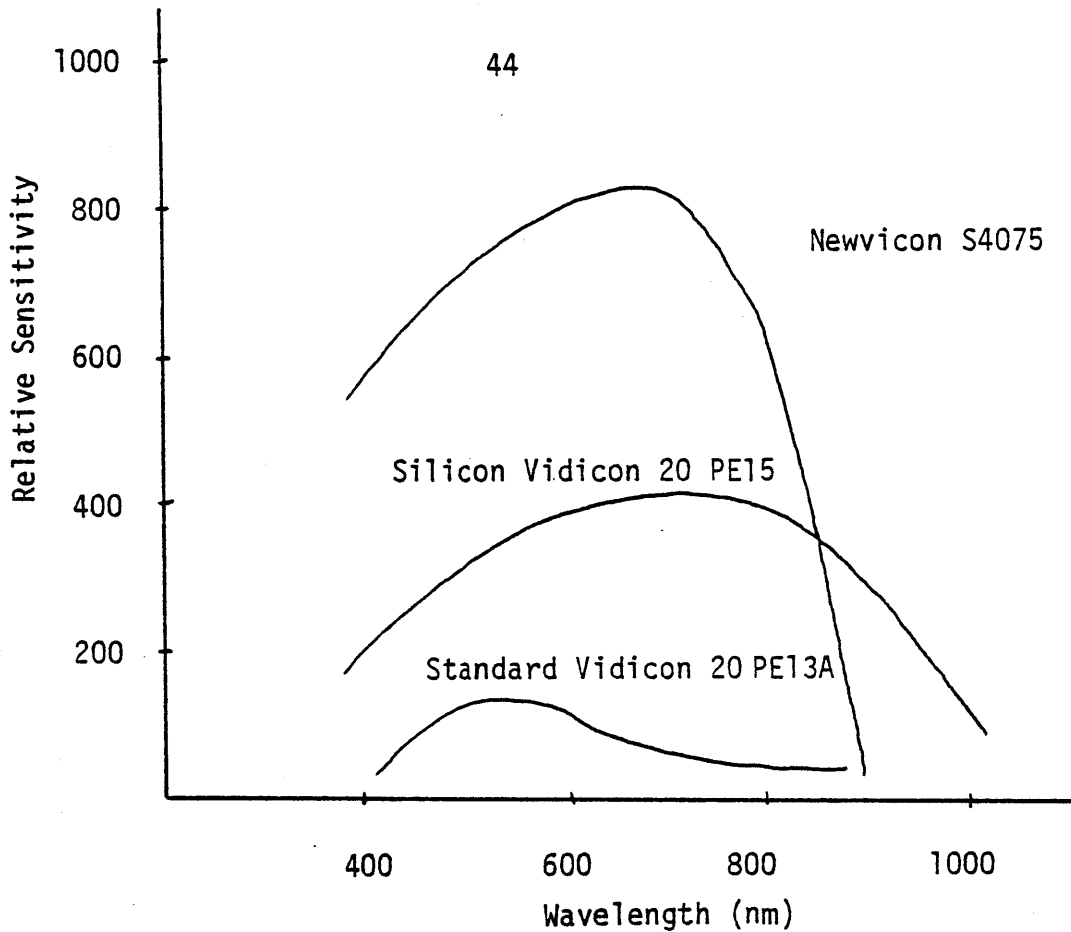


Figure 4.2 Spectral Sensitivity Chart Contrasting three Panasonic Tubes (Newvicon tube S4075 used in our set up)

#### 4.3.2 Camera Lens

In viewing the human eye, a number of key issues arise. First, equipment should be aligned as closely as possible to the ideal bright pupil arrangement, where the camera is 90° to the light source and the light source 90° to the eye. The beam splitter in line with the camera and subject should be oriented at 45° to reflect light into the eye and at the same time allow transmission of the image of the eye to the camera. Misalignment in any direction will decrease the amount of



light reflected into and from the eye, decreasing the illumination and therefore the contrast. All parts of the system should therefore be mounted on a single metal table or plate. A wood pallet supported the prototype set up and no great concern was given to precise and rigid mounting. This may have contributed somewhat to data variability and detracted from overall performance. Second, it is critical that one focus on the feature in the contact lens and not on the eye. This is difficult but aided by the shallow depth of field of the macro lens; when the lens feature is in focus the eye beneath is not. Thus, the feature stands out all the more, providing the video signal processor with a good target.

Third, in striving to fill the field of view with the iris and pupil alone, a 1 to 1 reproduction ratio is required. It is important to keep in mind that this will require a long lens and therefore a considerable mount of light, since when the image size and object size are equal, the distance to film plane from the lens and from lens to object must be equal as well. Likewise, the increased distance to the film plane requires increased light intensity. Use of the 'bright pupil' not only illuminated the eye at a sufficient level but since it 'fills' the pupil with light, the field of view contains a bright area corresponding to the pupil and a relatively dark surround. The camera tube assembly will accept any C-mount lens such as are used in television 16 mm format. An adapter is available to mount an 35 mm F-mount lens to this former format. Thus a high resolution Nikon f2 photomic 105 mm medical micro-Nikor lens

with extension tube fills the screen with an image of the iris and pupil alone.

#### 4.3.3 Video Tape Recorder

A high resolution, 330 lines monochrome, video cassette recorder allows for recording of eye movements for repetitive playback and analysis at some time after the experiment. If real time analysis is performed, simultaneous taping will assure that a copy of the complete data is available. The PANASONIC NV-9300 VTR <sup>( $\frac{3}{4}$ " bet)</sup> used has adjustable still frame which permits the user to stop on a particular video field and to manually feed the tape through the recording heads. This is especially convenient in examining the recording for detail.

## CHAPTER 5

## VIDEO SIGNAL PROCESSOR

An electronic device detects a specific pattern from a video picture of the eye. It uses a high speed differential comparator to find high contrast transitions in a filtered and enhanced version of the video signal. If the transition occurs within a user defined segment of the full video scan line, the horizontal and vertical coordinates of the transition are transferred to a digital computer in real time. There, they are stored on an RK05 disk for future data analysis. A quick means of assessing the operation of the detection is provided by overlaying the comparator output upon the video image. The key elements of the video signal processor (VSP) are depicted in the block diagram of Figure 5.1.

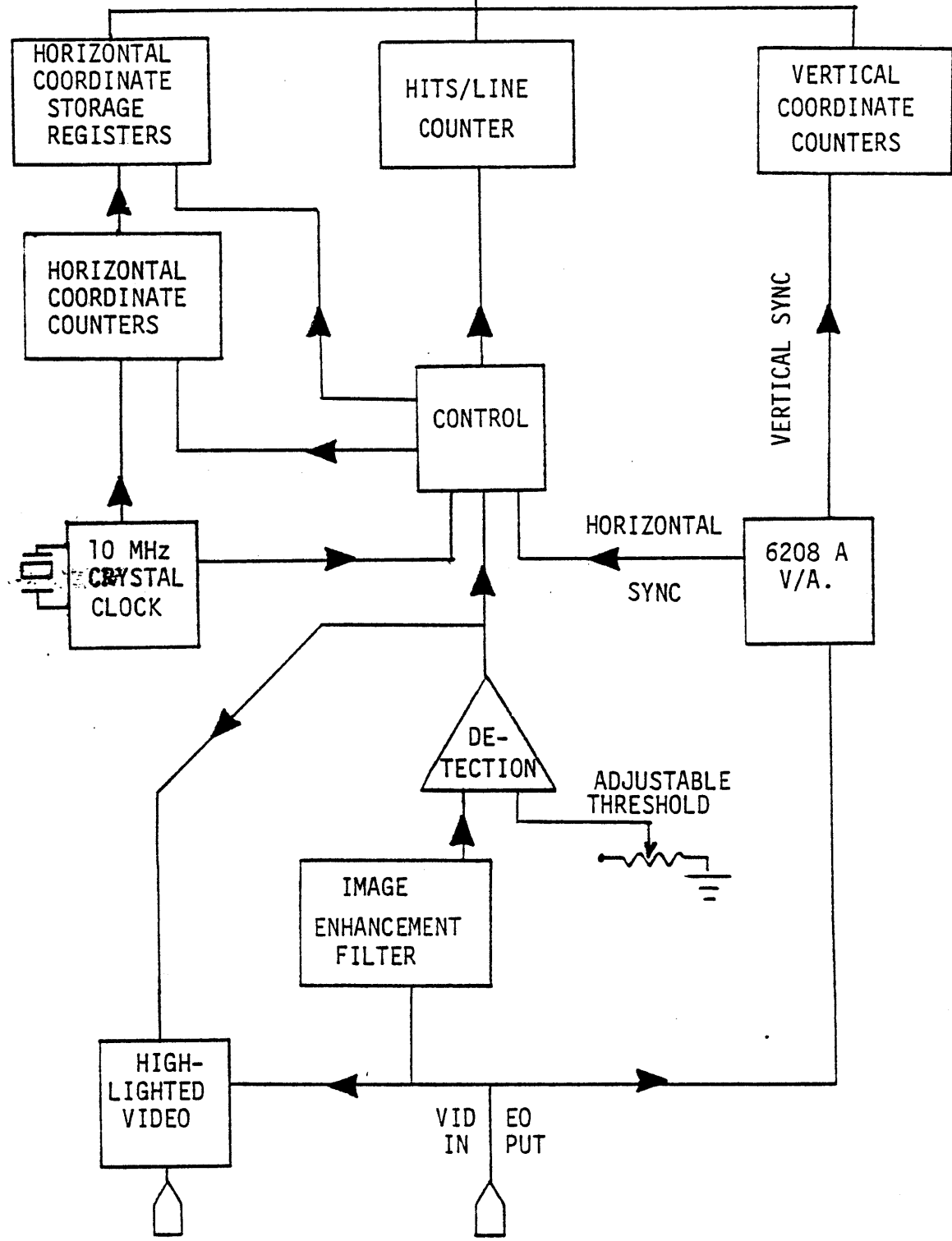


Figure 5.1 Block Diagram of the VSP

## 5.1 DC Restoration

The video signal is an amplitude modulated waveform consisting of video information and blanking and synchronization pulses (see Appendix E). Though there are regulated standards for the frequencies of these pulses, the amplitudes seem to vary from camera to camera, at times drastically. Furthermore, the signal is often corrupted by noise. To assure that the detection system was analysing a signal with constant reference, a DC restoration circuit was inserted. The signal, terminated with a  $75 \Omega$  resistor to ground, is passed through two capacitors in parallel. Negative excursions, such as sync signals, are then clamped to a desired level which may be potentiometer adjusted. A  $100 \text{ K}\Omega$  resistor to ground slowly ( $\tau \approx 1 \text{ sec}$ ) discharges the capacitors to assure that line hum or other artifacts do not erroneously shut off the diode by pulling the signal high.

## 5.2 Signal Enhancement

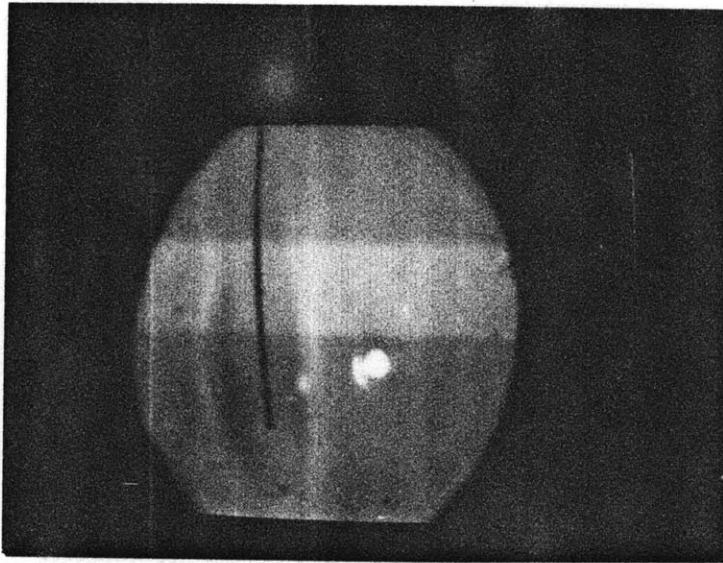
The characteristic rounded pulse-like shape of a hair in a contact lens sandwich suggests that it may be discriminated from other signals by some type of matched filter. A resonant, RLC circuit, may be the best suited, but two RC circuits were used to implement a band pass filter. The enhanced signal was compared with a threshold, set by a potentiometer voltage divider. Care was taken to keep all grounds in close proximity to minimize noise. A high speed differential comparator (LM 361) with complementary outputs and independent strobes is

used. Hysteresis reduced spurious transitions, leading to a sharper threshold and some noise and oscillation immunity as well. A 10 pf capacitor in parallel with the 100 K $\Omega$  feedback resistor eliminates high frequency spikes.

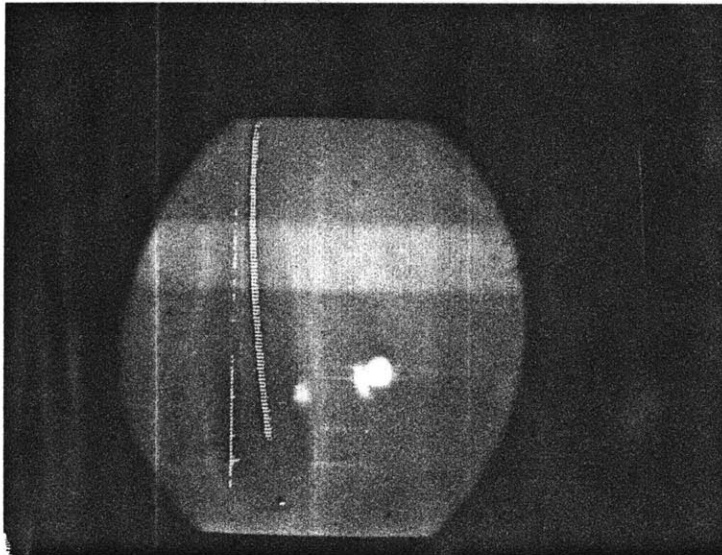
The comparator output is ANDed with two selection pulses to exclude unwanted transitions, such as corneal reflections, from appearing as detected features. The first pulse, the 'active line' signal, is set whenever the current video line is a scan from which data is being sampled. The second, the 'video gate' is generated by passing the inverted horizontal sync through two series monostable multivibrators. It sets a window within the video field whose width and location may be set by varying potentiometers controlling the single shot time constants. The gated signal represents acceptable data and is passed to the digital coordinate transfer circuitry. It is also used to 'highlight' the video image.

### 5.3 Highlighting

To provide the user with an immediate assessment of the detection circuitry operation, the acceptable data signal is overlaid on the video image. White dots are superimposed upon objects detected on active lines within the video window. In this manner, the threshold and window can be adjusted and corrected to provide the optimum data to the computer.



Photograph 5.1 Subject mounted Softlens-hair 'sandwich' at VSP video output (directly connected to video input)



Photograph 5.2 VSP highlighted video output version of photograph 5.1.

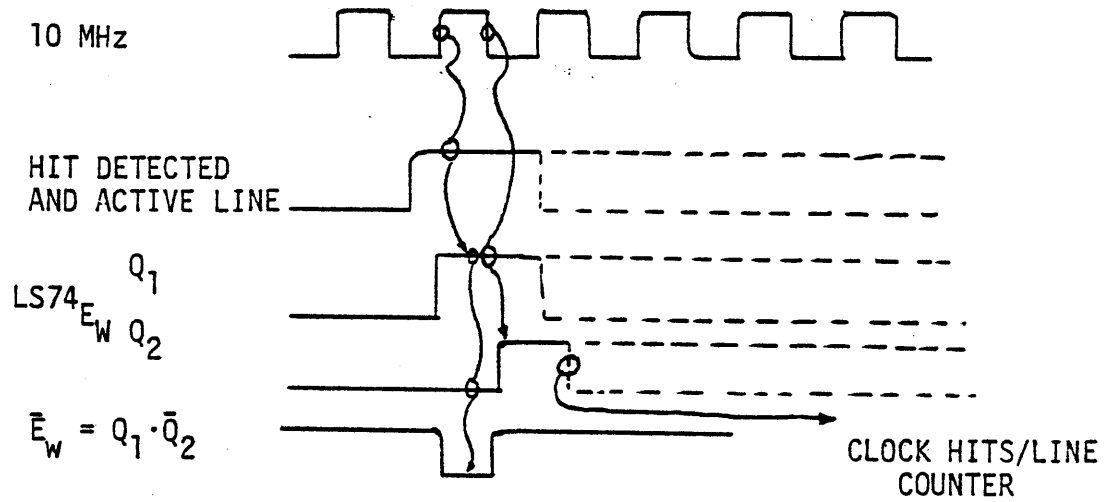
#### 5.4 Data Transfer

To assure data flow integrity, every other line must be skipped. This provides one video scan's time for storage of data in proper registers and computer reading of this information. A DIP switch is used to allow adjustable initialization of the synchronous binary counter which controls the line sampling rate. The count starts from this initial value and proceeds up to 16, whereupon the carry output is set activating the rest of the circuit as well as reloading the counter to the initial value. The activation includes enabling of the X-coordinate register and the updating of a counter that counts the number of comparator 'hits' per scanned video line. This four bit binary counter notes up to 16 comparator accepted images on a line. Its lower two bits ( $s_0, s_1$ ) are used as the write addresses for the X-coordinate storage registers. The  $s_0, s_1$  directed transfer of the count value from the X-coordinate counter to one of the four files takes place only when the latches are enabled. The formation of this pulse is depicted in Figure 5.2.

Computer data rate limitations constrain the amount of data that may be gathered in a given time. In the present configuration, the LPS is only fast enough to get one X,Y pair every two scan lines. Thus, if every other line (EOL) is to be sampled, only one of the four horizontal coordinates may be read along with the scan line value. If additional lines are skipped, as they may be set by the DIP switch, more points may be taken per line. This choice between points per line and lines per frame may be eliminated by implementation of a number of the suggestions in Chapter 8.



FIGURE 5.2 GENERATION OF HORIZONTAL REGISTER WRITE ENABLE PULSE



The horizontal position counters are cleared by the horizontal sync pulse extracted from the video waveform by the 6280A video to analog converter. This module, which is produced by Optical Electronics, Inc. (OEI), provides video output, separated vertical and horizontal sync pulses, vertical and horizontal ramps and blanking pulses, from a composite video input. Some of these pulses are used to clock various states of the circuitry in the device so that the electronic processing is in synchrony with the video image. It is set for standard television rates of 16 msec fields and 63.5  $\mu$ sec lines, but may be adjusted for other frame rates and sweep times.

While most of the clocking in the circuit is set by the module or signals from other components, the system sweep time is set by an external clock. A 10 MHz crystal oscillator provides a clock for the image position counters. At this rate, the horizontal coordinate binary counters sample a 63.5  $\mu$ sec video line approximately 635 times. The counters are cleared by the horizontal sync pulse and therefore count out points along every video line.

When the comparator signifies that a point is part of the desired pattern and the line counter circuit notes that the current line is desired or active, an enable pulse is formed to control the data acquisition. This pulse enables the LS670 storage file to accept counter data. The following timing diagram illustrates how this pulse is established to sample points only along active lines.

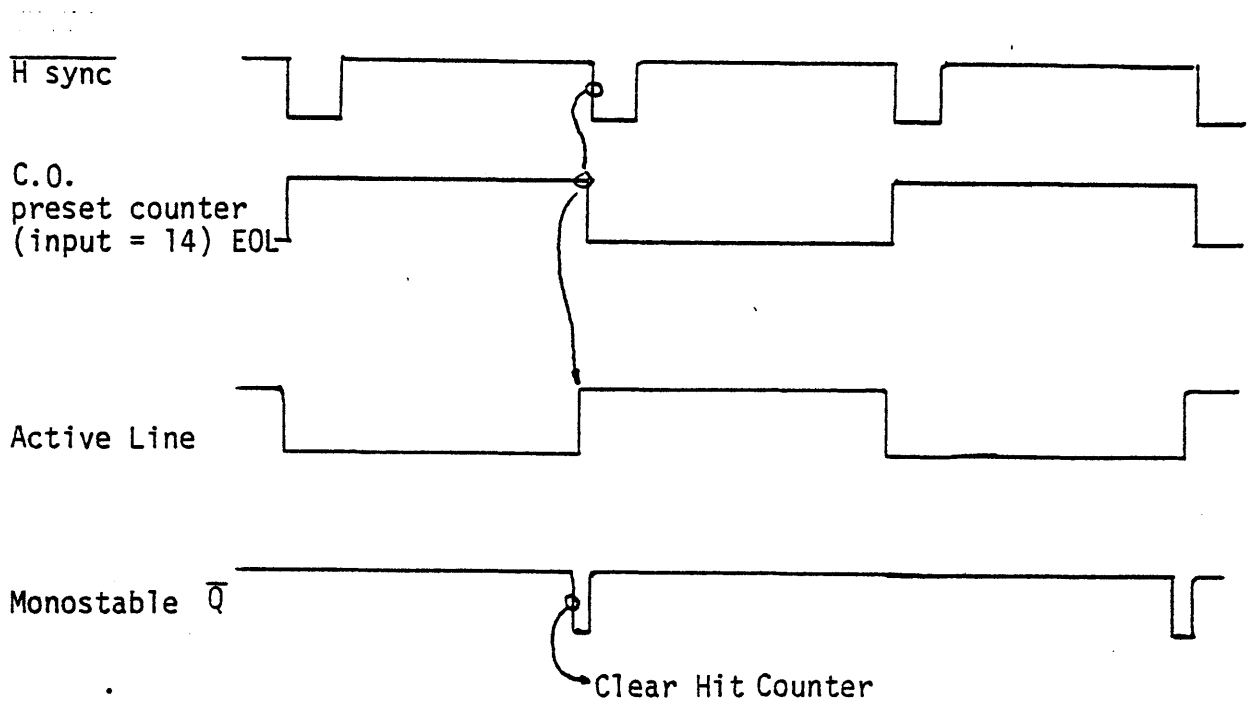


Figure 5.3 GENERATION OF ACTIVE LINE PULSE

The Y-coordinate or vertical position represents the line on which the detected image is found. It is read from two counters, clocked by the horizontal sync pulses and cleared after every field. This establishes a 60 Hz image refresh rate. A flip flop is available to halve this rate to 30 Hz.

Together, the horizontal point and vertical line counters establish the smallest video image element or pixel. The computer polls the storage registers and Y counters for data points, records their values on a disk and reconstructs the 'highlighted' video image.

Three types of data are, then, eventually stored in the computer; 12 bits of X coordinate, 8 bits of Y coordinate data and 8 bits of state information. Multiplexers select the data and pass it through the inverter buffers to the LPS of the PDP 11/34. The type selection is specified through the four lower order bits of the computer's Digital Output Buffer; bits 3 and 2 are used for the line select addresses, while bits 1 and 0 specify which of the four register files in the three storage latches are to be sent as X data. The lower bits function as read addresses in the same manner as the write addresses. When  $R_A$  and  $R_B$  are both set to 0, the first register file is opened and used as the X-data line into the line multiplexers. Schematics detailing all components of the processor are presented below. The following chapter discusses software and control of the video signal processor. Register sheets summarize the form of the three data types and a block diagram is provided to illustrate the synchronization of the computer and VSP. Device operation is described in the User's Guide of Appendix I.

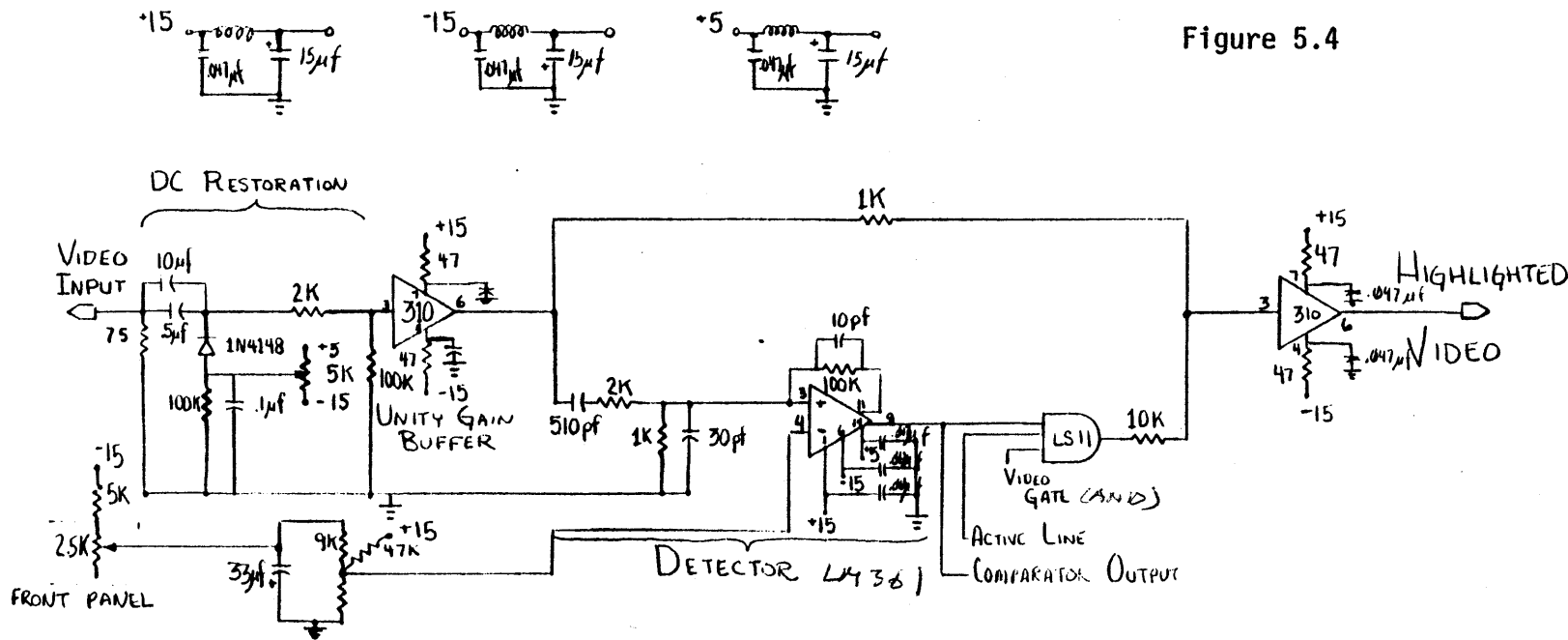
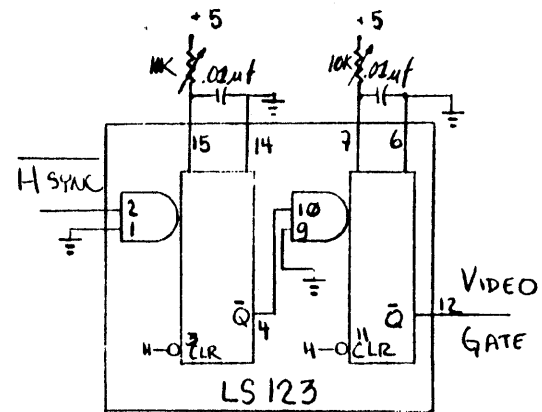
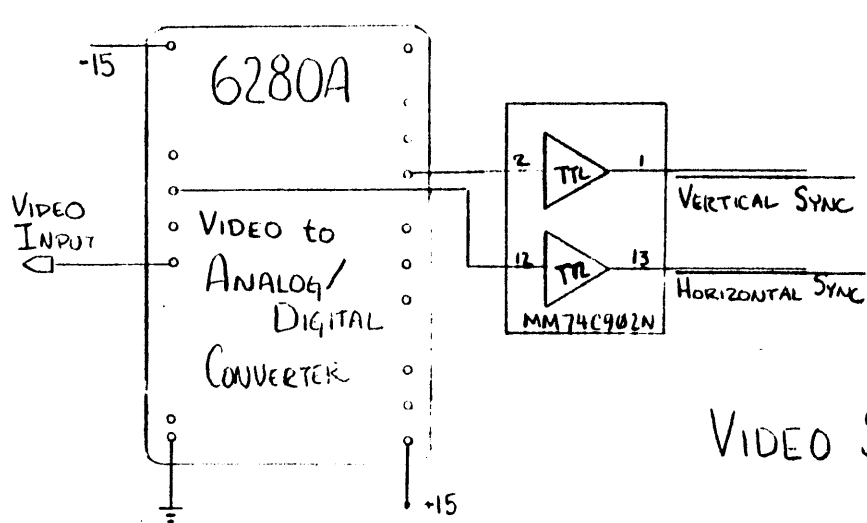
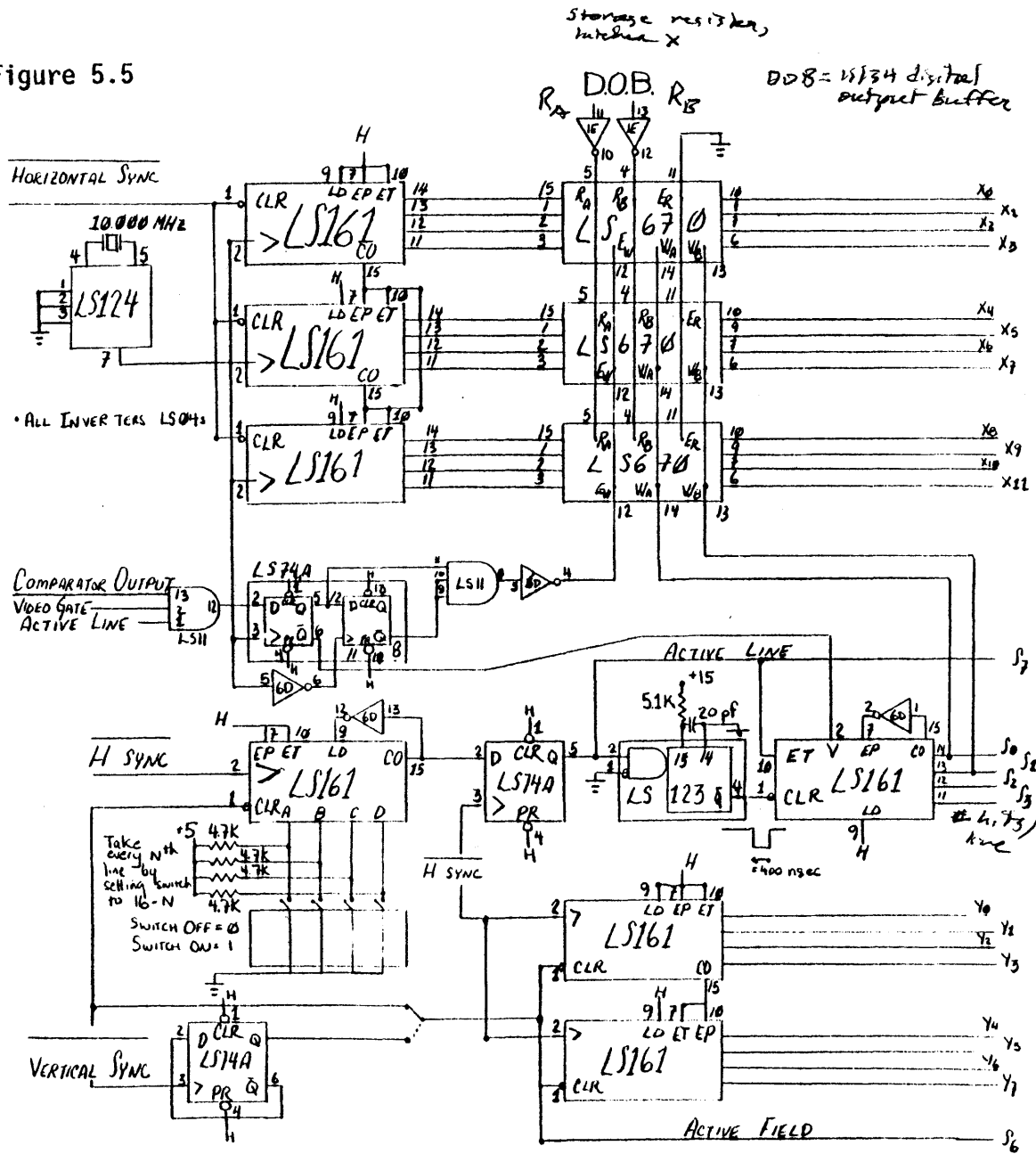


Figure 5.4

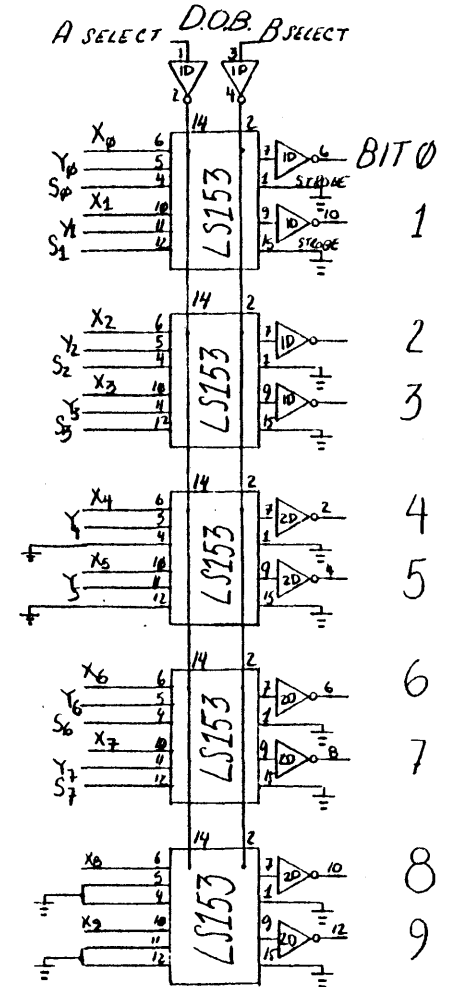


VIDEO SCANNING PROCESSOR SHEET I  
 E.R. EDELMAN  
 11-JUNE-1979

Figure 5.5

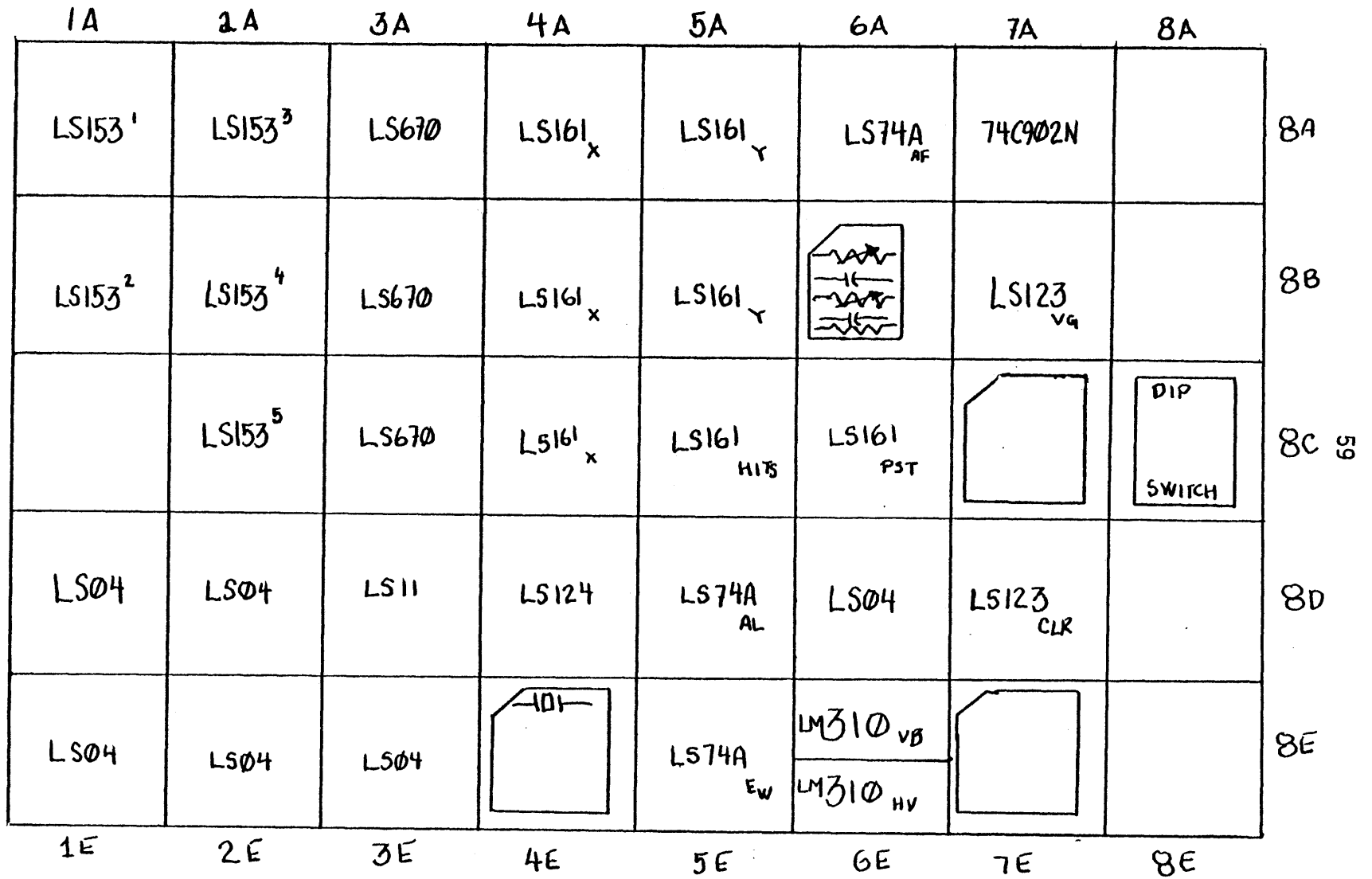


LS153  
4 line to 1 line  
multiplexer



VIDEO SCANNING  
PROCESSOR SHEET II  
E R EDELMAN  
5-JUNE-1979

Figure 5.6 Digital Component Layout



## CHAPTER 6

## VSP DATA TRANSACTIONS

In this prototype version data is stored in real time and analyzed later. That is, if a camera or video tape recorder is supplying a video signal to the VSP, the processed data can be written onto an RK05 disk at the 60 Hz video field rate. Once stored, extensive and repetitive processing can be used to extract the feature angle for each field. The real time analysis system would bypass this intermediate step by using a dedicated processor (microprocessor or minicomputer) to provide the angle in real time. The speed and processing requirements of such an analysis exceeds the capabilities of the PDP 11/34 available for this work. In addition, since this thesis represents the preliminary phases of a major project, it is logical to split the data analysis development into two distinct tasks. The first - investigating means for data transfer and the second - approaches for analyzing the data.

This separation makes it possible to establish the optimum analysis techniques independent of problems associated with high sampling rates. The same data may be evaluated many times with different schemes or for the same scheme with different parametric values. When the most effective method is found, the two tasks, transfer and analysis, may be combined and consideration given to real time implementation. Linear regression provided the most acceptable results to date; yet,



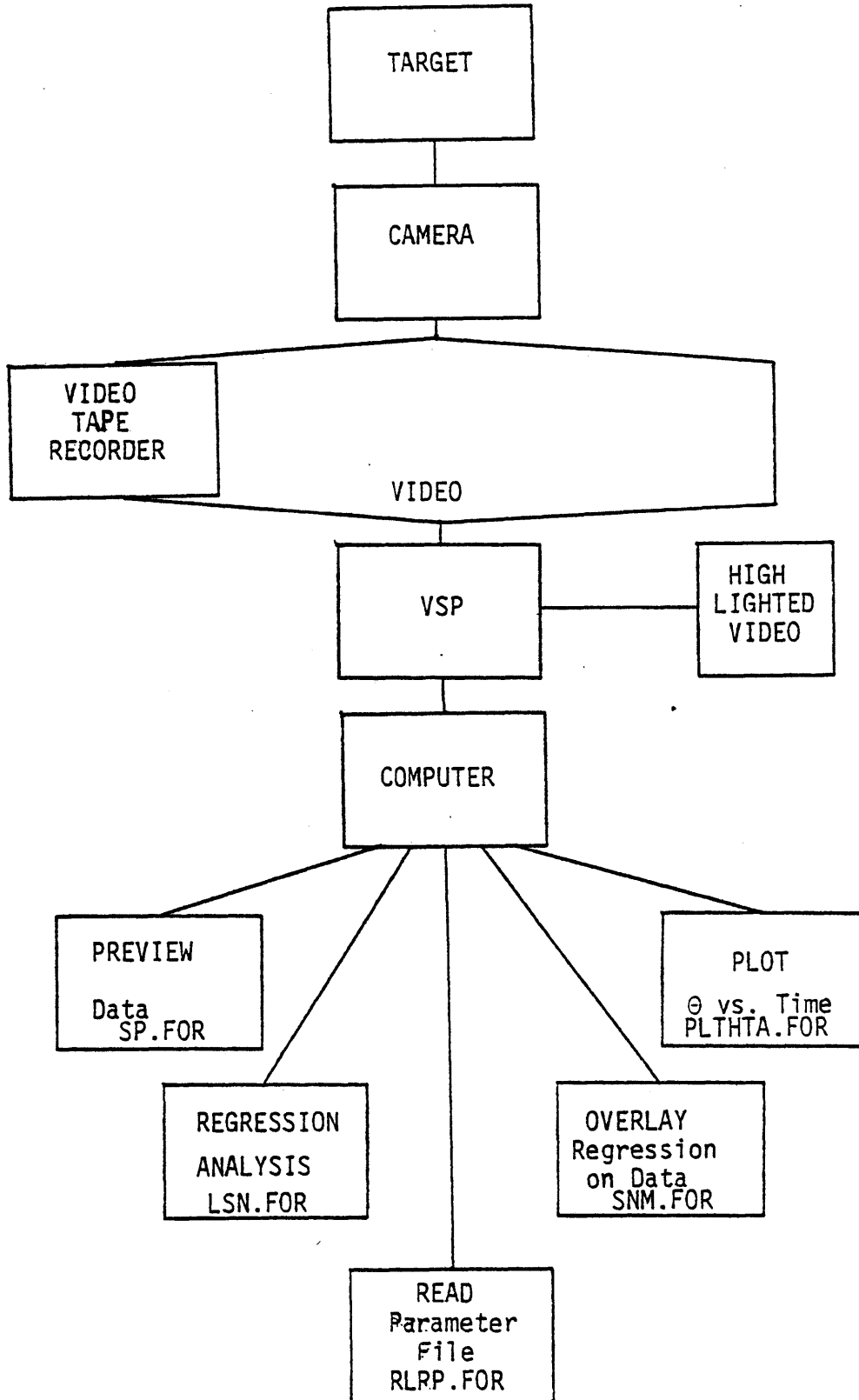


Figure 6.1 System Options. Programs names aside operating modalities control associated features.

a more complex polynomial fit may better suit the curved contact lens mounted feature.

The block diagram above illustrates the various data modalities and processing options available to the user in operation of the system. These include the choice between analysis of direct versus recorded video data and selection of different data handling modes. Names of the software routines are listed next to the tasks they control. Each option is described in this chapter along with a description of the challenges presented by the processing constraints and the compromises they necessitated. Segments of the implemented computer programs are presented to provide the reader with some appreciation for the structure of the code necessary for data transfer. Complete listings may be found in Appendix B. A flow chart emphasizing the synchronization between the computer and the VSP is included here as well.

### 6.1 Data Transfer

Vertical and horizontal coordinates of a detected image are passed from the VSP to the computer under the direction of the DEC Lab Peripheral System(LPS). The LPS is controlled by a computer program which initiates the sampling after assuring that the VSP scans are synchronized with the LPS reads. Real time writing was accomplished by first placing the data in one of two memory buffers. As one buffer is filled, an asynchronous write is started and the second buffer used for data acceptance. In this manner, data is read at 60 Hz and formatted such that each field establishes a disk block 200 words long.

The Lab Peripheral System data register module (LPSDR) controls LSP Input/Output. Its main functional units include a 16-bit buffered output register, a 16-bit input register, a status register, and an interrupt control section. The output register may be loaded from or read into by the central processor. When loaded, the register initiates an INTERNAL NEW DATA READY signal, a zero going pulse of 1  $\mu$ sec duration. This pulse is placed on the output lines in addition to the 16 data lines. The external device interfaced to the LPS receives the data and issues an EXTERNAL DATA ACCEPT signal, indicating that the output register may now be loaded with new data. Receipt of that signal sets the output flag of the status register and, if the output interrupt enable bit is set, causes an interrupt.

To load the input register, the external device applies data to the lines and generates the signal EXT NEW DATA READY (ENDR), which loads the register and sets the input flag of the status register. When the central processor has read the data, the signal INTERNAL DATA ACCEPT is transmitted back to the external device, which can then send another ENDR. If two signals are sent before the first is acknowledged, data from the first signal is lost.

In our system, a software I/O 'handshake' generated the EXTERNAL NEW DATA READY pulse. Bit 4 on the digital output line is connected to the ENDR pin at the I/O interface. A software pulse is generated by alternately setting and clearing this bit. Bits 0 and 3 are used

TABLE 6.1

## LPSDR Input/Output Pin Assignments

<u>Pin</u>	<u>Digital Input</u>	<u>Digital Output</u>
1	Ground	Ground
2	EXT NEW DATA RDY	INT NEW DATA RDY
3	INT DATA ACC	EXT DATA ACC
4	IN DATA 03	EXT DATA 03
5	IN DATA 00	EXT DATA 00
6	Ground	Ground
7	IN DATA 05	EXT DATA 05
8	IN DATA 07	EXT DATA 07
9	Ground	Ground
10	IN DATA 10	EXT DATA 10
11	IN DATA 14	EXT DATA 14
12	IN DATA 04	EXT DATA 04
13	IN DATA 06	EXT DATA 06
14	Ground	Ground
15	IN DATA 02	EXT DATA 02
16	IN DATA 01	EXT DATA 01
17	Ground	Ground
18	IN DATA 08	EXT DATA 08
19	IN DATA 11	EXT DATA 11
20	Ground	Ground
21	IN DATA 15	EXT DATA 15
22	IN DATA 09	EXT DATA 09
23	Ground	Ground
24	IN DATA 12	EXT DATA 12
25	IN DATA 13	EXT DATA 13





to instruct the VSP as to which data is to be provided to the data multiplexers and from there to the LPS interface. Bits 0 and 1 select one of four possible horizontal hits by directing the LS670 through its read pins  $R_A$  and  $R_B$ , while bits 2 and 3 specify the type of data to be sent along the input lines from the LS153 4 line to 1 line multiplexers to the I/O interface. Thus, when the DOB presents an 00XX to the VSP, horizontal data is presented to the LS153's from the LS670's. XX determines which of the first four comparator hits along a vertical line scan are to be sent; 00 hit 1, 01 hit 2, etc. If, instead, a 01 in bits 2 and 3 of the DOB requests the Y, vertical coordinate of the line and a 10 requests status information. This includes the number of hits per line and state of the ACTIVE FIELD and ACTIVE LINE signals. The register sheets above summarize these different buffer modalities.

The following segments of the data transfer computer program may explain the actions described above still further.

	DIGITAL OUTPUT BUFFER	ENDR PULSE	
	bits 4 3 2 1 0		
MOV # 1, @#DOB ;	0 0 0 0 0		Get second
MOV #21, @#DOB ;	1 0 0 0 0		horizontal
MOV # 1, @#DOB ;	0 1 0 0 0		hit coordinate
MOV @#DOB, RO ;	Read data on input lines in software register 0		

As noted, VSP status information is also provided. This data is used to evaluate the signal processor's operation and to synchronize the VSP and LPS before the reads take place. The four lowest order

status bits are the number of comparator detections for a given line. They may be used to assess the proper level of the comparator threshold. A very large number signifies that the threshold is too low and too much of the image is being passed as the tracking feature, while a very small number or 0 might indicate the reverse. Though not currently in use, a feedback loop may be implemented to control the threshold in this manner.

Bits 6 and 7 are used as synchronization pulses. They are examined prior to data sampling to assure that this sampling starts at the top of a video field and that data may be read from the beginning of active lines. The machine code fragment below illustrates that by looking for a transition in the AL or AF signals, data sampling will occur at the correct places and not within an active field or line.

```
MOL: MOV #10,@#DOB ; generate ENDR pulse and ask
      MOV #30,@#DOB ; for VSP status information
      MOV #10,@#DOB ;
      MOV #DIB,R0 ; read digital input lines
      CLR @#DGS ; clear digital status register
      BIT #100,R0 ; is bit 6 set?
      BEQ MOL ; yes, loop since middle of AL
                ; no, wait since on nonactive line
```

```
NAL: MOV #10,@#DOB
      MOV #30,@#DOB
      MOV #10,@#DOB
      MOV #DIB,R0
      CLR @#DGS
      BIT #100,R0 ; is bit 6 set? No, loop till
      BNE NAL ; Yes signifying transition to AL
```

The same code is used for AF synchronization by changing bit test query to BIT #200,R0; examining bit 7.



This scheme, however, presents severe drawbacks, for every time a line is to be scanned a full series of synchronization evaluation instructions must be executed along with the actual data read. Chapter 6 discusses means of eliminating some of this code and allowing added time for actual data sampling.

In short, the horizontal coordinate of a comparator hit is recorded alone, with its scan line position once synchronization has verified that sampling may be initiated. Currently, 99 such lines are scanned per field. A field counter recorded at the start of each field and a termination indicator at the end are added to yield 200 words of data per field. This is executed every 16 milliseconds, at the 60 Hz video field rate. Normal WRITES to disk are therefore ruled out, since they require 350 msec for completion.

Instead, a dual buffering scheme has been set up to work with asynchronous WRITES. These writes to disk occur when time is available and allow for continued independent program operation requiring only that enough time for the write be allocated before the next write request of that save variable. Thirty-two video fields are written into a memory buffer, and when filled, a write is initiated and the second buffer called upon to receive the next thirty-two fields. When it is filled, its write is initiated and the first buffer, already written, is once again ready to accept more fields to repeat the cycle.

The disk handler queue has been expanded to accept additional write requests. This assures that write requests will not be blocked by other processes. At the same time, interrupts are locked out during data sampling so as not to disturb data transfer from the VSP.

Appendix C describes the choice of buffer size and a description of the operation of the collection and storage routines may be found in the systems user's guide. Precise details as to the workings of the DEC-Lab Peripheral System may be found in the LPS11-Laboratory Peripheral System User's Guide (DEC-11-HLPGA-B-D).

An overview of the transfer procedure as implemented in the software is depicted in the flow chart in Figure 6.14

## 6.2 Data Analysis

Once data has been recorded on disk, movement of the feature, as represented by the data, must be extracted. The main concern of this work is the evaluation of purely cyclotorsional eye movements; torsion about the anteroposterior axis. Thus, an angular shift from field to field must be assessed. To do this, a line is fitted to the data and an angle computed for each line. Artifacts such as noise and the curvature of the line feature required that certain points be rejected before the fit. This chapter discusses the problem noted above, the considerations that went into implementation of the existing analysis routines and suggestions for future development.

Various forms of line fit were investigated. Regression analysis provided the most effective means of filtering data and rejecting outliers. In addition, though it is now linear in nature, it may be expanded to higher order terms with few modifications.

The linear regression routine defines a slope  $b$  and an  $x$ -intercept for each field. These values approximate an actual first order linear regression of the form  $X = A + BY$ . The regression on  $Y$  is used because this system is searching to locate the horizontal coordinate along a given vertical line. Quite conveniently, the targets are near vertical also dictating desirability of an  $X$  on  $Y$  regression. A standard deviation of the horizontal coordinates from the regressed results is used on repeated passes through the same data to reject points lying outside a specified limit, as illustrated in the figure on the next page. The limit is composed of a user specified multiple,  $S$ , of the standard deviations  $\sigma_x$ , plus some fixed constant  $\Delta$ , which may also be varied at execution time; so  $\text{lim} = S\sigma_x + \Delta$ . A vertical software window simultaneously excludes noise points from regions above and below the actual feature.

The user may repeat the analysis along the same field of data as many times as desired before moving on to the next field. Noise free signals will require only one or two additional passes after the first, while noisy images may need several iterations for best fit. (See results section for discussion.)

At the program start, the user is queried for the data file to be analyzed and a file name for the data file into which the linear regression parameters are to be entered. A second query allows for limitation of the number of fields. Thus, the entire data file or only a small segment of it may be analyzed. The analysis currently starts from the first field, but the simple adjustment to the program code will allow for examination to start on any field, as is the case in the program SP.FOR that permits data viewing.

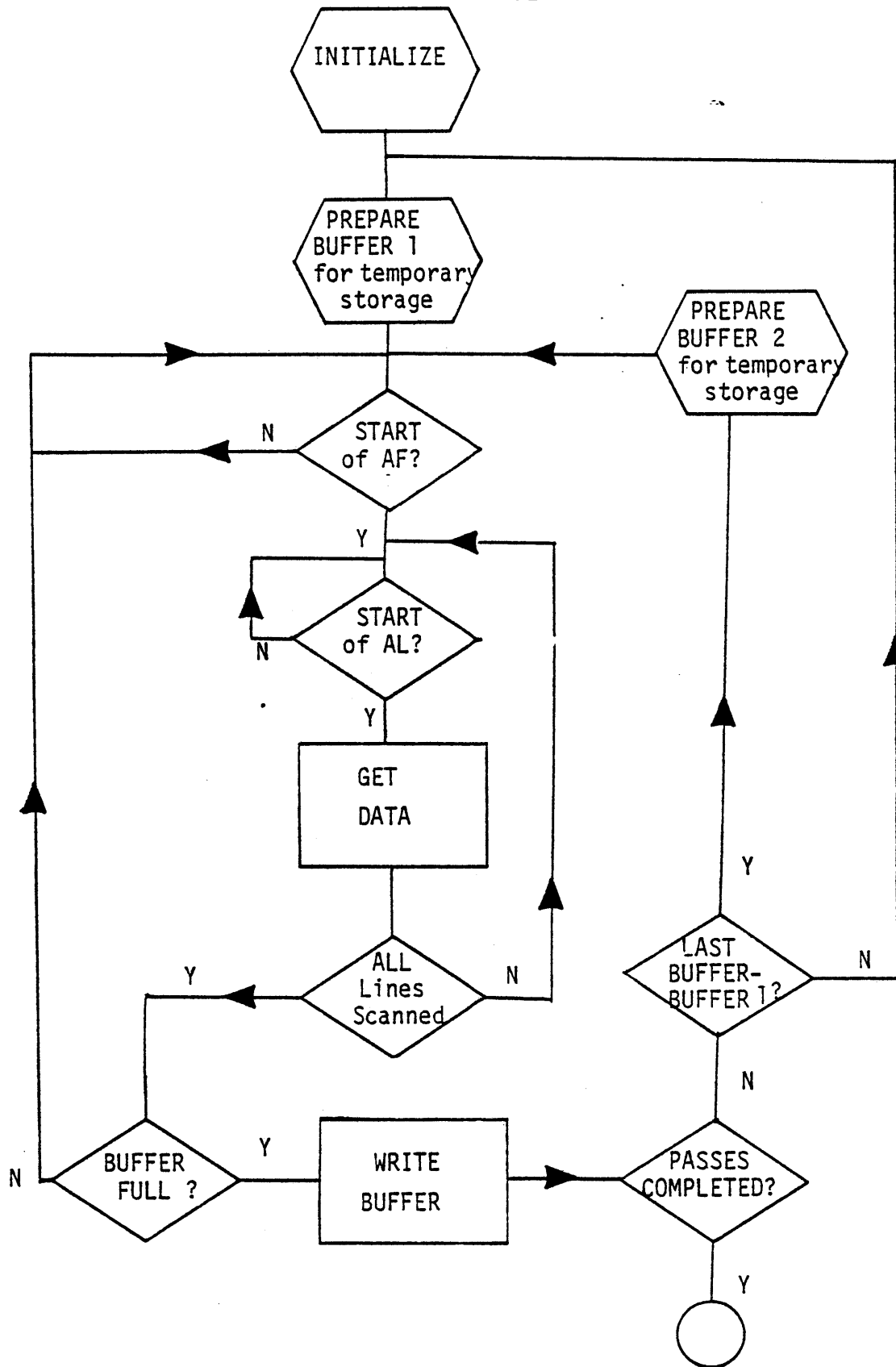


Figure 6.4 Data collection flow diagram emphasizing computer-VSP synchronization

### 6.2.1 Vertical Window

Very often bad data will appear at the top and bottom of the video field. These points may represent a region of the scan above or below the pupil, or that part of the pupil with no target across it. An adjustable vertical window can be used to delimit valid data. The window limits may be specified with a light pen sighting or through specific reference to a certain scan line. If the light pen is used, the system operator is asked to pinpoint two points from a display of the first field of data. The program searches the data array for the actual point closest to the light pen indication and then takes the scan lines they lie on as the top and bottom boundaries of the window. After selection, the window limits are displayed against the data points to provide the user with an illustration of the possible effect of rejecting points outside the window, and the opportunity to reposition these boundaries.

### 6.2.2 Data Rejection

When the window is set, the analysis begins. Horizontal data points, starting from the top of the window, are compared to what is predicted from the previous pass's linear regression. If the difference is greater than the limit mentioned above, the point is excluded from analysis for that field. If two or less points remain, the entire field is rejected. The first pass through the first field is a straight regression with no point rejection. While the first pass through for each field after that uses the last field's standard deviation in its limit.

Each successive pass of the same field uses the previous pass's linear regression line and standard deviation for comparison.

The slope and x-intercept are determined from N accepted points in NF accepted fields to provide the fit  $x = a + by$ , where

$$a = \frac{1}{\Delta} \begin{vmatrix} \Sigma x_i & \Sigma y_i \\ \Sigma y_i x_i & \Sigma y_i^2 \end{vmatrix} = \frac{1}{\Delta} [\Sigma y_i^2 \Sigma x_i - \Sigma y_i \Sigma y_i x_i]$$

$$b = \frac{1}{\Delta} \begin{vmatrix} N & \Sigma x_i \\ \Sigma y_i & \Sigma y_i x_i \end{vmatrix} = \frac{1}{\Delta} [N \Sigma y_i x_i - \Sigma y_i \Sigma x_i]$$

$$\Delta = \begin{vmatrix} N & \Sigma y_i \\ \Sigma y_i & \Sigma y_i^2 \end{vmatrix} = N \Sigma y_i^2 - (\Sigma y_i)^2$$

This has been simplified for computational purposes to (see Bevington, 1969; Draper and Smith, 1966; Brown and Hollander, 1977):

$$b = \frac{N \Sigma y_i x_i - \Sigma y_i \Sigma x_i}{N \Sigma y_i^2 - (\Sigma y_i)^2} \quad \text{and} \quad a = \frac{\Sigma x_i - b \Sigma y_i}{N}$$

Finally, an angle for the line may be determined by adding  $90^\circ$  to the arctangent of the slope. The  $90^\circ$  is needed to bring the computer arctangent function into the regions corresponding to the video coordinate system where positive y is down the screen, since the scans are generated starting from the top.

### 6.2.3 Scaling

In standard television systems, the aspect ratio, or the ratio of frame width to frame height is 4 to 3. Furthermore, increments in horizontal direction do not equal those in the vertical. A 10 MHz crystal controlled clock establishes 520 samples along the 52  $\mu$ sec of each of the 240 scan lines in a video field. Thus, before any analysis takes place, it is essential that the X and Y video be normalized to the same units. A scaling constant, DK, has been determined to be equal to 0.6745 from normalization of a 45° line. If desired, this value may be determined afresh before each experiment to account for camera variations.

### 6.2.4 Statistics

The analysis routine also generates a series of statistical parameters that provide indication of the accuracy of fit. This information is provided at the completion of the regression, whereupon the user is given the opportunity to rerun the analysis for a different series of parameters. If he chooses not to do so, the program is terminated and the regression parameters and summary information written into the data file specified when the program was started.

This summary includes: the number of fields analyzed, as well as the number and location of the fields rejected; the vertical window limits, top and bottom; the user specified number of intrafield standard deviations to be used in point rejection; and an average

slope, standard deviation from this average for all fields, and the average standard error of angle estimate.

```

190 fields      2 loops, line 1 t 89
had limited excursion of 0.9330 pt. s.d.s + 5.000
average slope= 105.72 dgrs,  s.d. from <slope>= 24.352 mins
average standard error of angle estimate= 12.615 mins

```

0 Fields were rejected, including numbers:

### Number of Fields

Some fields are rejected because they contain noisy data, others because the fit is bad, etc. The number of fields analyzed is thus presented along with the number of rejected fields.

### Average Theta and Standard Deviation

Associated with the analysis of a large number of fields is an average angle  $\bar{\theta}$  and an estimate of the standard deviation from this mean,  $\hat{\sigma}_{\theta}$ .



$$\bar{\theta} = \frac{\sum_{i=NSF}^{NEF} \hat{\theta}_i}{N}$$

where NSF = starting field  
NEF = end field  
including only the accepted  
fields

and

$$\sigma_{\hat{\theta}} = \sqrt{\frac{\sum_{i=NSF}^{NEF} (\hat{\theta}_i - \bar{\theta})^2}{N-1}}$$

The angle estimate  $\hat{\theta}$  should only be regarded as an estimate of the true angle  $\theta$  which may be obtained from the regression of the data points. The reliability of this estimate may be evaluated by computing a confidence interval for  $\hat{\theta}$ . This will provide a means of assessing how much faith should be assigned to this angle estimate. Such an interval may take the form of

$$\hat{\theta} \pm t_{\alpha/2, n-2} * \sigma_{\hat{\theta}}$$

where the value  $t_{\alpha/2}$  is the upper  $\alpha/2$  percentile of Student's t-distribution with  $n-2$  degrees of freedom,  $\sigma_{\hat{\theta}}$  is the standard error of the angle estimate, and  $100*(1-\alpha)$  is the confidence coefficient.

There are a number of ways of estimating the standard error of  $\hat{\theta}$  only two of which were utilized. Both require knowledge of  $\epsilon_y$ ; the standard error associated with the regressed estimate of the linear fit. This is equal to the ratio of the standard deviation of  $x$  after it has been regressed on  $y$ , to the sum of the deviations in  $y$ .

$$\epsilon_b = \frac{\sigma_{x,y}}{\frac{NEF}{\sum_{i=NSF} (y_i - \bar{y})^2}}$$

where

$$\sigma_{x,y} = \sqrt{\frac{\frac{NEF}{\sum_{i=NSF} (x_i - [a + by_i])^2}}{N-2}}$$

Note, two degrees of freedom are lost, one for the determination of the regressed values and the other for the error estimate.

A conservative estimate of  $\epsilon_\theta$  may be found by determining a minimum and maximum angle for each fit based on the low and high limit errors of estimate about the regressed slope. In short, for

$$\begin{aligned} b_+ &= b + \epsilon_b, & \hat{\theta}_+ &= \tan^{-1}(b_+) \\ b_- &= b - \epsilon_b, & \hat{\theta}_- &= \tan^{-1}(b_-) \end{aligned}$$

The standard error of angle estimate may then be thought of as the averaged difference of these two angles, or,  $\epsilon_\theta = (\theta_+ + \theta_-)/2$ , as depicted below.

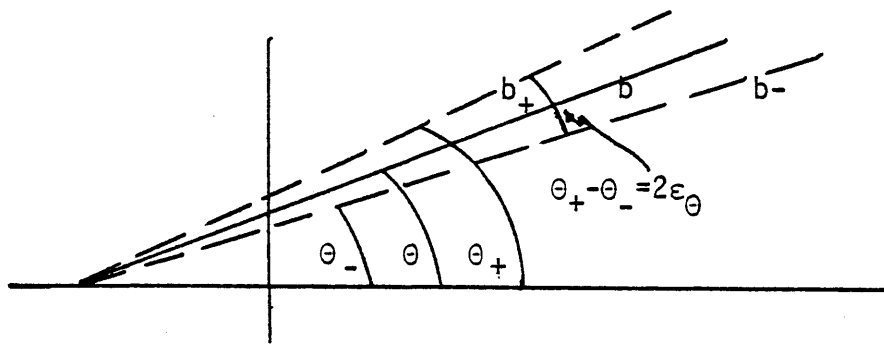


Figure 6.5 Illustration of  $\epsilon$  as computed by averaging the difference of maximum and minimum possible angle estimates

Problems arise with this due to the non-linearity of the arctangent function. To a first approximation, however, this provides a good estimate of  $\epsilon_\theta$ .

A second means attempts to bring the standard deviation of the slope through the arctangent function, by relying on the following argument.

For  $y = f(x)$ , the first term of a Taylor expansion will provide

$$y = y_0 + f'(x_0)(x - x_0) \quad \text{where } y_0 = f(x_0)$$

leading to

$$y - y_0 = f'(x_0)(x - x_0) \text{ and}$$

$$\Delta y = f'(x_0) \Delta x$$

If we let  $y = \theta$  and  $x = b$  and allow the differentials to represent the standard errors then

$$\epsilon_\theta = f'(b) \epsilon_b$$

If  $f(b)$  is the arctangent function, its derivative with respect to  $b$  is  $1/(1 + b^2)$ . Thus,  $\epsilon_\theta = (1/(1 + b^2))\epsilon_b$  radians. This is only a linearization ignoring higher order terms. However, since we are dealing with extremely small deviations, the estimate is reasonably valid.

Both methods were implemented and yielded approximately the same results. Yet, because of the non-linear arc tangent function, the second was favored and used in the reported results for tracking of a contact lens mounted feature and a moving abstract target.

## CHAPTER 7

## RESULTS

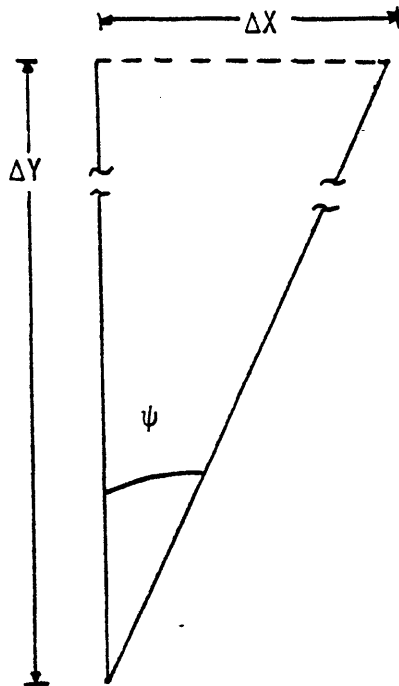
A series of tests were performed to characterize the performance of the system as it might be used for the measurement of ocular counter-rolling. Though far from extensive, they included: assessment of minimum resolvable angle and accuracy or goodness of fit. Evaluations were based on analysis of static straight lines, rotating straight lines, and contact lens mounted features adhered to a subject's eye. This chapter presents a summary of these experiments and some theoretical limitations of the system and then contrasts them to other techniques for measuring OCR as discussed in Chapter 3.

### 7.1 Theoretical Resolution

The use of video not only imposes the 60 Hz field rate but a vertical resolution of approximately 1 in 480 as well. The 10 MHz clock rate allows for 520 divisions along each active part of a video scan line. This leads to a 1 part in 520 horizontal resolution.

With this information, it is possible to establish a theoretical minimum resolvable angle,  $\psi$ . A most conservative estimate can be found by linking two endpoints to form a line and then rotating the line through  $\psi$  about one endpoint such that the other is displaced a single horizontal

element  $\Delta X$ . Thus,  $\psi = \arctan \frac{\Delta X}{\Delta Y}$  which may be simplified to  $\psi = \frac{\Delta X}{\Delta Y}$  using the small angle approximation.



where  $\Delta Y$  is the number of scan lines intersecting the tracking feature

Figure 7.1 Minimum resolvable angle,  $\psi$ , as determined by rotation about one endpoint.

Ninety-nine scan lines may intersect a given feature. Since every other line is sampled and because of the interlacing of field lines in a video frame this represents a possible high  $\Delta Y$ , of 396 lines. If  $\Delta X = 1$ , after normalization  $\psi = 5.8'$ . This value only represents what may be expected from an analysis joining only the two endpoints. It may even increase if one were to require that the center of rotation lie on the feature itself. In this case, as depicted in Figure 7.2 below,  $\psi$  is doubled to  $11.6'$ .

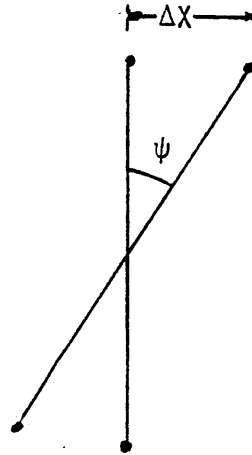


Figure 7.2 Minimum resolvable angle,  $\psi$ , as assessed from rotation about a point along the feature.

Still further, the angle may increase if a curved feature occupying less of the video field is used. Thus, it is essential that additional points be used to demarcate the feature. These extra values will not only average out the probability of error associated with assigning a detected point to its actual value, but will also allow for the discrimination of line features with horizontal excursions less than  $\Delta X$ . Susceptibility to large deviations from the mean will be minimized and the problems that other techniques which use only 2, 3, or 5 points per image avoided. Chapter 8 provides some suggestions as to how further points may be achieved. Nonetheless, better than 6 minutes of arc has been resolved with the present scheme.

## 7.2 Empirical Resolution

As an empirical determination of the minimum resolvable angle, an abstract target consisting of a black line on white background was attached to a protractor accurate to 0.1 degree. Angles were determined after rotating the protractor arm the smallest discernable angle. Repeated tests indicated that when the protractor was displaced a tenth of a degree, the system indicated precisely this amount. Rotations on the order of 3 minutes were observed by rotating the protractor less than the smallest demarcation, but due to this limit in demarcation, no exact measurement less than 0.1 degree could be made. It is felt that the system is capable of discerning these smaller movements but characterization of such is unnecessary due to the variabilities and uncertainties introduced by other parts of the system. These include not only electronic noise and computational error but also astigmatism in the camera tube and vibration of equipment that was secured to a wooden base. Nonetheless, this experimental evidence falls close to the theoretical computation of the minimum angle presented above.

## 7.3 Fixed Straight Line

Numerous fields of stationary lines at orientations from 0 to 180° were examined by the system to establish system accuracy and repeatability. Over 190 fields average deviations from mean angles were found to range from 1 to 5 minutes, increasing as the feature was rotated farther and farther from vertical. This increase corresponds



to the decrease in the number of scan lines intersecting the feature. At approximately  $15^\circ$  and  $165^\circ$ , as measured from the horizontal, so few lines crossed the target that no line could be fit with assurance greater than a few degrees.

The decrease in lines and eventual 'drop out' indicates that the best orientation for any target should be near vertical.

The standard error of angle estimates  $\epsilon_\theta$  used as an assessment of goodness of fit. Both methods discussed in the last chapter were implemented and both found to vary from 0.1 to 2 minutes of arc, and increased with non-vertical orientation.

The test data was, for the most part, so noise free that only one or two points out of the total of 99 did not lie directly on the target. These points were easily rejected by large ranges of values for  $S$  and  $\Delta$ . One had only to be careful that for targets at about  $90^\circ$ ,  $\Delta$  not be set to zero. In this case, most of the points lie on  $\bar{X}$ , and  $\sigma_x$  becomes negligible. Thus,  $S\sigma_x$  plays little, if any, part in point rejection and if  $\Delta = 0$ , a point limit of zero would be set into effect. The figure below is a characteristic hard copy output generated by the routine that overlays the regressed line upon actual data. The vertical window is also depicted and in this figure.

#### 7.4 Rotating Straight Line

The same lines used in the fixed case were mounted on a hub capable of being rotated at speeds up to  $90^\circ$  per second. Tests performed indicated that the system could reliably track rotations

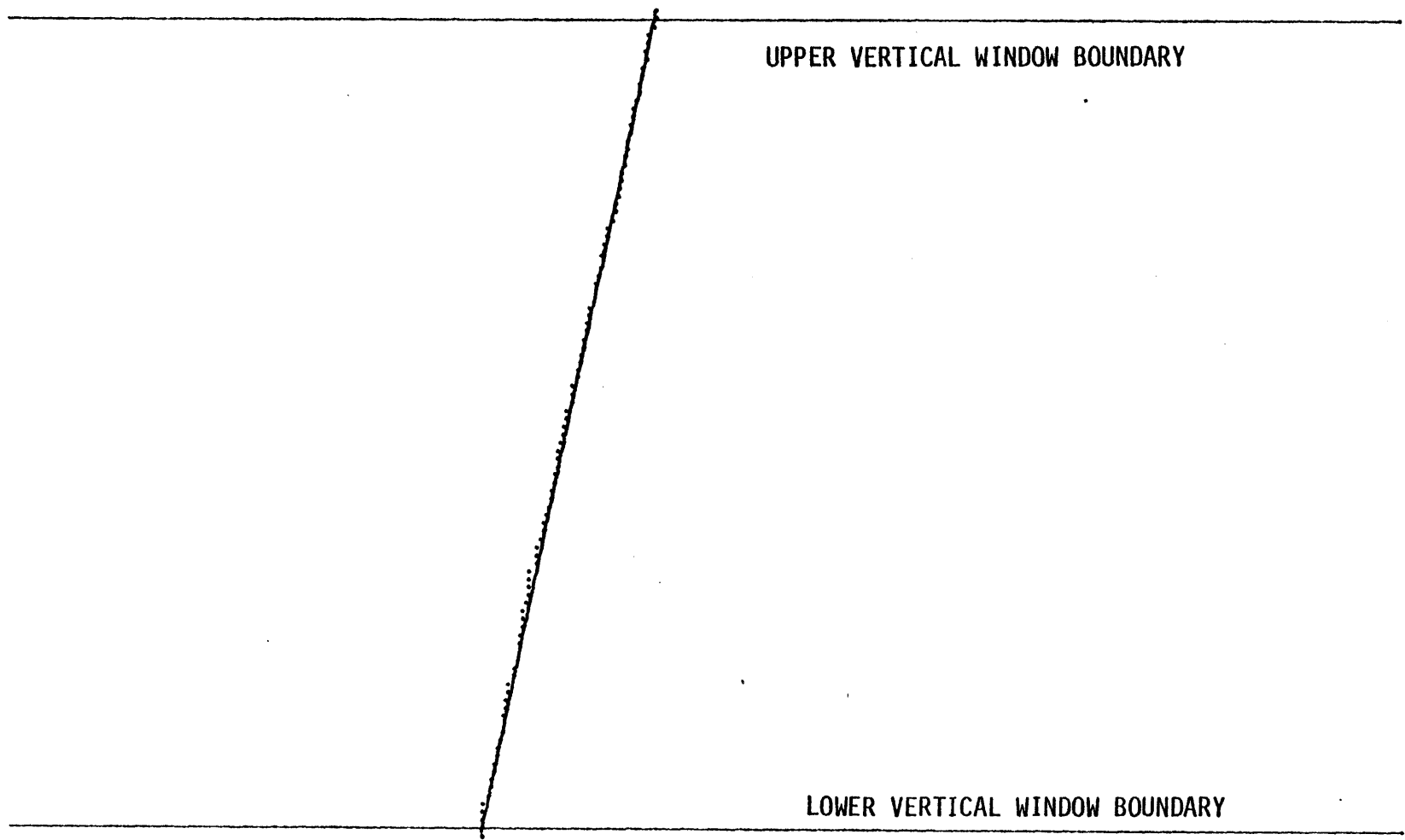


Figure 7.3 Hard copy output of computer routine that overlays regressed line upon actual data

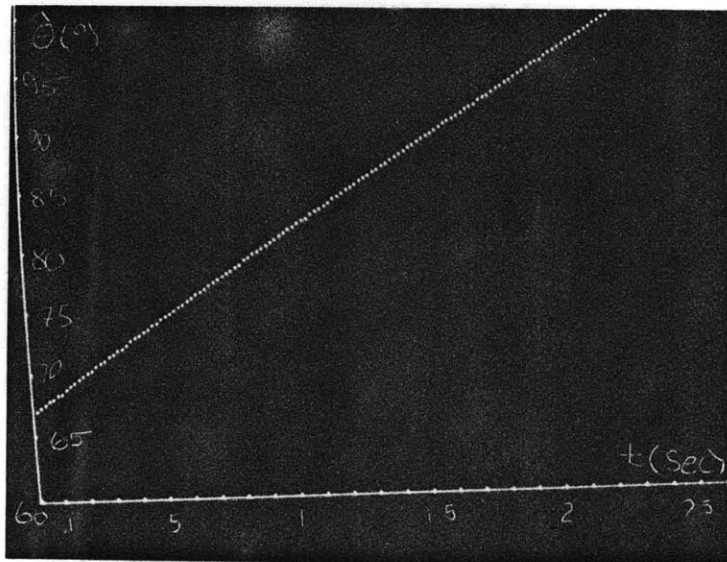
at these velocities. Drop outs occurred, as before, as the line rotated toward horizontal where few points could be deciphered as belonging to a line.  $\sigma_{\hat{\theta}}$  was no longer a valid statistic since the line was rotating and  $\bar{\theta}$  signified only the midrange of rotation.  $\epsilon_{\theta}$  ranged from approximately 1.0 to 5 minutes within regions where analysis could be performed. S values of 0.933 to 2 worked best with  $\Delta$ 's of 5 to 20. The second method of computing  $\epsilon_{\theta}$ , that setting it equal to  $1/(1+b^2) * \epsilon_b$  was used in these tests to avoid problems associated with the nonlinearity of the tangent function. Quite understandably,  $\epsilon_{\theta}$  varied with angle. For, when b increases, the feature is becoming more vertical, more lines are intersecting the target and both  $1/(1+b^2)$  and  $\epsilon_b$  decrease slightly.

The photograph below shows a plot of  $\theta$  versus time for a line rotating  $15^\circ/\text{sec}$ . Abcissal tick marks occur every 0.1 sec and on the ordinate every  $5^\circ$ . One may notice that at 1 second  $\theta$  has indeed increased  $15^\circ$ , 2 seconds  $30^\circ$  and so on.

### 7.5 Subject Contact Lens Mounted Feature

Two subjects were placed in the experimental setup a number of times and both experienced compelling circularvection showing a variety of eye movements. The most important for this work was an apparent rotary nystagmus or jitter overlaid upon a static cyclotorsional shift in eye position. The movements were quite fast but observable on video tape, usually just prior to vection or soon after losing it.

$\epsilon_{\theta}$  for regression in contact lens features ranged from 7 to 20 minutes of arc. Larger values representing noisier signals with a number



Photograph 7.1 Orientation angle versus time, plot for a line rotating at  $15^\circ/\text{sec}$

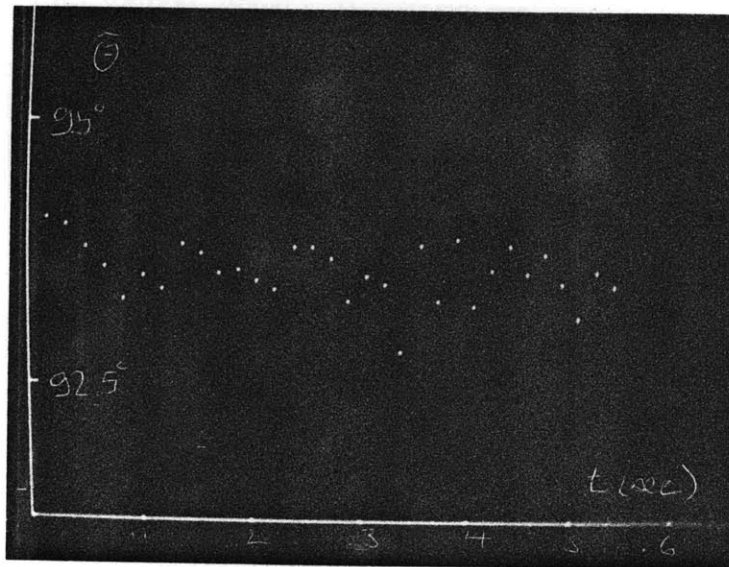


Figure 7.2 Eye angle versus time plot of what may be OCR or torsional saccades.

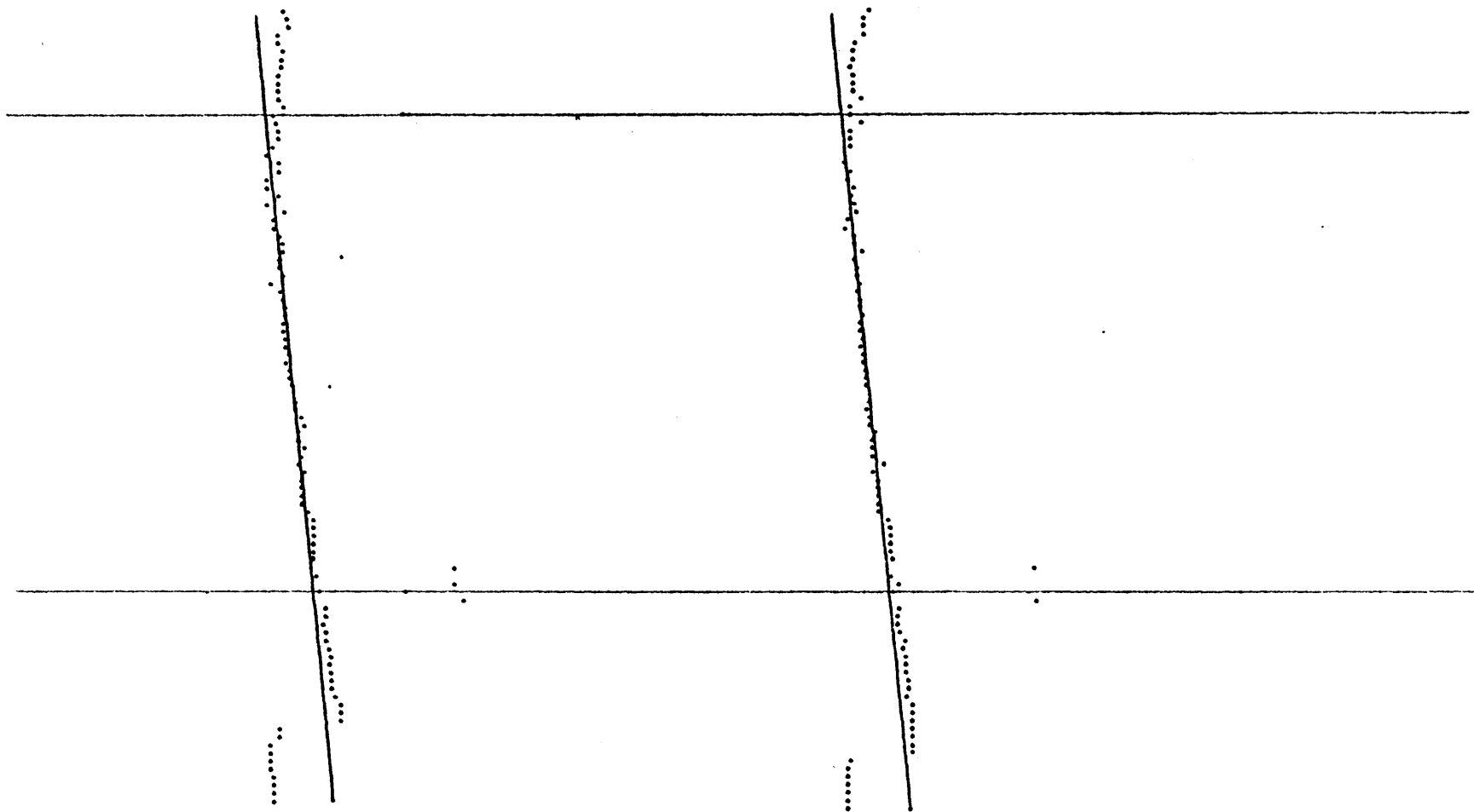


Figure 7.4 Two overlays of fitted lines to data extracted from contact lens mounted features.

of outlying points and variations along the detected line. A  $\Delta$  of 5 was usually used with values of  $S$  ranging from 0.933 to 2 and together with two iterations provided the best answer in most cases. It is not clear at this time what affects small values of  $S$  have. If  $S$  is set to less than 1, artificial biasing of the fit may occur. Further study of the effect of variations in these parameters must be done. A regressed line-data overlay is provided as an example of the fit in Figure 7.4.

Photograph 7.2, of eye angle versus time, seems to show saccadic movements, 1.5 to 2 degrees in magnitude at a frequency of 10 Hz. These movements, as noted, were observed on video tape as jerky rotary eye movements. Though, it is not clear that they represent ocular counter-rolling in the strict sense of the word, they do fall within the wide range of frequencies and magnitudes reported from previous experiments. A summary of the discussion in Chapter 3 is repeated here to highlight the variation.

Robinson (1963) irrigated the ear with water at 47°C to calorically stimulate almost a degree of torsional saccades rotating half a degree per second. Martin (1964) invoked 5 minute 3 Hz nystagmoid motions through vestibular caloric stimulation. Melvill Jones (1964) brought an airplane into aerodynamic spin to elicit 10° roll saccades at 2 Hz. More recently, Galoygan et al (1973, 1976) found 0.5-8.0° of OCR at velocities ranging from 100 to 200°/sec by using both head tilt and galvanic and caloric inner ear stimulation.

Thus, large variations in observations of dynamic OCR have been recorded in the photographs of eye angle versus time fit within the range of these values. The observed 1 to 2 degrees in magnitude

closely follows Finke and Held's (1978) observation of visually induced static torsional nystagmus. The 10 Hz frequency may seem a bit fast but extrapolation of Galoygan results yield a range of 12.5 to 400 Hz. Nonetheless, it is hoped that further investigations will verify the finding of this work. It is important that more rigid and secure experimental apparatus be used along with implementation of a number of other suggestions presented in Chapter 8. Yet, what is clear is that significant components of roll nystagmus may very well be found at frequencies higher than 10 or 15 Hz. The most commonly used torsional measurements accomplished through extensions of Miller's photographic technique have, at best, a 5 Hz bandwidth. Thus, serious consideration should be given to reassessing existing practices.

#### 7.6 Summary of System Performance

A minimum resolvable angle of better than 6 minutes was observed in analysis of abstract targets. Accuracy tests indicated a maximum of 20' for contact lens images and minimum of .1' for a fixed straight line. (See Table 7.1) Student's t-test for 64 to 90 points on a line provided an average confidence interval of approximately half a degree with 99% confidence. Finally, system stability of 1' - 5' was observed for analysis of 190 sequential fields of a fixed line target. In addition, no difference was noted in the analysis of the same numerical data. That is, once the data was collected, the same analytical parameters yielded the same results on any run of the analysis routines.



Minimum Resolvable Angle      <math>0.1^\circ</math> (6' of arc)

	$\sigma_{\theta}$	$\epsilon_{\theta}$
FIXED LINE	1-5'	1-2' of arc
ROTATING LINE	-	1-5'
CONTACT LENS FEATURE	-	7-20'

Table 7.1 Summary of System Performance

### 7.7 Contact Lens

The second aspect of this work was the development of a contact lens mounted feature. As described above, numerous objects were used as tracking targets before they were replaced by thin human hair. This feature provides a high constant image against the brightened pupil. The lens adheres on the average of 20 to 30 minutes after initial placement in the eye. Excessive tearing or blinking may cause the adherence to the eye to decrease, but at all times the lens sandwich remained intact. Further, the lens can easily be reattached by administering a few drops of distilled water.

The bottom lens of the sandwich can become slightly dried out on occasion. This leads to a slight puckering of the lens and greater adherence in a few spots. These spots appear as dark images to the video system but are easily eliminated by a voluntary blink. This last action smooths out the lens somewhat and refreshes it with tears. At the same time, however, it may decrease the duration of adherence. Ongoing research into a single lens molded about a dark fiber is expected to alleviate it, not eliminate this problem. Further details on this are in the next chapter.

In general, the lenses are easy to handle and quite tolerable to wear. Both subjects participated in experiments after wearing the lenses for the first time though neither had worn contact lenses before. One subject became quite adroit at inserting and removing the lenses by himself. It is, however, recommended that a second person aid in placement to assure proper alignment. A further modification, as discussed in Chapter 8, will allow for quick assessment of the contact lens feature orientation.

## 7.8 Comparison of Technique with Previous Methods

Table 3.1 summarizes some of the representative techniques for measuring OCR as discussed in Chapter 3. Three major concerns are used as points of focus, including: sampling rate or for continuous systems bandwidth; accuracy, which in some cases was reported as a noise level; and ease and safety of operation. This last category should not be overlooked, for in many ways it may affect the results and analysis. Schemes that require extremely precise optical alignment are not acceptable. Furthermore, though Robinson, Matin and Yamada provide a real time readout, their use of mirrors and coils in contact lenses poses safety problems. They all also require topical anesthesia.

All methods but the two reported by Fluor which rely most heavily on human observation of direct eye movements have an accuracy of a degree or less. Photographic techniques suffer because of length of time from experiment to results. Film must not only be processed but analysed frame-by-frame. In addition, the maximum sampling rate of 10 Hz may miss the fast eye movements such as rotatory nystagmus. Melvill Jones 64 Hz cine-photographic scheme expands the rate but still requires frame-by-frame correlation and even at that suffers from an accuracy of  $\pm 1^\circ$ .

In summation, the two major developments of this research, the VSP (hardware) - data analysis (software) electronic processing and the soft contact lens mounted feature establish this work as a viable alternative to existing techniques for measuring eye movements. The

use of a video camera provides a 60 Hz data rate, and the option of electronic processing circumvents the time, limitations and errors associated with manual alignments by utilization of many points per field. In addition, the system may be used to track a number of eye movements and adopted to other areas of scientific research.

Furthermore, the feasibility of a real time dedicated device of this nature has been illustrated.

Secondly, a soft contact lens has been developed that not only does not require topical anesthesia but is also safe and easy to use and readily adaptable to other systems.

## CHAPTER 8

## SUGGESTIONS FOR FUTURE INVESTIGATIONS

A prototype model of an instrument capable of monitoring torsional eye movements has been built. Many aspects of the project are open for improvement. In the following discussion, I have detailed some of the more promising ones.

Aside from the verification of results and further study into matters such as analysis control parameters, the most critical problems arise because of timing constraints of the PDP 11/34. Upgrading of the present computer with, for example, DMA interface to the unibus may be considered. However, it is hoped that eventually a stand-alone unit will be developed. This might require more sophisticated digital hardware or may involve the use of a microprocessor. If the remainder of the system simplifications and suggestions are implemented, it is possible that such a device could be built.

### 8.1 Monitoring Other Eye Movements and Head Immobilization

This video method is not limited to tracking ocular cycloverision alone. It can, in its present form, monitor other types of eye movements. Vertical and horizontal nystagmus are two important measures of vestibular function which can be observed. The regression

yields a center of gravity (the first moment) as a pair,  $\bar{X} \bar{Y}$ , as well as A the X intercept. Preliminary tests have shown the horizontal translation may be observed by noting the change of A or  $\bar{X}$  with time and vertical nystagmus by tracking  $\bar{Y}$ . No data is currently available but these movements, slower than rotatory nystagmus, most assuredly may be traced by the system. One must, however, assure that the center of moment is indeed the feature's center of rotation. This can be accomplished by allowing the entire line to fall within the vertical window.

As noted in Chapter 4, data variability can be decreased by aligning the light, camera and beam splitter precisely, as well as securing them properly. In this work, a wooden pallet was used as a base on which to mount the key equipment components. However, future research should utilize a straight metal slab or table. Mountings should be secure and rigid in addition to adjustable. It is anticipated that this will lead to more accurate measurements.

As a second step, one might deal with a better means of immobilizing the head. Subjects tend to perform compensatory postural or head movements with the onset of vection. A bite board was used along with a standard three pressure point head rest but this did not provide sufficient support. Furthermore, the subject was forced to stand leaning somewhat forward into the rest, which not only provided tactile and proprioceptive cues, but also was somewhat tiring.

A new apparatus should be built around the more stable equipment mounting mentioned above. Fiduciary marks, such as a line or series of dots held constant with respect to the head, in front of the eye, may allow less severe head restraint. Lichtenberg (1979) used these marks successfully in photographic OCR measurements. He connected an aluminum extension with two block dots to a bite board. The dots, immobile with respect to the skull, rested just below the bottom eye lid and provided two constant features for sighting in analysis.

A swing or bench may allow the subject to sit comfortably and at the same time may remove motion cues received through the feet or from perception of lean.

## 8.2 Enhancing Feature Extraction

Currently the VSP-computer interface as controlled by the DEC Lab Peripheral System allows for a transfer of one set of coordinates every other scan line. Several means may be used to increase the data flow and thereby better demarcate the contact lens feature. One may consider the purchase of a Direct Memory Address (DMA) unibus interface or the implementation of interrupt control. Ultimately, however, one would like to circumvent the LPS and refer to each of the VSP coordinate registers as memory location. If this could be done tremendous overhead could be avoided. Secondly, the number of these locations may be compacted by applying to the higher order bits on the digital input lines. Since there are at most 12 bits of X data and 8 of Y these two signals may be placed at bits 13 and 14. In this manner, they will always be available for examination.

As an aside, it is advised that the cable be rewired. It is now a single cable of 13 twisted pairs of wire. Some data lines are thus wrapped about each other. Two cables should be wired, one input and one output, and each data line should have a ground line as its twisted mate. Another means of increasing the integrity of the feature extraction is to sample fewer lines but more points per line. Since only one coordinate may be selected for each collection, some bad data may be accepted to the exclusion of desirable points. A more sophisticated transfer routine would collect many points along a line and then select which of these points fit on the feature.

### 8.3 Real Time Evaluation of Eye Position

An important aspect of this work is that it is adaptable for real time implementation. Since two iterations after the first analysis pass yield the same results as 10, 20 or 50 additional passes, extensive iterations appear to be unnecessary. Thus, analysis may be done by a smaller dedicated processor such as an LSI-11. Certain software tasks may be performed within the hardware. Vertical windowing can be accomplished by delaying the scan a specified number of lines. In short, it is quite possible to free the Man Vehicle Laboratory PDP 11/34 to operate on more important tasks such as the control of other



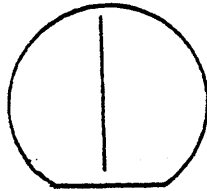
devices. In this manner, the VSP system may be used with a number of ongoing MVL experiments requiring eye movement monitoring.

#### 8.4 Contact Lens Implementation

In the course of our work, Dr. Cavallerano and I have been using the lens sandwich described in Chapter 4. This has worked quite well, yet two final extensions of this work may enable use of this both in eye movement research and in vision correction. The first extension involves the molding of a fine hair or wire into the lens itself. This would do away with the bulk and multiple layers associated with the sandwich and allow for repetitive alignment of the feature in the same orientation for each subjects' lens. Indications are that standard molding techniques could possibly be directly modified to accomplish this. This would also permit the addition of another line feature that would allow more veridical discrimination of torsional movements from translational displacements. The second target might form an L with the first lens. Furthermore, objects previously used in other eye monitoring schemes may be embedded within the SOFLENS, including the Robinson search coil (Robinson, 1963), the Collewijn ring (Collewijn et al, 1965), and the Ish-Shalom ferromagnetic ring (Ish-Shalom, 1978). These modifications will make the lens

a permanent research tool, far less expensive, far easier to handle, and more sanitary than existing contact lens mounted features.

Dr. Cavallerano has suggested truncating or cutting off the bottom of a molded lens with a vertically oriented feature. This would greatly aid in aligning the nearly invisible feature on the eye.



The second extension follows this lead into the field of vision correction. This, first proposed in my bachelor's thesis, involves molding a hard contact lens within soft contact lens material. The advantage of hard lenses, visual acuity and correction of astigmatism, would be provided without the associated irritation of standard hard lenses. Recent innovations with gas permeable lenses may also be taken advantage of.

## 8.5 Higher Order Fit

Current techniques fit the data outlining a target with a linear regression fit of the form  $X = A + BY$ . The contact lens feature, however, has an apparent curvature which increases in radius as it is displaced from the central meridian of the eye. That is, when the target is aligned across the camera's axis of scan, it will look nearly linear, but as it moves across the eye it will appear increasingly curved. A higher order of fit can be used. One must first assess how the angle will be extracted from this regression. It may be the case that the first order fit and computation tangent to a higher order fit are equivalent. Secondly, such implementation may pose limitations on a real time analysis.

### 8.5.1 Regression Coefficients and Statistical Parameters for $n^{\text{th}}$ Order Polynomial Fit

The implementation of a higher order regression is of no major problem. Standard statistical techniques exist for fitting curves of all types to data. Polynomial regressions extend the basics of linear regression to the  $n^{\text{th}}$  order. A power series polynomial, such as  $X = A + BY + CY^2 + \dots + MY^n$  can be most effective in reconstructing curved data.

In this case, one would simply expand to  $n + 1$  simultaneous equations for  $n + 1$  coefficients in the following manner.

$$\Delta = \begin{vmatrix} N & \Sigma y_i & \Sigma y_i^2 & \dots \\ \Sigma y_i & \Sigma y_i^2 & \Sigma y_i^3 & \dots \\ \Sigma y_i^2 & \Sigma y_i^3 & \dots & \dots \\ \dots & \dots & \dots & \dots \end{vmatrix}$$

$$a = \frac{1}{\Delta} \begin{vmatrix} \Sigma y_i & \Sigma y_i & \dots \\ \Sigma x_i y_i & \Sigma y_i^2 & \dots \\ \Sigma y_i^2 x_i & \dots & \dots \\ \dots & \dots & \dots \end{vmatrix}$$

$$b = \frac{1}{\Delta} \begin{vmatrix} N & \Sigma x_i & \dots \\ \Sigma y_i & \Sigma y_i x_i & \dots \\ \Sigma y_i^2 & \Sigma y_i^2 x_i & \dots \\ \dots & \dots & \dots \end{vmatrix}$$

and so on, replacing the  $j^{\text{th}}$  column in  $\Delta$  with the first column in  $a$  to achieve the  $j^{\text{th}}$  coefficient. The experimental standard error of estimate remains

$$S = \sqrt{\frac{1}{N-n-1} \sum [X_{\text{actual}} - X_{\text{predicted}}]^2}$$

where  $N-n-1$  is the number of degrees of freedom  $\nu$  for a fit of a polynomial of degree  $n$ , to a set of  $N$  data points. (Recall the linear case where  $n=1$  and  $\nu=N-2$ . See also Bevington(1969).)

### 8.5.2 Slope Determination

A critical consideration for implementation of a higher order fit is the extraction of an angle for the curve. For first order regressions where  $X=A+BY$ ,  $\frac{dx}{dy}=B$ . But, as the degree of the polynomial increases the slope does too, and  $\frac{dx}{dy} = B+CY+\dots+MNY^{N-1}$ , including not only higher order terms but a dependence upon a specific  $y$  value as well. The question must be raised whether, in any event, the linear regression does not provide a more suitable value for the slope. Currently, it has only been established that within certain bounds a linear fit is reasonable. There are however, limitations; mainly that the lens mounted feature be close to the center of the eye where the data will appear primarily linear. It has been found that even in the most eccentric cases it is possible to utilize the linear fit by excluding the endpoints from analysis as illustrated in the figure below.

### 8.6 Polar Mapping

One may desire to leave the Cartesian coordinate system altogether and attempt analysis of rotational movements in polar coordinates. The distribution of points along a certain vector magnitude or angle may be an effective means of assessing line orientation or torsional shift.

Duda and Hart (1973) describe a number of means of  $\rho, \theta$  mappings.

### 8.7 Further Rejection

The statistics generated by the regression analysis provides valuable insight into the variability of the data and the accuracy or goodness of the fit. Large values of  $\hat{\sigma}_{\theta}$  and  $\epsilon_{\theta}$  may signify that a certain field is of questionable reliability. This, then, may be used as a criteria for rejecting fields altogether or assigning a weighting of significance to an estimate of a specific angle.

### 8.8 Phase Lock Loop on Horizontal Clock

The 10 MHz horizontal data sampling clock is initiated at the start of every horizontal line. There may be a slight discrepancy from scan line to scan line, thus, one might introduce a phase lock loop to synchronize all line rates. This will add to data integrity and may reduce  $\hat{\sigma}_{\theta}$  and  $\epsilon_{\theta}$ .

### 8.9 Increased Magnification

Increased magnification may fill the entire video field with the pupil alone or just that portion of the pupil containing the feature and the locus of its excursion. While, this would increase expected resolution, it will also require rigid head restraint, for head movements will pull the eye out of the camera view.

## APPENDIX A

## System Users Guide

Four operations are required to monitor eye movements and to perform the necessary data analysis as well as evaluation of this analysis. The following pages contain step-by-step discussion of the experiment, computer data collection, data analysis and analysis evaluation. A number of examples are provided where appropriate.

### I. Experimental Set Up

The computer programs that analyze the eye movements require positional coordinates of a target. Thus, as noted in the recommendations for further work, this system may be used for a variety of applications. This section deals with what form a rotating target such as a contact lens mounted object should take to be converted to such positional information and how the user may conclude if the desired feature is accepted.

#### I.1 Video Signal Processor

The signal processor will accept any video compatible signal of any image and detect transitions that rise above a certain voltage threshold. The coordinates of the first four transitions are stored and upon computer request sent for data storage along with their scan line. This section discusses the workings of the VSP. The user must only deal with: the video input, output and highlighted output signals; the threshold

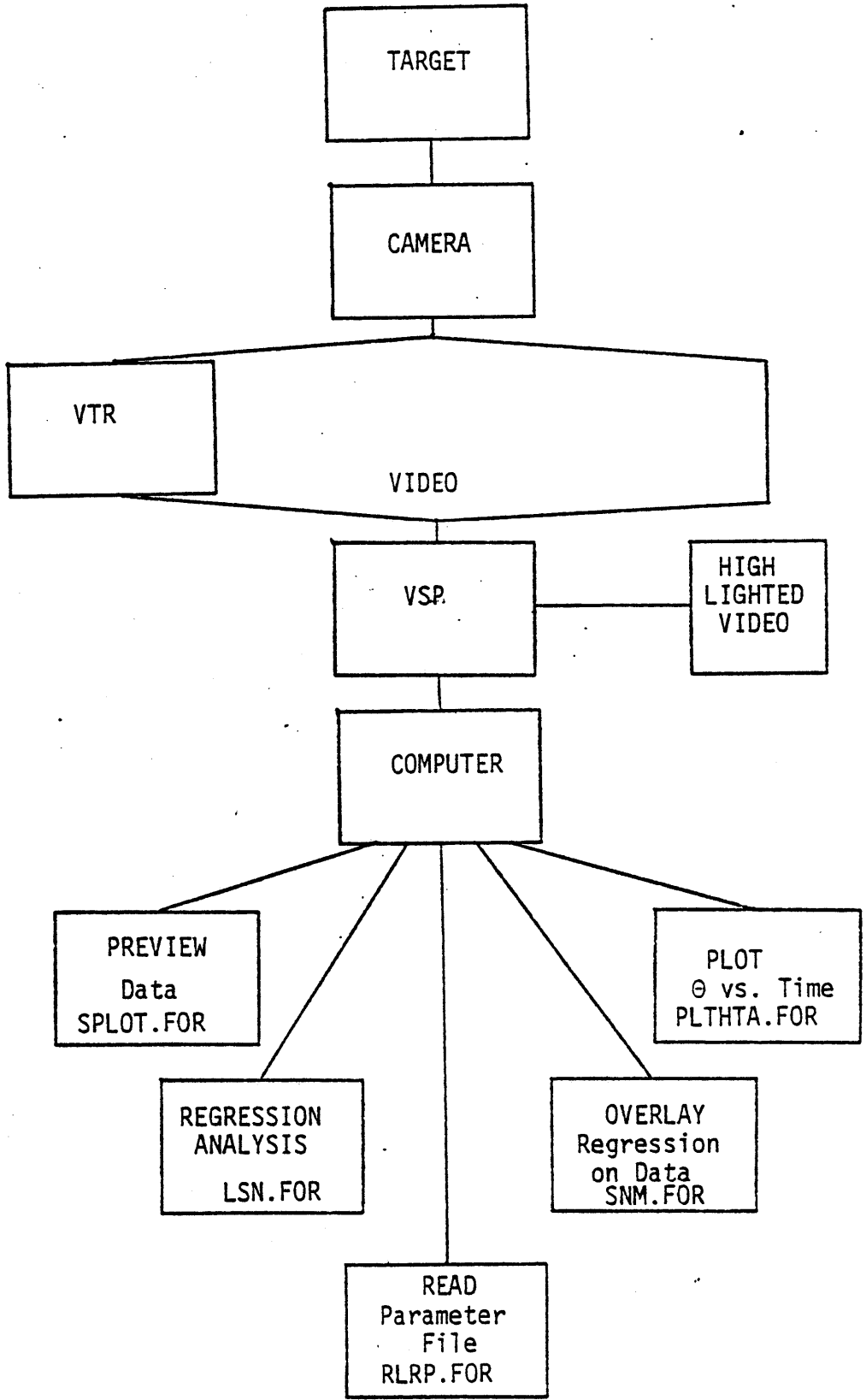
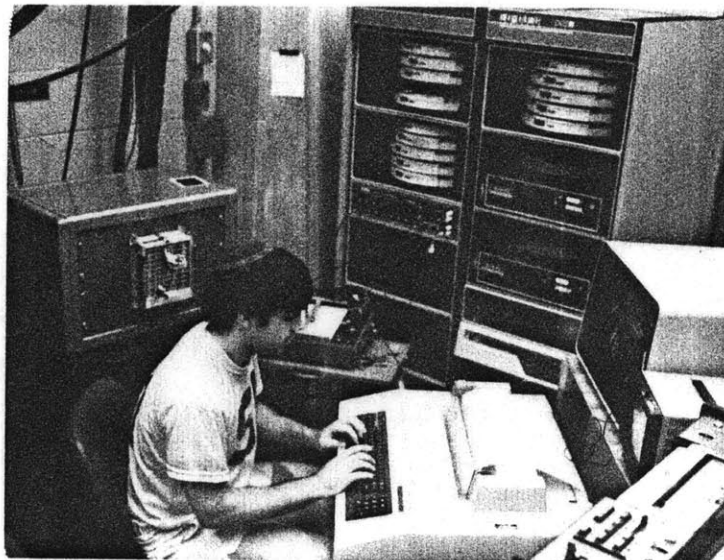
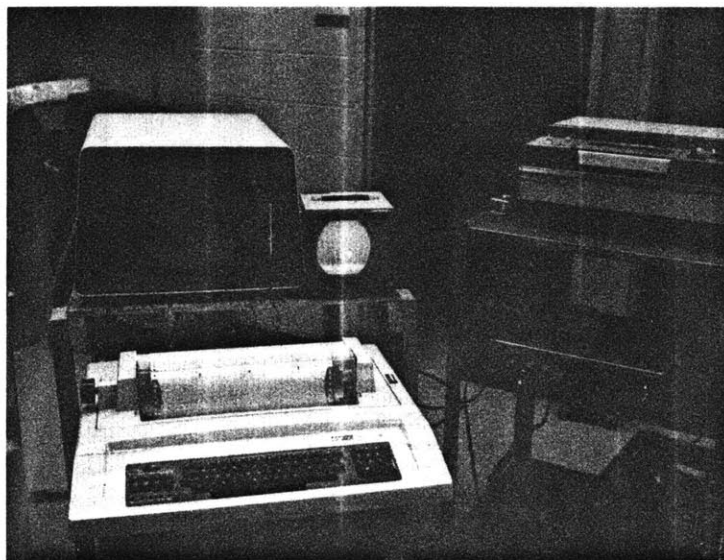


Figure A.1 System Options





Photograph A.1 User, computer, plotter, etc.



Photograph A.2 Front view of setup. Note: VSP and VTR on cart, monitor displaying VSP highlighted output.

adjustment; vertical window alignment; and computer digital output and input control.

### I.1.1 Video Input, Output, Highlighted Video

A video camera or tape recorded video image may be used as input to the VSP. For that matter, any video signal may be analyzed. The middle of the three UHF jacks on the VSP front panel is for video input. It may be tapped at the output, jack 1, for monitoring of the direct image. This signal is analyzed and then presented to the computer for analysis in digital form. A potentiometer controlled voltage divider provides a threshold for the direction circuitry. This pot appears on the front panel between the on-off switch and the video jacks. Its operation raises and lowers the threshold and its effect can be noted by viewing the highlighted video output. The highlighted video signal is an overlay of the computer output upon the video image. When an image is detected by the VSP within the horizontal video window, a corresponding "very white" signal appears on the highlighted video image. In this manner, a full field image of the passed and rejected features are presented to the user. If the signal is acceptable, data collection and disk storage can be initiated. If not, the threshold may need to be adjusted or the window realigned.

The window is designed to limit the extent of the video image presented to the detection circuit. It is set by two monostable multivibrators with adjustable time constants, set by potentiometers. These pots lie on the digital circuitry board and are

readily accessible. The affect of their adjustment may also be noted within the highlighted image by turning the threshold way down leaving the part of the lines within the video gate whitered.

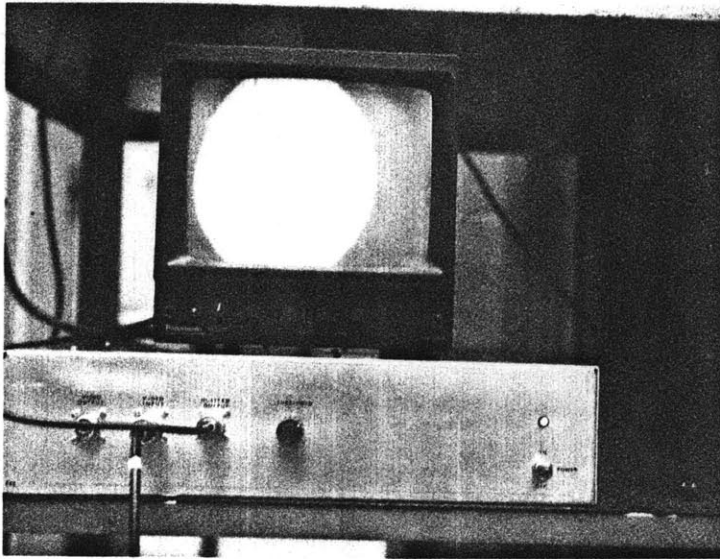
Two 25 pin jacks on the back panel accept the digital input and output lines from the computer. These lines run from the back of the PDP 11/34 Lab Peripheral System (LPS) carrying synchronizing information and data.

When the user has decided that the desired feature lies within the video window and the threshold is properly set, collection and data storage may begin.

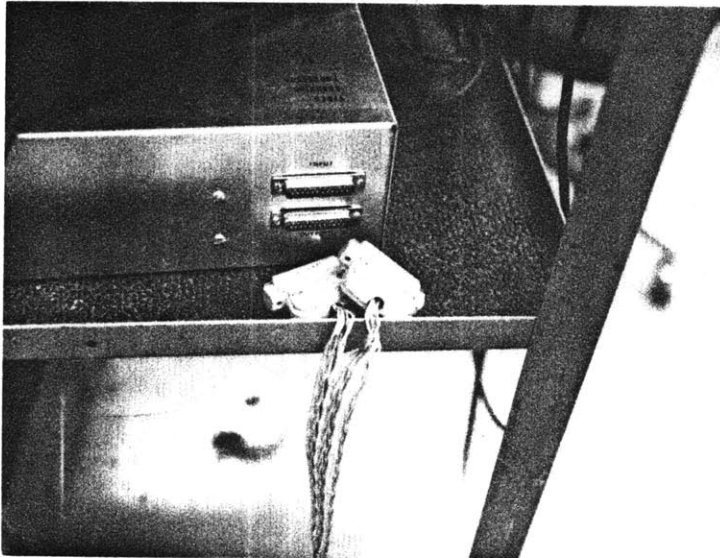
## II. Computer Data Collection

Currently, data is collected every other line on every field. This represents an effective 12 KHz data rate. As discussed in Chapter 3, limitations on the computer allowed for collection of only one horizontal coordinate and a vertical scan line. The video signal processor has provisions for selecting up to four hits along any line. The user must decide which of the four to choose. Four separate computer data collection programs are available: X0M, X1M, X2M, X3M, one for each point. Each program is a self-contained assembly language routine requiring no user input other than the RUN command. They were written for speed and utilize the double buffer technique discussed in Chapter 3. Data is written into X\_M.DAT data files which may be renamed later if they are to be saved.

The first few lines of the program contain the number of lines to be scanned per field, the number of fields to be placed in a buffer and



Photograph A.3 Highlighted video displayed on video monitor. (Note, front panel)



Photograph A.4 Cable and jacks of VSP panel. Power cord receptacle on opposite side not shown.

the number of passes to be made through the double buffering scheme. The first two numbers indicate the buffer length at

$$BL = \frac{\text{number of lines}}{\text{field}} * \frac{\text{number of fields}}{\text{buffer}}$$

If they are changed, the buffer length designated in the WRITE statements and the dimension statements at the program end must be modified as well.

It should be noted that a disk block expects to be a multiple of 256 words. Even if each field does not contain 256 words, it is essential that each buffer be a multiple of this number. Currently, there are 200 words per field. This includes: a field counter, a field terminator marker (a-1), and a horizontal and vertical coordinate for the 99 lines scanned. At 32 fields per buffer, this data will occupy 25 disk blocks.

The number of passes allows for specification of repetitive collection. Each pass accepts 64 fields or 1.066 seconds of data and places this into 50 blocks. Thus, 6.4 seconds occupies 300 blocks and the entire 1.2 Mword RK05 disk will be filled with approximately 2.7 minutes of data in 80 passes.

If these numbers are to be altered, a batch file X\_M.BAT contains the necessary code to recompile and link the edited version.

In short, when the user has decided that the video signal processor in extracting the target in the best manner, he need only run one of four collection routines and the data will be recorded in a corresponding data file.

### III. Data Preview

A quick illustration of the quality of the data that has been collected can be seen by running PRVW. This program generates and plots x,y pairs from the data as well as listing their values. Any field within the file may be examined upon specification of the user. In this manner, noisy or faulty data will stand out clearly and another collection of data can be initiated before any data analysis has been started. A hard copy output of the data points may be printed on the x,y plotter. A sample run is provided along with an example of the output.

.R RLRP

ENTER FILENAME:\*DK1:PE1

NF	Top	Bot	S	Del	<Theta>	S.D.	<SE>
190	45.	211.	0.933	5.000	91.875	20.073	12.51

#Fld	#Pts	A	AU	B	BU	Theta	SDM
1.	80.	145.880	216.279	0.039	0.058	92.256	13.734
2.	78.	145.842	216.223	0.039	0.057	92.212	13.622
3.	77.	145.831	216.206	0.036	0.053	92.043	14.493
4.	76.	145.615	215.886	0.033	0.049	91.896	12.877
5.	68.	146.336	216.954	0.029	0.043	91.656	15.025
6.	79.	146.208	216.766	0.032	0.048	91.839	11.766
7.	77.	146.641	217.406	0.030	0.045	91.739	14.124
8.	79.	145.881	216.280	0.036	0.054	92.084	12.886
9.	71.	145.655	215.945	0.035	0.052	92.019	15.352
10.	72.	145.851	216.236	0.033	0.049	91.875	12.584
11.	77.	145.422	215.600	0.033	0.049	91.903	12.576
12.	79.	145.273	215.378	0.032	0.047	91.821	13.065
13.	77.	145.363	215.512	0.031	0.046	91.759	12.778
14.	66.	144.916	214.850	0.036	0.054	92.088	13.839
15.	77.	145.405	215.575	0.037	0.054	92.093	12.987
16.	73.	145.669	215.966	0.035	0.052	92.009	14.627
17.	75.	145.967	216.408	0.029	0.044	91.686	11.977
18.	74.	144.828	214.719	0.033	0.049	91.884	12.892
19.	74.	144.681	214.501	0.032	0.047	91.822	14.727
20.	72.	146.311	216.918	0.023	0.034	91.306	13.336
21.	72.	145.346	215.487	0.037	0.055	92.135	14.190
22.	73.	147.124	218.122	0.030	0.044	91.711	10.889
23.	72.	146.103	216.609	0.038	0.057	92.193	15.911

PAUSE -- To continue hit RETURN

#Fld	#Pts	A	AU	B	BU	Theta	SDM
24.	74.	146.855	217.724	0.029	0.044	91.682	13.532
25.	75.	146.109	216.618	0.034	0.051	91.964	11.987
26.	75.	145.295	215.412	0.038	0.056	92.162	14.356

.R SP

116

Enter data filename:\*DK1:E4

0

Hard Copy?(Y or N):Y

PAUSE -- -If plotter set hit RETURN-

PAUSE -- ZERO PLOTTER NOW, THEN HIT CR

Enter Y to replot:N

Hit <RETURN> to see next set of points, or  
enter E to exit, S if you want to set NREC yourself:S

Enter NREC:56

55

Hard Copy?(Y or N):N

Hit <RETURN> to see next set of points, or  
enter E to exit, S if you want to set NREC yourself:

56

Hard Copy?(Y or N):Y

PAUSE -- -If plotter set hit RETURN-

PAUSE -- ZERO PLOTTER NOW, THEN HIT CR

Enter Y to replot: Y

PAUSE -- -If plotter set hit RETURN-

PAUSE -- ZERO PLOTTER NOW, THEN HIT CR

Enter Y to replot:N

Hit <RETURN> to see next set of points, or  
enter E to exit, S if you want to set NREC yourself:E

PAUSE --  
TYPE <CR> TO EXIT



#### IV. Data Analysis

When acceptable data is stored within a data file, an analysis will fit a line to the data and establish an angle for that line. Statistics are generated for the analysis to examine the strength of fit and accuracy of the angle. The latest version of the analysis routine is a program known as LSN. It performs a linear regression on the horizontal data to achieve a  $X = A + BY$  fit. Points that may represent erroneous data are rejected in a number of fashions. The user is expected to interact closely with this program, and in the following sections, the various queries and expected responses are presented, mostly by way of example.

##### .R LSN

Once the program has been initiated, the user is expected to enter the name of the disk file containing the data to be analyzed and the file into which the analysis results will be written.

```
*ENTER DATA filename: DK1:X1M.DAT
```

```
*ENTER PARAMETER datafile: DK1:PX1M.DAT
```

These files are opened, the data file to be read from and the parameter file to be written into. The first field of data is displayed on the screen and a subroutine WINDM is called to set a window about the points.

R LSN

Enter INPUT Filename:\*OK1:E3

Enter OUTPUT Filename:\*OK1:PE3

PAUSE -- -Hit <CR> to display the first set of comparator HITS-

P<RET> will enable Light Pen,(\$<RET> terminates):P

PAUSE -- Position light pen and hit <RETURN>:

Is 15.47 an acceptable boundary?(Y or N):Y

PAUSE -- Position light pen and hit <RETURN>:

Is 196.83 an acceptable boundary?(Y or N):Y

Window between 1 & 90

Are you happy with the window settings.

Y(yes) enters limits, N(no) restarts limit settings.

S(set) allows the user to enter values for ITOP and IBOT:S

Please enter two integers for ITOP and IBOT: 1,890

ITOP or IBOT may not exceed 99 please reenter values: 1,89

Are you happy with the window settings.

Y(yes) enters limits, N(no) restarts limit settings.

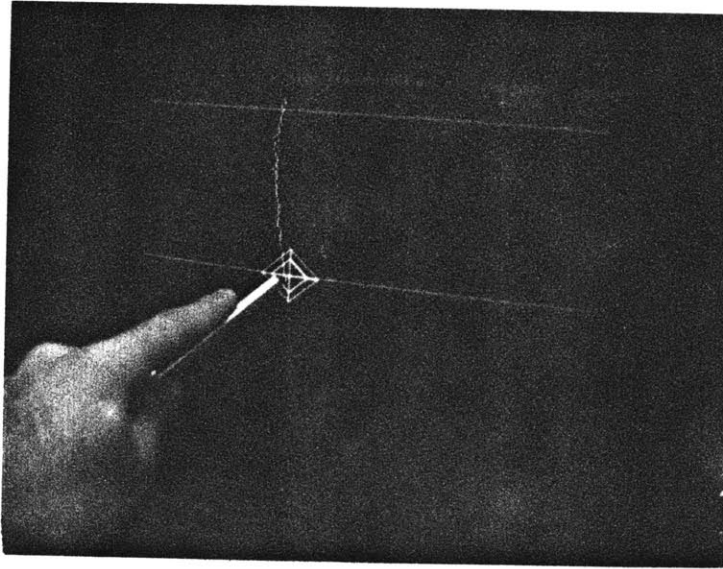
S(set) allows the user to enter values for ITOP and IBOT:Y

89 Points, from line 17. to 195.

Enter NF(#fields),ILSP(#self loops),

RPV(SDX multiplier) and DEL(pt. rej. constant):190,3,.933,5.

PAUSE -- Press <RETURN> to start analysis - -



Photograph A.5 Light pen window definition. Current pen position displayed in upper right hand corner of display terminal.

PAUSE -- Hit <RETURN> for summary information.--

190 fields 2 loops, line 1 to 89  
 had limited excursion of 0.9330 pt. s.d.s + 5.000  
 average slope= 94.68 dars, s.d. from <slope>= 19.790 mins  
 average standard error of angle estimate= 14.247 mins

0 Fields were rejected, including numbers:

<dif>=2.8

Enter a Y to RERUN program, N to EXIT;n  
 PAUSE --  
 TYPE <CR> TO EXIT

Scan lines at the top and bottom of the field are excluded. They represent the parts of the eye with no feature, or just points that are obviously bad. The program requests specification of a window top and bottom and permits this specification by means of a light pen hit upon a particular point or by direct line specification. If the light pen is used, the user sights it upon a point perhaps representing the endpoint of a tracking feature or points slightly above or below it and then signifies that the choice is to be entered. Until this signal is sent, the light pen can be moved about anywhere on the screen and its coordinates displayed to the user at the top of the CRT screen. When a point is entered, it may be reentered before the next is specified. Once both are specified, the program searches the array of data points for the scan line closest to the light pen indication. The lines are drawn on the screen over the points and, if unacceptable, the limits may be reentered by direct specification of two lines or once again through the light pen. The process may be run again and again until the user is satisfied that obviously bad points are excluded and that good data from following fields will not be affected by these limits.

The user must decide how the analysis should be done. A regression is performed that rejects outlying points, i.e. points that lie outside a certain window. This window is determined by adding some multiple of the standard deviation of the horizontal coordinates and a constant value,  $lim = S\sigma_x + \Delta$ . The user is asked to specify  $S$  and  $\Delta$ , as well as the number of fields to be analyzed and the number of iterations on each field. The outlier rejection uses the standard

deviation of the horizontal coordinate ( $\sigma_x$ ) of the previous field for the first pass through a field of data and updates this value upon each iteration.

These values may be determined by the initial preview of the data. Very good data will not be aided by numerous iterations or large windows, while for poor data the reverse may be true. In some cases,  $S$  or  $\Delta$  may be set to zero. Repeated use will give a user the best feel for what these values should be. Chapter 4 discusses some of the selection criteria.

## V. Analysis Evaluation

The final phase of the system is the evaluation of the analysis. The primary means of review is provided by the summary of information at the end of the analysis. The user is left with an immediate indication of what occurred. The entire parameter data file may be read by running RLRP. A printout containing the summary information and the subsequent line by line regressed values appears. These lines include the field number, the number of points evaluated per field, the slopes and intercept, normalized and unnormalized, as well as the angle and its associated error of estimate. In this manner, the user may note whether a field was rejected or a significant number of points found unacceptable. In short, a quick overall assessment of the data can be achieved.

The routine SNM, on the other hand, provides a graphic illustration of the results. It prints out the results within the parameter data file and displays the data along with the window and line fit. Poor fits are immediately evident, good fits are easily recognizable. There, as in S, the user may choose to examine any field within the file, skipping forward or backward at will. It should be noted, however, that there is some distortion due to display screen astigmatism and the line over the points should not be visualized as an absolute indication of goodness of fit. A hard copy output may be requested and plotted with default or user specified scaling parameters.

Finally, the user may plot the data versus time by running PLHTA. This program has a zoom feature which allows for an overall view of all the points over the entire range of angles, 0 to 360 degrees.

A user may ask to see only a part of the points within a few degrees. The axes, lengths, and tick marks are externally scaled. The ordinate ticks are incremented every  $5^\circ$ , and the abscissa incremented every 0.1 second.

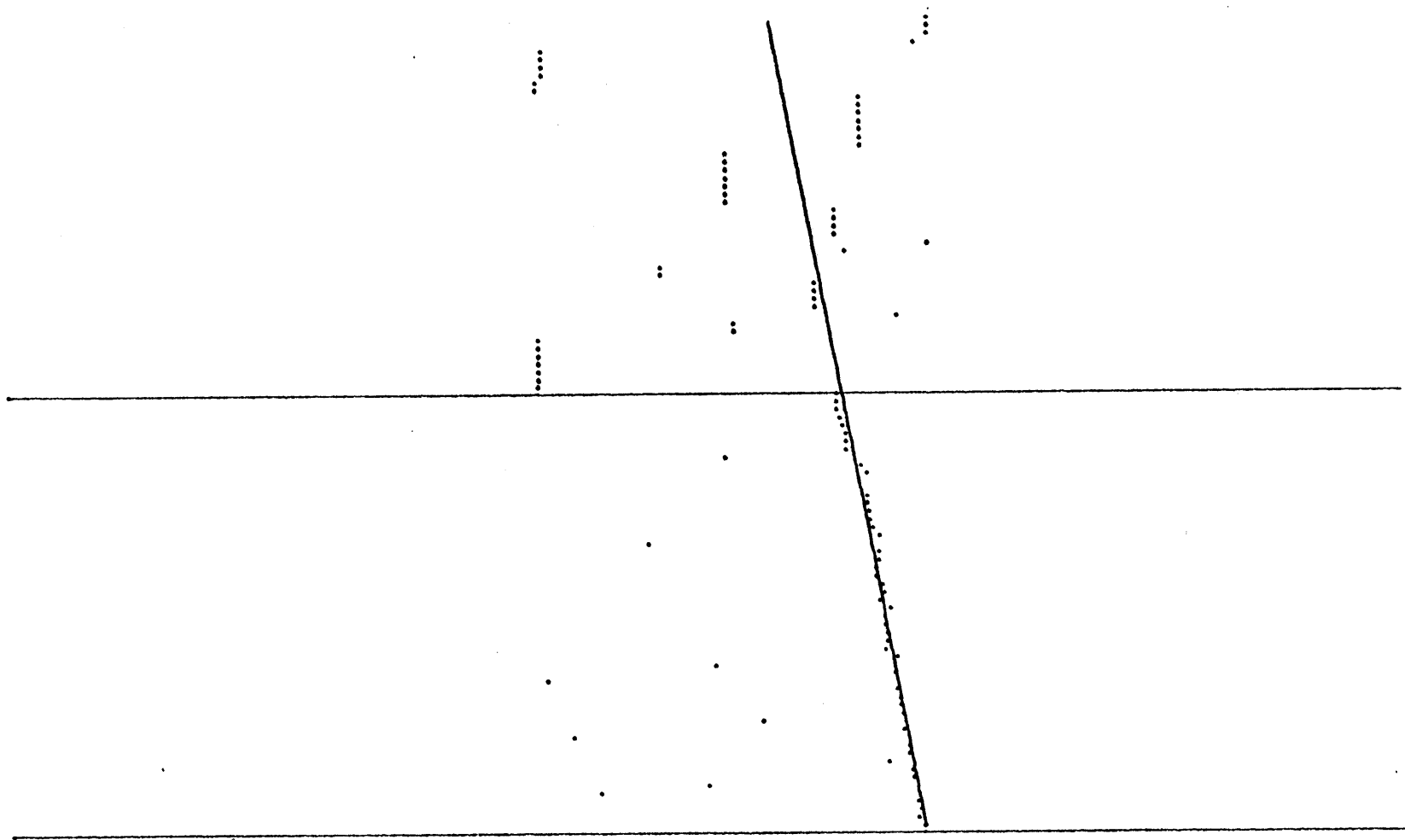


Figure A.2 Overlay of fit to a hair mounted over bottom half of the pupil. Vertical window excluded noise including that found in region of pupil above contact lens feature.



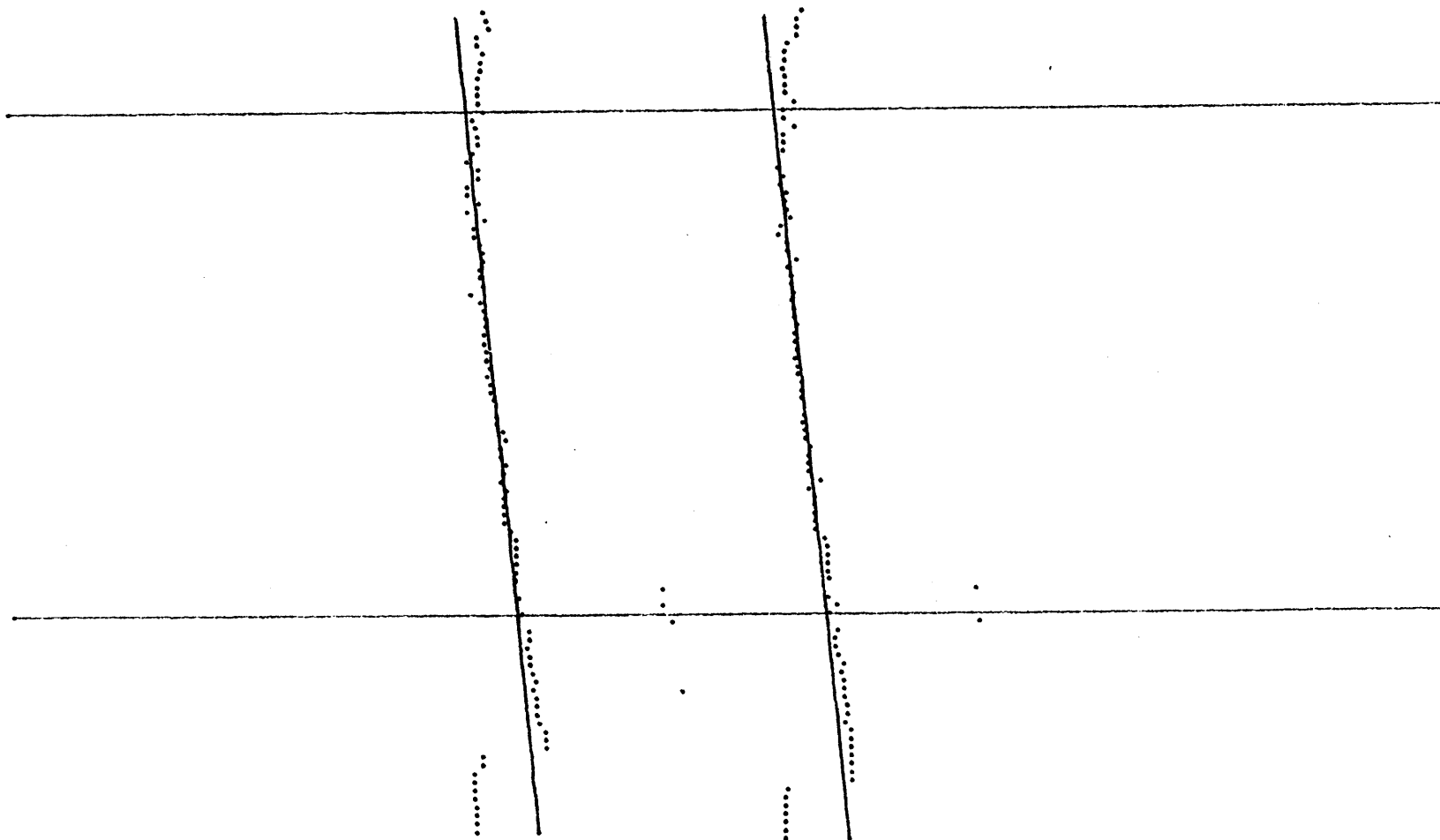


Figure A.3 Overlay of fit to two contact lens features.  
Curvature resulted from positioning of hair adjacent  
to pupil-iris border. Vertical window limited analysis  
to linear region.

.R SNM

Enter data filename:\*DK1:E1

Enter filename containing lin. res. parameters:\*DK1:PE1

This analysis of 190 fields yielded:  
an average slope of 91.875 degs, s.d. 20.07  
average standard error on angle estimate 12.51mins  
rejection window: 0.9330 s.d.s + 5.0000  
1 1 80 145.880 0.039 92.256 13.734  
Hard Copy(Y or N)? N

Hit <RETURN> to see next set of points, or  
enter E to exit, S if you want to set NREC yourself:S

Enter no. fields want to skip(+/-):105

106 106 79 152.089 0.045 92.595 11.324  
Hard Copy(Y or N)? S

Hit <RETURN> to see next set of points, or  
enter E to exit, S if you want to set NREC yourself:S

Enter no. fields want to skip(+/-):-34

72 72 75 144.396 0.027 91.519 13.992  
Hard Copy(Y or N)? Y

Enter D to use Default parameters:D

Amin= 0.00-400.00 Amax= 520.00 38.00 V0= 0.00 0.00  
PAUSE -- ZERO PLOTTER NOW, THEN HIT CR

PAUSE -- ZERO PLOTTER NOW, THEN HIT CR

PAUSE -- ZERO PLOTTER NOW, THEN HIT CR

PAUSE -- ZERO PLOTTER NOW, THEN HIT CR

Type Y to replot(rescale);Y

Enter D to use Default parameters;N

Enter Axmin,Asmin,Axmax,Asmax,Ux0,Uy0;0.,-256.,520.,0.,0.,0.

PAUSE -- ZERO PLOTTER NOW, THEN HIT CR

type Y to replot(rescale);N

Hit <RETURN> to see next set of points,or  
enter E to exit, S if you want to set NREC yourself;E

PAUSE --

TYPE <CR> TO EXIT

.R PLTHTA

Enter data filename:\*DK1:PE1

190 45.00 211.00 0.933 5.000 91.875 20.073 12.5109

Enter YMIN & YMAX,NSF,NEF: 0.,180.,-45,4567

To rerun program type R,then <RETURN>;R

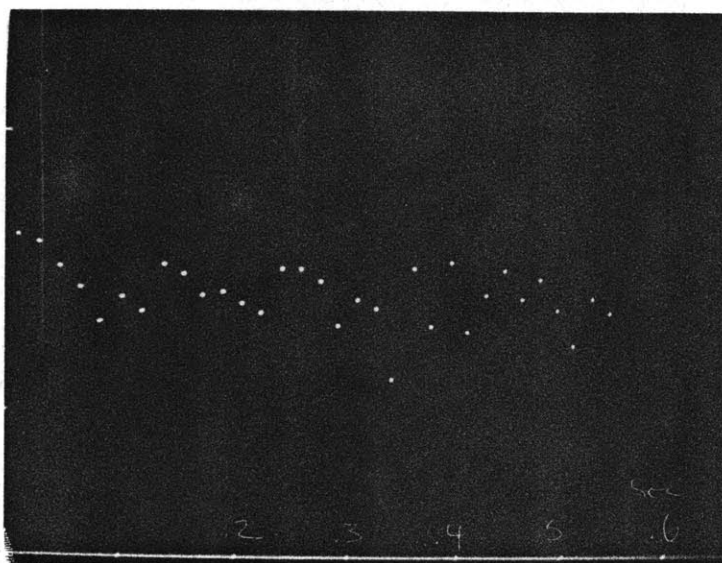
190 45.00 211.00 0.933 5.000 91.875 20.073 12.5109

Enter YMIN & YMAX,NSF,NEF: 85.,95.,0,42

To rerun program type R,then <RETURN>;N

PAUSE --

TYPE <CR> TO EXIT



Photograph A.6 Eye angle versus time plot generated by PLHTA.FOR. Abscissal tick marks of 0.1 sec and ordinatal demarcations of  $2.5^\circ$  are evident along the axes.

## APPENDIX B

This appendix contains listings of the computer code for the routines described above.

1 XIM	MACRO	Synchronizes sampling, controls data transfer from the VSP to the LPS, and, using a dual buffer system and asynchronous writes, places data on RK05 disk.
2 SP(1ot)	FORTTRAN	Displays data on VT-11 CRT for preview and is capable of generating hard copy output.
3 LSN	FORTTRAN	Regression analysis routine.
4 WINDMI	FORTTRAN	Subroutine of LSN used to establish vertical window about data points.
5 RLRP	FORTTRAN	Reads file containing results of regression.
6 SNM	FORTTRAN	Provides overlay display of regressed fit on actual data for each field. Hard copy may be called for.
7 PLTHTA	FORTTRAN	Plots eye angle versus time, zoom feature allows scrutiny of any subset of points.

```

.TITLE X1M
.GLOBL X1M, BUF1, BUF2
.MCALL ..V2,,,WRITE,.EXIT
.MCALL .CLOSE,.ENTER,.FETCH,.QSET
..V2..          ;VERSION II MCALL instructions

```

```

R0=%0          ;Temporary data register
R1=%1          ;block count
R2=%2          ;buffer pointer
R3=%3          ;no. sampled video scan lines/field
R4=%4          ;no. of fields per buffer
R5=%5          ;no. passes through dual buffers
SP=%6
PC=%7

```

```

DGS=170410     ;Digital Status Buffer
DIB=170412     ;Digital Input Buffer
DOB=170414     ;Digital Output Buffer

```

```

NLINES=143     ;look at 99 lines, if start at 17 -> 215
NFLDS=40       ;32 fields/buffer
NPSSSES=3      ;no. fields/(2*no. fields/buffer)

```

```

X1M:  .FETCH #HSPACE,#PGNAM    ;Load device handler

      MOV #NPSSSES,R5
      CLR R1                    ;CLEAR block count register
      .ENTER #EAREA,#1,#PGNAM  ;enter file on channel 1
      .QSET #R1,#5             ;add 5 elements to the I/O queue
                                   ;starting at Q1

LP:   MOV #BUF1,R2              ;load BUF1 pointer
      MOV #NFLDS,R4            ;field/buffer test register

LPP1: MOV FCNT,(R2)+            ;Place frame no. at top of array
      INC FCNT                 ;Increment Frame no.
      MOV #NLINES,R3          ;Load scan line counter register

;Wait for beginning of a field
BOFW1: MOVB #10,@#DOB          ;SELECT BITS OF LS153
      MOVB #30,@#DOB
      MOVB #10,@#DOB
      MOVB @#DIB,R0
      CLR @#DGS
      BIT #100,R0              ;AF bit set?
      BNE BOFW1

BOFW0: MOVB #10,@#DOB
      MOVB #30,@#DOB
      MOVB #10,@#DOB
      MOVB @#DIB,R0
      CLR @#DGS
      BIT #100,R0              ;AF?
      BEQ BOFW0

```

```

        MFPs @#OLDPSW          ;save current interrupt level
        MTPS #7                ;disable interrupts

;Wait for beginning of active line
EOW1:  MOVb #30,@#DOB
        MOVb #10,@#DOB
        MOVb @#DIB,R0
        CLR @#DGS
        BIT #200,R0          ;AL bit set?
        BEQ EOW1

EOW0:  MOVb #30,@#DOB
        MOVb #10,@#DOB
        MOVb @#DIB,R0
        CLR @#DGS
        BIT #200,R0          ;AL?
        BNE EOW0

        MOV #24,@#DOB          ;Pulse V.S.P. to set YVAL
        MOV #4,@#DOB
        MOV @#DIB,R0
        BIC #177400,R0        ;Mask out upper byte
        MOV R0,(R2)+          ;Read in YVAL

        MOV #21,@#DOB
        MOV #1,@#DOB          ;Select X data
        MOV @#DIB,R0          ;Read in XVAL
        BIC #170000,R0        ;Mask out user 4 bits
        MOV R0,(R2)+

        SOB R3,EOW1           ;if less than NLINES scanned,continue
        MOV #177777,(R2)+     ;-1 signifies array termination

        MTPS @#OLDPSW        ;restore interrupt level

        DEC R4                ;DECrement field loop counter
        BEQ W1                ;if completed #fields WRITE
        JMP LRF1              ;otherwise set another field of data

W1:    .WRITE #WAREA,#1,#BUF1,#14400,R1
        ADD #31,R1            ;increment block number by 25.

```



```

LP2:    MOV #NFLDS,R4          ;start on BUF2

LPF2:   MOV @#FCNT,(R2)+
        INC @#FCNT
        MOV #NLINES,R3

BOFW3:  MOVB #10,@#DOB        ;SELECT BITS OF LS153
        MOVB #30,@#DOB
        MOVB #10,@#DOB
        MOVB @#DIB,R0
        CLR @#DGS
        BIT #100,R0          ;AF bit set?
        BNE BOFW3

BOFW2:  MOVB #10,@#DOB
        MOVB #30,@#DOB
        MOVB #10,@#DOB
        MOVB @#DIB,R0
        CLR @#DGS
        BIT #100,R0          ;AF?
        BEQ BOFW2

        MTPS @#OLDPSW
        MTPS #7

EOW2:   MOVB #30,@#DOB
        MOVB #10,@#DOB
        MOVB @#DIB,R0
        CLR @#DGS
        BIT #200,R0          ;AL bit set?
        BEQ EOW2

EOW3:   MOVB #30,@#DOB
        MOVB #10,@#DOB
        MOVB @#DIB,R0
        CLR @#DGS
        BIT #200,R0          ;AL?
        BNE EOW3

        MOV #24,@#DOB
        MOV #4,@#DOB
        MOV @#DIB,R0
        BIC #177400,R0
        MOV R0,(R2)+

        MOV #21,@#DOB
        MOV #1,@#DOB
        MOV @#DIB,R0
        BIC #170000,R0
        MOV R0,(R2)+

        SOB R3,EOW2

```

```

MOV #177777,(R2)+

MTPS @#OLDPSW

DEC R4
BEQ W2
JMP LPF2

W2:  .WRITE #WAREA,#1,#BUF2,#6400.,R1
      ADD #25.,R1                ;INCRement block number

      DEC R5                      ;DECrement PASS counter
      BEQ CLS                    ;CLOSE file if through processing
      JMP LP                      ;otherwise start again

CLS:  .CLOSE #1                  ;close channel 1

      .EXIT

```

```

EAREA: .BLKW 5          ;Version II MCALL parameter storage
FCNT:  .WORD 0         ;Intialize FIELD counter
;FLD:  .WORD 0         ;Initialize filed loop counter
OLDPSW: .BLKW 1        ;Save space for old interrupt level
;PSS:  .WORD 0         ;Intilaize number of passes
Q1:    .BLKW 7*5       ;Queue area (35 decimal words)
WAREA: .WORD 0,0,0,0,0 ;.WRITE(..V2..) parameter storage

PGNAM: .RAD50 'DK1'    ;device
      .RAD50 'X1M'    ;filename
      .RAD50 'DAT'    ;extension
HSPACE: .BLKW 400     ;DK HANDLER

BUF1:  .BLKW 14400
BUF2:  .BLKW 14400
;buflen=#flds/buffer*((#pts/line*#lines/fld)+FCNT +(-1))
;6400 = 32 *(( 2 * 99 )+ 1 + 1 )

.END X1M

```

## PROGRAM SPLOT

```

C           Version VI           3-June-79
C   SERIES OF SNAPSHOTS

DIMENSION IBUF(1500),IVLIST(200),A(2,99)
DIMENSION AMIN(2),AMAX(2),V(2,99)
LOGICAL*1 SET,YES,YNS,EXT,YOX
DATA SET/'S',YES/'Y',EXT/'E',NO/'N'/

TYPE 5
5  FORMAT(1H,' Enter data filename:',$)
   CALL ASSIGN(1,,-1)
   DEFINE FILE 1 (256,200,U,NREC)
     NREC=1

DK=.6745
NLD=99

30  READ(1,NREC) IVLIST

TYPE 40,IVLIST(1)
40  FORMAT(I5)

CALL FREE
CALL INIT(IBUF,1500)
CALL SCAL(0.,400.,520.,-38.)  !range of 438 Y values

IX=NLD           !X array argument

DO 100 IL=2,(2*NLD)+1,2      !DISPLAY loop

      X=IVLIST(IL+1)
      Y=IVLIST(IL)
      CALL APNT(X,Y,1)      !plot points

      A(1,IX)=X*DK
      A(2,IX)=-Y
      IX=IX-1

100          CONTINUE

```

```

TYPE 150
150  FORMAT(1H,' Hard Copy?(Y or N):', '$)
      ACCEPT 160, YNS
160  FORMAT(A1)
      IF(YNS. EQ .YES) GOTO 165      !Plot? yes, goto 165
      GOTO 190                      !Else skip

C ***** Hard Copy Plot
165  PAUSE '-If plotter set hit RETURN-'

      CALL MAXMIN(NLD,A,AMIN,AMAX)    !Find max and min
C      XMIN(1)=0.
C      XMIN(2)=0.
C      XMAX(1)=520.
C      XMAX(2)=384.
      CALL SCALER(NLD,A,AMIN,AMAX,V) !Scaled X array in V
      CALL ZERO(A(1,1),A(2,1))
      CALL POINT(NLD,V)              !Plot points

TYPE 170
170  FORMAT(1H,' Enter Y to replot:', '$)
      ACCEPT 180, YNS
180  FORMAT(A1)
      IF (YNS. EQ .YES) GOTO 165

C ***** Next Field?
190  TYPE 200
200  FORMAT(1H,' Hit <RETURN> to see next set of points, or ', /
      1 ' enter E to exit, S if you want to set NREC yourself:', '$)
      ACCEPT 210, YNS
210  FORMAT(A1)

      IF(YNS. NE. .SET) GOTO 250
      TYPE 230
230  FORMAT(1H,' Enter NREC:', '$)
      ACCEPT 240, NREC
240  FORMAT(I5)
      GOTO 30

250  IF(YNS. EQ .EXT) CALL EXIT

      GOTO 30                      !Otherwise Just loop

END

```

```

PROGRAM LSN

C      Version XXI                24-MAY-79
C      Does analysis specified times on self
C      Rejects overlapping frames

COMMON /IVLIST/IVLIST,/ITP/ITP,/IBT/IBT,/N/N
COMMON /TOP/TOP,/BOT/BOT
DIMENSION RTS(500),RDAT(8),IB(100)
LOGICAL YON,YES
INTEGER*2 IVLIST(200)
DATA YES/'Y'/

DK=.6745

PI=3.14159265
RTD=180./PI                !Radians to Degrees

TYPE 10
10  FORMAT(1H,3X,'Enter INPUT Filename:','$)
    CALL ASSIGN(2,,-1)
    DEFINE FILE 2(512,200,U,IUU)

TYPE 15
15  FORMAT(1H,3X,'Enter OUTPUT Filename:','$)
    CALL ASSIGN(3,,-1)
    DEFINE FILE 3(512,16,U,IU)

20  IUU=1
    IU=2

READ (2,1) IVLIST          !display 1st field of data
CALL WINDM1                !call window routine

TYPE 30
30  FORMAT(1H,' Enter NF(#fields),ILSP(#self loops), '/',
1   ' RPV(SDX multiplier) and DEL(pt. rej. constant):','$)
ACCEPT 40,NF,ILSP,RPV,DEL
40  FORMAT(2I5,2F7.3)

C      NF=no. frames to be analysed, N=no. lines in window
      NLF=NF                !Preserve NF for LOOPing
      NS=N                  !Preserve no. lines

DRT=0.

SSDT=0.
SMT=0.
SMTSQ=0.

PAUSE 'Press <RETURN> to start analysis - -'

I=1                        !intailize slope vector counter
IBFLD=0                    !initialize bad field counter

```

```

DO 200 IF=1,NLF

ISL=-ILSP                               !initialize same field loop

READ(2'IUU) IVLIST

C Reject fields with overlapping data
C Test to see that successive scan lines indeed follow each other.
C Reject those fields were two successive lines have a value less
C than the preceding line. Ie. reject if line i+1 had line i+2
C have a line value less than line i. Dual test allows for some
C noise.
DO 222 ILT=150,199,2
  IF (IVLIST(ILT). GT .IVLIST(ILT-2))GOTO 222
  IF (IVLIST(ILT+2). GT .IVLIST(ILT-2))GOTO 222
  IBFLD=IBFLD+1
  IB(IBFLD)=IVLIST(1)
  NF=NF-1                                !Decrement Field counter
  GOTO 200
222 CONTINUE

50 N=NS                                   !Reinitialize N
  SUMY=0.                                !must compute since
  SUMXY=0.                                !reject certain points
  SUMX=0.
  SUMXX=0.
  SUMYY=0.
  SDIF=0.

DO 100, ILL=ITP,IBT
  IL=(ILL-1)*2
  Y=IVLIST(2+IL)
  X=IVLIST(3+IL)

C ***** Point limit test and rejection
IF (IF.EQ.1.AND.ISL.EQ.-ILSP) GOTO 85 !1ST FLD,1ST PS NO R.

  RLP=A+B*Y                               !predicted point
  DIF=ABS(RLP-DK*X)                       !current point-RLP

  RJW=RPV*SDX+DEL                         !Rejection window=K*sd+del
  IF(DIF. LT .RJW) GOTO 85
  N=N-1                                    !# points=#-1

C Ignore point that falls out of excursion, GOTO 100 avoid SUMmins
C If less than 2 points in the field fit the criteria skip analysis.
C ignore field and GOTO 80 and then 200
IF (N-2) 80,80,100
80 NF=NF-1 !decrement field counter
  IBFLD=IBFLD+1                            !inc rejected field counter
  IB(IBFLD)=IVLIST(1)                      !add field to rejected list
  GOTO 200                                  !and skip analysis

```

C \*\*\*\*\* Points SUMmins

```

85          SUMXY=SUMXY+X*Y
           SUMX=SUMX+X
           SUMXX=SUMXX+X*X
           SUMY=SUMY+Y
           SUMYY=SUMYY+Y*Y
           SDIF=SDIF+DIF*DIF

```

100 CONTINUE

C \*\*\*\*\* Slope, Intercept and Angle determination

```

DEN=N*SUMYY-SUMY*SUMY
IF (DEN. NE .0) GOTO 190

```

```

B=0.
BU=0.
AU=SUMX/N
A=AU*DK
THETA=90.

```

GOTO 195

```

190  BU=(N*SUMXY-SUMX*SUMY) / DEN      ! unnormalized slope
      B=BU*DK

```

```

AU=(SUMX-BU*SUMY)/N
A=(DK*SUMX-B*SUMY)/N      !Y intercept,X=A+BY

```

```

SDY=SQRT(DEN/(N*N))      !SD=SQRT(Diff Sum of Sqs/N)
SDX=DK*SQRT((N*SUMXX-SUMX*SUMX)/(N*N))

```

```

195  ISL=ISL+1            !increment loop counter
      IF (ISL) 50,50,196  !loop till reaches zero

```

```

196  THETA=90.+RTD*ATAN(B)

```

```

      ASDIF=SDIF/N      !average |Xpred.-Xact.|

```

```

      SDXY=SQRT(SDIF/(N-2))  !regression s.d.
      SDB=SDXY/SQRT(DEN/N)   !slope s.d.

```

```

      RBP=B+SDB           !slope+s.d. of slope=mt
      RTP=ATAN(RBP)       !angle assoc. w/ mt
      RBN=B-SDB           !slope-s.d. of slope=m-
      RTN=ATAN(RBN)       !angle assoc. w/ m-

```

C Standard error of angle estimate

C method I: del(thetaz)

```
SDT=60.*(RTP-RTN)/2.
```

C method II: 1st term taylor expansion

```
SDT=60.*SDB*RTD/(1.+R*B)
```

```

RTS(I)=THETA          !vector of angles
I=I+1                !INCRement vector counter

DRT=THETA-ROT        !Angular shift
ROT=THETA            !update last frame's slope

SSDT=SSDT+SDT        !sum of SDT's
SMT=SMT+THETA        !sum of slopes
SMTSQ=SMTSQ+THETA*THETA !sum of squares

RDAT(1)=IF           !field number
RDAT(2)=N            !no. points accepted this field
RDAT(3)=A            !normalized regressed x-intercept
RDAT(4)=AU           !unnormalized x-intercept
RDAT(5)=B            !normalized regressed slope
RDAT(6)=BU           !unnormalized slope
RDAT(7)=THETA        !angle of line
RDAT(8)=SDT          !s.d. of angle

WRITE(3'IU) RDAT

200 CONTINUE

ASDT=SSDT/NF         !average SDM
AVT=SMT/NF           !average slope

DF2=0.
DO 225 I=1,NF
    DF=RTS(I)-AVT
    DF2=DF2+(DF*DF)
225 CONTINUE
SDAT=SQRT(DF2/NF)*60. !s.d.(min.s)

PAUSE '--Hit <RETURN> for summary information.--'

TYPE 250,NF,ILSP,ITP,IBT,RPV,DEL,AVT,SDAT,ASDT
250 FORMAT(1H,/,I6,' fields ',I5,' loops, line ',I3,' to ',I3,
1 /,' had limited excursion of ',F7.4,' pt. s.d.s + ',F7.3,
1 /,' average slope= ',F6.2,' dgrs, ',
1 ' s.d. from <slope>= ',F6.3,' mins'//,
1 ' average standard error of angle estimate= ',F6.3,' mins'//)

TYPE 275,IBFLD
275 FORMAT(1H,I6,' Fields were rejected,including numbers:')

IF (IBFLD) 285,285,277 !skip printing if no fields rejected

277 DO 285 ILS=1,IBFLD,8
    WRITE(7,280) (IB(ILS+J),J=0,7)
280 FORMAT(8I6)
285 CONTINUE

```



```

TYPE 286,ASDIF
286  FORMAT(1H,/,', <dif>=',F10.5,/)

      RDAT(1)=NF           !number of fields analysed
      RDAT(2)=TOP         !scan line at window top
      RDAT(3)=BOT        !scan line at window bottom
      RDAT(4)=RPV        !point rejection SDX multiplier
      RDAT(5)=DEL        !point rejection constant
      RDAT(6)=AVT        !average angle for NF fields
      RDAT(7)=SDAT       !SD from average angle
      RDAT(8)=ASDT       !average SDM
      WRITE(3'1) RDAT

TYPE 300
300  FORMAT(1H,' Enter a Y to RERUN program, N to EXIT:',$,)
      ACCEPT 350,YON
350  FORMAT(A1)
      IF (YON, EQ .YES) GOTO 20

      CALL EXIT

      END

```

LSN.BAT

!LSN BATCH FILE

```

$JOB/RT11
.R FORTRAN
*LSN,LSN=LSN/W
.R LINK
*LSN,LSN=LSN,UTLIB/F/C
*WINDM1
$EOJ
*
```

```
PROGRAM RLRP
C READs linear regression parameter files
```

```
C The first 25 lines of the specified file
C are read before the user is queried as to
C wether he wishes to continue or not. The
C same occurs at line 50, from then on the
C reading is uninterrupted.
```

```
DIMENSION RDAT(8)
```

```
WRITE(7,100)
100 FORMAT(2X,'ENTER FILENAME: '$)
```

```
CALL ASSIGN(1,,-1)
DEFINE FILE 1 (256,16,U,NREC)
NREC=1
```

```
READ(1'NREC) RDAT
NF=RDAT(1) !number of fields analysed
TOP=RDAT(2) !scan line at top of vertical window
BOT=RDAT(3) !scan line at bottom of vertical window
RPV=RDAT(4) !SDX multiplier in point rejection window
DEL=RDAT(5) !constant in point rejection window
AVM=RDAT(6) !average of NF angles
SD=RDAT(7) !standard deviation from AVM
ASDM=RDAT(8) !average standard error of estimate on angle
```

```

WRITE(7,160)
160  FORMAT(1H,3X,'NF',4X,'Top',5X,'Bot',8X,'S',6X,'Del',
1    4X,'<Theta>',4X,'S.D.',5X,'<SE>')

WRITE(7,175)NF, TOP, BOT, RPV, DEL, AVM, SD, ASDM
175  FORMAT(X, I5, 2F8.0, 2X, 2F8.3, X, 2F9.3, F9.2, /)

WRITE(7,180)
180  FORMAT(1H,5X,'#Fld',3X,'#Pts',4X,
1    'A',5X,'AU',9X,'B',7X,'BU',4X,'Theta',4X,'SDM')

IL=1          !intialize block count

150  CONTINUE

      READ(1'NREC)RDAT

      WRITE(7,200)RDAT
200  FORMAT(3X,2F7.0,6F8.3)

      LCNT=25*IL      !print blocks of 25 and then

      IF (NREC-LCNT) 150,400,400      !QUERY to continue

400  PAUSE 'To continue hit RETURN'

      IL=IL+1          !another 25 blocks read
      WRITE(7,180)      !print heading

      GOTO 150

500  END

```

PROGRAM SNM

C  
C

Version VIII

2-June-79

SERIES OF SNAPSHOTS

```

DIMENSION IBUF(1500),IVLIST(200),RDAT(8)
DIMENSION AR(2,99),SA(2,99),AMIN(2),AMAX(2)
DIMENSION APR(2,99),SPR(2,99),VZERO(2)
DIMENSION ATP(2,2),STP(2,2),ABT(2,2),SBT(2,2)
LOGICAL*1 DEF,DOS,EXT,SET,YES,YNS,YDX
DATA DEF/'D'/,EXT/'E'/,SET/'S'/,YES/'Y'/

```

TYPE 4

```

4 FORMAT(1H,' Enter data filename:',$)
CALL ASSIGN(1,-1)
DEFINE FILE 1 (512,200,U,NREC)

```

TYPE 6

```

6 FORMAT(1H,' Enter filename containing lin. res. parameters:',$)
CALL ASSIGN(2,-1)
DEFINE FILE 2 (512,16,U,NRC)

```

READ(2'2)RDAT

```

      IFF=RDAT(1)
      NREC=IFF      !set first field
      NRC=1

```

READ(2'NRC)RDAT

```

      NF=RDAT(1)      !number fields analysed
      TOP=RDAT(2)     !vertical window top
      BOT=RDAT(3)     !vertical window bottom
      RPV=RDAT(4)     !SDX multiplier for point rej. window
      DEL=RDAT(5)     !point rejection window constant
      AVT=RDAT(6)     !average angle
      SDAT=RDAT(7)    !s.d from average angle
      ASDT=RDAT(8)    !average standard angle error
                      !of estimate

```

TYPE 9,NF,AVT,SDAT,ASDT,RPV,DEL

```

9 FORMAT(1H,'This analysis of ',I5,' fields yielded:',/,
1 ' an average slope of ',F8.3,' degs, s.d. ',F8.2,/,
1 ' average standard error on angle estimate ',F8.2,' mins',/,
1 ' rejection window:',F8.4,' s.d.s + ',F8.4)

```

NLD=99

DK=.6745

30 READ(1'NREC) IVLIST

```

READ(2,'NRC') RDAT
  IF=RDAT(1)
      NREC=IF+1      !sync data and parameter files
N=RDAT(2)           !# points analysed this field
A=RDAT(3)           !regressed x-intercept
AU=RDAT(4)         !unnormalized intercept
B=RDAT(5)          !regressed slope
BU=RDAT(6)         !unnormalized slope
THETA=RDAT(7)      !angle of line feature
SDT=RDAT(8)        !standard error of est. on THETA

CALL FREE
CALL INIT(IBUF,1500)
CALL SCAL(0.,400.,520.,-38.)      !range of 438 Y values

IX=NLD                !Array argument

DO 100, IL=2,(2*NLD)+1,2          !DISPLAY loop

      Y=IVLIST(IL)
      X=IVLIST(IL+1)
      CALL APNT(X,Y,1)           !PLOT points

      AR(1,IX)=X                !Actual value
      AR(2,IX)=-Y

      APR(1,IX)=AU+BU*Y         !predicted value
      APR(2,IX)=AR(2,IX)

      IX=IX-1

100      CONTINUE

C ***** Draw Window limits

      CALL APNT(20.,TOP,0,-5)
      CALL LVECT(480.,0.)

      CALL APNT(20.,BOT,0,-5)
      CALL LVECT(480.,0.)

C ***** Plot Linear Regressed line over data points

      FPY=-25.
      RLPY=275.

      FPX=AU+BU*FPY             !X regressed predictions
      RLPX=AU+BU*RLPY

      DY=RLPY-FPY
      DX=RLPX-FPX

      CALL APNT(FPX,FPY,0,-5)
      CALL LVECT(DX,DY)         !draw line

```

```

170 WRITE(7,170) (NREC-1),IF,N,A,B,THETA,SDT
    FORMAT(2X,3I5,4F12.3)

C ***** Hard Copy?

    TYPE 171
171 FORMAT(1H,'Hard Copy(Y or N)? ',%)
    ACCEPT 172,YNS
172 FORMAT(A1)

    IF (YNS. EQ .YES) GOTO 173      !Hard Copy? YES, GOTO 173
    GOTO 199                        !else, skip and GOTO 199

173 TYPE 174
174 FORMAT(' Enter D to use Default parameters:',%)
    ACCEPT 175,DOS                  !Default Or user Set
175 FORMAT(A1)

    IF (DOS. NE .DEF) GOTO 177      !GOTO 183 to let user set MAXMIN

C ***** Default scaling factors
    AMIN(1)=0.
    AMIN(2)=-400.
    AMAX(1)=520.
    AMAX(2)=38.
    VZERO(1)=0.                    !plotter zero
    VZERO(2)=0.

    TYPE 176,AMIN,AMAX,VZERO        !Print values for user reference
176 FORMAT(1H,' Amin=',2F7.2,' Amax=',2F7.2,' V0=',2F7.2)

    GOTO 180                        !Skip scaling settings

177 TYPE 178
178 FORMAT(1H,' Enter Axmin,Aymin,Axmax,Asmax,Vx0,Vy0:',%)
    ACCEPT 179,AMIN,AMAX,VZERO
179 FORMAT(6F7.2)

180 CALL SCALER(NLD,AR,AMIN,AMAX,SA) !SA is scaled AR
    CALL ZERO(VZERO)                !zero plotter
    CALL POINT(NLD,SA)              !Plot points

    CALL SCALER(NLD,APR,AMIN,AMAX,SPR) !SPR scaled PAR
    CALL ZERO(VZERO)                !zero plotter
    CALL LINE(NLD,SPR)              !link regressed points

```



## SUBROUTINE WINDM1

```

C          Version VIII          12-June-79
C      Based on a snapshot of the first frame an upper and lower
C      limit is set on the video scan lines. These limits, ITOF and
C      IBOT will be sent to the angle determination routine, ANG.
C      Only points within these scan lines and the video gate
C      hardware window will be processed for rotation.

COMMON /IVLIST/IVLIST, /ITP/ITP, /IBT/IBT, /N/N
COMMON /TOP/TOP, /BOT/BOT
LOGICAL*1 ANS, BDOL, BP, BR, OK, NO, SET, YES, YON
DIMENSION IBUF(1500), RY(2), IVLIST(200)
DATA BDOL/'$'/, BP/'P'/, NO/'N'/, SET/'S'/, YES/'Y'/

CALL FREE
CALL INIT(IBUF, 1500)

C      CALL SCAL(0., 0., 1545., 1300.)   Scales for rectangular display
C      Using this same ratio for x=520 y becomes 438.
C      The fourth quadrant is used here. Later in the program everything
C      is changed to have the negative values, positive; but, Y still
C      increases down the screen.
      CALL SCAL(0., 400., 520., -38.)   !400.+38.=438 Y values

      NLD=99                          !No. lines down scan

      CALL APNT(180., 0., 0., -7)
      TX=20.                          !initial light pen position
      TY=20.

      CALL TEXT('Light Pen Coordinates: X= ')
      CALL NMBR(1, TX, 'F8.2')
      CALL TEXT(' Y= ')
      CALL NMBR(2, TY)

C          PLOT POINTS

      PAUSE '-Hit <CR> to display the first set of comparator HITS-'

90          DO 100, ILL=1, NLD          !DISPLAY loop

              IL=(ILL-1)*2

              X=IVLIST(3+IL)
              Y=IVLIST(2+IL)

              CALL APNT(X, Y, 1)       !plot points

100         CONTINUE

```



C \*\*\*\*\*Enable light Pen

```
110  WRITE(7,120)
120  FORMAT(' P<RET> will enable Light Pen,($<RET> terminates):'$)

      ACCEPT 130,BR
130  FORMAT(A1)
      IF(BR .EQ. BP) GO TO 140
      IF(BR .EQ. BDOL) CALL EXIT

      GOTO 110          !If no acceptable response requery

140  CALL TRAK(TX,TY)  !Call light pen tracking feature

145  DO 190, IY=1,2    !loop for top & bottom limits

      PAUSE ' Position light pen and hit <RETURN>:'

150  CALL NMBR(1,TX) !Updated light pen positions
      CALL NMBR(2,TY)

180  RY(IY)=TY

      TYPE 185,RY(IY)
185  FORMAT(1H,'Is ',F7.2,' an acceptable boundary?(Y or N):','$)
      ACCEPT 186,YON
186  FORMAT(A1)

      IF (YON. NE .NO) GOTO 190      !to get next level or
                                      !to exit, otherwise
      PAUSE 'Reposition $ hit <RETURN>(Position updated above)'
      GOTO 150                        !set new value

190  CONTINUE
```

C \*\*\*\*\* Find actual values closest to window limits

```

OLDY=ABS(RY(1)-IVLIST(2))           !set top limit
TOP=IVLIST(2)
ITOP=1

```

```

DO 200, IFIX=2,NLD                   !Search data array for
  IFL=2+(IFIX-1)*2                   !actual line closest to
  RNWY=ABS(RY(1)-IVLIST(IFL))       !light pen hit
  IF(RNWY. GT .OLDY) GOTO 200
  TOP=IVLIST(IFL)
  ITOP=IFIX
  OLDY=ABS(RY(1)-IVLIST(IFL))

```

200 CONTINUE

```

OLDY=ABS(RY(2)-IVLIST(2))           !set bottom limit
BOT=IVLIST(2)
IBOT=1

```

```

DO 210, IFIX=2,NLD                   !Search for closest lin
  IFL=2+(IFIX-1)*2
  RNWY=ABS(RY(2)-IVLIST(IFL))
  IF(RNWY. GT .OLDY) GOTO 210
  BOT=IVLIST(IFL)
  IBOT=IFIX
  OLDY=ABS(RY(2)-IVLIST(IFL))

```

210 CONTINUE

TYPE 212,ITOP,IBOT

212 FORMAT(1H,' Window between ',I6,' & ',I6)

C \*\*\*\*\* Plot WINDOW limits

```

215 CALL APNT(20.,BOT,0,-5)
    CALL LVECT(480.,0.)
    CALL APNT(20.,TOP,0,-5)
    CALL LVECT(480.,0.)

```

```

TYPE 220
220  FORMAT(1H,' Are you happy with the window settings.',/,
1    ' Y(yes) enters limits, N(no) restarts limit settings.',/
2    ' S(set) allows the user to enter values for ITOP and IBOT: ',$,)
ACCEPT 230,OK
230  FORMAT(A1)
      IF (OK. EQ .NO) GOTO 145
      IF (OK. EQ .SET) GOTO 240
      GOTO 270                ! assumes <CR> represents YES response

240  TYPE 250
250  FORMAT(1H,' Please enter two integers for ITOP and IBOT: ',$,)
255  ACCEPT 260,ITOP,IBOT
260  FORMAT(2I9)
      IF (ITOP.GT.NLD.OR.IBOT.GT.NLD) GOTO 265
          BOT=IVLIST(2+(IBOT-1)*2)
          TOP=IVLIST(2+(ITOP-1)*2)
      GOTO 215

265  TYPE 266,NLD
266  FORMAT(1H,' ITOP or IBOT may not exceed ',I5,
1    ' please reenter values: ',$,)
      GOTO 255

270  ITP=MIN0(ITOP,IBOT)      !Independent of order entered
      IBT=MAX0(ITOP,IBOT)    !ITP lower limit, IBT upper limit

      TOP=AMIN1(TOP,BOT)     !TOP loer scan line
      BOT=AMAX1(TOP,BOT)     !BOT upper scan line

      N=IABS(ITP-IBT)+1

      TYPE 280,N,TOP,BOT
280  FORMAT(1H,3X,I4,' Points, from line ',F5.0,' to ',F5.0)

      END

```

## PROGRAM PLHTA

```

C                                     20-May-79
C THETA(Y) vs. time(X) is plotted using the results of LSMRT.
C The time scale may be user specified and the time scale set
C by the program in accordance with the number of fields
C that were analysed.

      DIMENSION IBUF(1500),RDAT(8)
      LOGICAL*1 QRY,RERUN
      DATA RERUN/'R'/

      DK=1545./1300.  !screen aspect ratio

      TYPE 5
5     FORMAT(1H,' Enter data filename:',$,)
      CALL ASSIGN(1,,-1)
      DEFINE FILE 1 (256,16,U,NREC)
50    NREC=1

      READ(1,NREC) RDAT
      NF=RDAT(1)      !number of fields analysed
      TOP=RDAT(2)    !scan line at top of vertical window
      BOT=RDAT(3)    !scan line at bottom of vertical window
      RPV=RDAT(4)    !SDX multiplier in point rejection window
      DEL=RDAT(5)    !constant in point rejection window
      AVT=RDAT(6)    !average of NF angles
      SDAT=RDAT(7)   !standard deviation from AVT
      ASDT=RDAT(8)   !average standard error of estimate on angle

      WRITE(7,175)NF, TOP, BOT, RPV, DEL, AVT, SDAT, ASDT
175   FORMAT(X, I5, 2F8.2, X, 2F8.3, X, 2F9.3, F9.4, /)

      TYPE 180
180   FORMAT(1H,'Enter YMIN & YMAX, NSF, NEF: ', $)
      ACCEPT 185, YMIN, YMAX, NSF, NEF
185   FORMAT(2F8.2, 2I5)
      IF (NSF. LT .2) NSF=2  !first record is summary of data
      IF (NEF. GT .NF) NEF=NF !cant go beyond last file
      NFT=NEF-NSF           !total #fields analyzed

      DIX=1000./60.        !time increments in msec
      XMIN=NSF*DIX         !#1st field * 16.66 msec/field
      XMAX=(NEF+12)*DIX    !#fields+12 * 16.66 msec/field

      YL=ABS(YMAX-YMIN)    !width of Y axis
      TLX=YL/250.         !tick length
      TLY=NF/20.

      CALL FREE
      CALL INIT(IBUF,1500)
      CALL SCAL(XMIN,YMIN,XMAX,YMAX)

```

```

C ***** Construct AXES

      CALL APNT(0.,0.,0,-5) !soto origin
      CALL VECT(XMAX,0.) !draw X-axis
      LIX=1+(NFT+12)/6 !X loop increment
      TIX=-6.*DIX !tick increment along X-axis
      DO 100 IX=1,LIX
C      X=XMIN-TIX*(IX-1.) !tick value in msec
C      CALL RDOT(0.,-15.,0.,-5) !position X axis numbering
C      CALL NMBR(1,X,'F5.1')
      CALL VECT(0.,TLX) !draw tick mark
100    CALL RDOT(TIX,-TLX,0,-5) !return to X-axis & move back .1 sec

      CALL APNT(1.,YMIN,0,-5) !soto end of Y-axis
      CALL VECT(0.,YL) !draw Y-axis
      LIY=1+YL/5 !Y loop increment
      TIY=-5. !tick increment along Y axis
      DO 200 IY=1,LIY
C      Y=YMAX-TIY*(IY-1.) !degrees
C      CALL NMBR(2,Y)
      CALL VECT(TLY,0.) !draw tick mark
200    CALL RDOT(-TLY,TIY,0,-5) !return to Y axes & drop TIY dsrs

      NREC=NSF
      DX=DIX !initialize time increment

      DO 400 IF=NSF,NEF+1

          READ(1'NREC)RDAT

          IF (IF.GT.NSF) GOTO 350
              ILF=RDAT(1)-1 !intialize last field
              DX=NSF*DIX !intialize X value

350          RT=RDAT(7) !theta
              ICF=RDAT(1) !current field
              DF=ICF-ILF !field increment
              DF=1.
              DX=DX+DF*DIX !time increment
              !16.666 msec/field

          CALL APNT(DX,RT,1)
              ILF=ICF !save field counter

400    CONTINUE

      TYPE 425
425    FORMAT(1H,' To rerun program type R,then <RETURN>:(',$,)
      ACCEPT 450,GRY
450    FORMAT(A1)

      IF(GRY. EQ .RERUN) GOTO 50
      CALL EXIT !otherwise EXIT

      END

```

## APPENDIX C

In choosing the number of words per field and number of fields per buffer, certain I/O timing and disk formatting requirements had to be adhered to. The discussion of these considerations not only lend an appreciation for the critical time factor under which the system is currently operating, but also provides future users with a means of assessing the effect of modification to the data collection and disk storage routines.

The Digital Equipment Corporation PDP 34/11 computer in use with the VSP has a core memory and all timing values below are for this unit alone.

#### 1 DISK SPACE

The RK05 disk used with this computer has approximately 4800 tracks. Each track contains 12 sectors of 256 words yielding 3072 words per track. Each of the dual buffers must therefore be a multiple of 256. Theoretically, this would fit the video field ideally, since it contains 256 scan lines. However, the first 17 and last 17 scan lines contain only sync information, and on occasion every third line is sampled by the VSP. Thus, less than 128 lines are scanned per field.

#### 2 WRITE TIMING

Each time an empty track is to be located on the average 50 msec (85 msec maximum) is required. Each word that is to be written occupies

11.1  $\mu$ sec and a disk revolution takes 40 msec.

With these requirements in mind, 32 fields of 200 words were used for each buffer. The 200 words represented 99 lines of X, Y pairs, a field counter and a field termination indicator. Unfortunately, these buffers will occupy 1 sector more than 2 tracks. Yet there is more than enough time to collect and store all the data with no loss even by the most conservative estimate. This latter would include: 3 track positionings, 6400 word writes, etc., plus some margin, amounting to about 460 msec per buffer. Thirty two fields, on the other hand, allow a 512 msec respite before a buffer must be cleaned to accept new data. An extra 50+ msec is available or about 3+ video fields.

It should be noted once again that if the buffer sizes are altered, the time and space requirements noted here must be reconsidered.

## APPENDIX D

## CONTACT LENS 'SANDWICH': DEVELOPMENT AND THEORY

A contact lens mounted feature was chosen for tracking for determination of ocular counterrolling. For this purpose, a new "soft" contact lens "sandwich" was designed. Relevant characteristics of the lens material, certain chemical phenomena and the mechanics of the lens developed are presented below as an update of work presented in my bachelors thesis.

Standard hard contact lens material, polymethylmethacrylate has been and is still widely used in the formation of corneal and scleral lenses and shells. If handled with care and precision, hard lenses may be fit successfully, yet lenses of this material possess a number of serious drawbacks. Friction and pressure of the rigid polymer is at the very least uncomfortable and may lead to mechanical damage to surface tissues in contact with the lens. Gases, water and many physiological solutes are restrained from flowing across the lens due to the nature of its permeability. Attempts to alleviate some of these deficiencies include grooves and holes cut into the lens. However, these methods have not proved efficacious. Aside from the mechanical trauma, the effects of corneal epithelial hypoxia are also often evident (Ruben, 1972). Adhesion of such lenses to a human eye to provide a tracking image for eye monitoring presents even greater hazards. Mounted objects such as mirrors and coils increase the chances of cornea abrasions, deformation and edema. In addition, fluid is evacuated from behind the lens to establish a negative pressure that forces this lens onto the eye. This may



This may very well lead to damage to the ocular accommodation muscles. Polyhydroxyethylmethacrylate (poly-HEMA) has been used as just such a substitute. It is far from perfect material, however, it does present both physical (comfort, permeability) and chemical (highly stable) advantages over the harder materials. (Ratner and Hoffman 1976).

The Bausch and Lomb SOFLENS contact lens comes in a limited number of sizes (three for prescription lens use and one for non-prescription plano lenses). They therefore avoid the impositions associated with custom fitting. Further, subjects wearing these lenses, even the relatively bulky sandwich types, feel little, if any, discomfort. The development and use of a sandwich of two soft contact lens bonded about a fine fiber, such as a human hair, was described in Chapter 4. This sandwich provides clear and distinct images to a video monitoring system. It may prove to be a viable alternative to other systems as well, and may be adapted to hold the coils, cores and rings previously embedded in other types of lenses

Two subjects participated in experiments involved in this research. Both reported no loss in their powers of visual discrimination and we have observed no impediment to eye movement. No anesthesia is required prior to insertion and fluid evacuation is not needed to establish a negative pressure to adhere the lens to the eye. The worst observed effects were those of expected adaptation problems of subjects who had never worn contact lenses. There was some initial tearing, which soon disappeared. Yet both the subjects were examined with the eye movement monitor after wearing the lenses for the first time. Neither had worn contact lenses prior to this time. Subsequent examination by an optometrist in the MIT Medical Department showed no edema or other corneal damage.

The purpose of this appendix is then to discuss the use of a softlens sandwich as it may be used in an eye monitoring system. Theoretical ideas as to why the composite lens is so stable and binding; and, why it can be made to adhere so well, for desired time periods, to surfaces with which it comes in contact, are also provided.

#### THE SOFLENS MATERIAL

The soft contact lens materials, SOFLENS (polymacon), consists of approximately 60% poly (2-hydroxyethylmethacrylate) and 40% water (by weight when immersed in normal saline solution). Poly-(HEMA) is an organic polymer, thus its properties can best be understood by considering the characteristics of polymers.

Primary chemical bonds along polymer chains are generally entirely satisfied. The only forces between molecules are secondary forces of attraction (these forces will be of relatively minor importance in the 'lens sticking theory'), which are relatively minor compared to the primary bond forces. The high molecular weight of polymers allows these forces to build up enough to impart excellent strength, dimensional stability and other mechanical properties to the the substance.

The SOFLENS material is a hydrogel, a subclass of polymers which exhibit the ability to swell in water and retain a significant fraction of water within their structure without dissolving.



## Hydrogels

Hydrogels are three dimensional, water swollen, networks of hydrophilic polymers, generally ionically or covalently crosslinked, consisting of two components: the polymer network and an aqueous solution. The Bausch and Lomb SOFLENS contact lens, for example, consists of 61.4% HEMA polymer and 38.6% water by weight in its hydrated state. The network, as described above, is composed of a large number of chemically related subunits bonded together. It is constant in quantity, presenting no significant physical change with changes in the environment. There is mobility of polymer segments, particularly in the interfacial zone (that region functioning as a boundary to other environments) and this mobility will be of specific interest with regard to the adherence characteristics of tackiness of the lens.

The polymer network interacts with the second component, the aqueous solution, by swelling to some equilibrium value. Unlike the polymer network, the solution is variable and in the SOFLENS, the water content may range from 37 to 42% by weight for the HEMA hydrogel. At equilibrium swelling, the chemical potentials of the water in the gel and the water surrounding the gel are equal. The variance in water content may then be seen as being influenced by the tonicity of the surrounding solution.

The combined aqueous gel network can be relatively strong or weak, generally becoming weaker as the amount of water in the hydrogel decreases. The mechanical behavior of the gel, which we believe contributes to the unique adherence properties of the SOFLENS, is influenced by the swelling of the lenses as well as certain other key properties,

including the nature of the poly-network, tacticity, etc.

The surface and interfacial properties of the hydrogels are somewhat similar to those of natural biological gels and tissues, and are therefore highly biocompatible, receiving increasing attention in utilization for biomedical applications. In addition, a number of analogies have been made between the hydrogel/water interface and the living cell/physiological solution interface. These comparisons aid our understanding of the mechanics involved in certain physical properties of the gels and permit us to extrapolate and establish further theories regarding the interaction of hydrogels with themselves as well as other surfaces and materials.

The most important feature of hydrogels, as far as we are concerned, is their ability to equilibrate with and 'follow' many environmental changes. The addition of macromolecules, too large to penetrate the hydrogel, to the solution surrounding the gel lowers the chemical potential of the water in the solution. Water will then flow out of the hydrogel, causing the polymer network to contract. This action leads to a balancing of the potential of the water in the network with that of the water in solution. The process of such equilibration in essence creates a swelling pressure equal to the osmotic pressure and it is this pressure which leads to some of the interesting mechanical side effects with regards to the adherence of poly-HEMA materials.

In polymer chemistry, the peculiar characteristics which cause two polymer or rubber surfaces to adhere or coalesce is known as tack or autoadhesion. It has been shown to depend upon the interdiffusion

of segments of polymer molecules across the rubber surface (Ledwith and Norton, 1975; Morton, 1973). Some synthetic polymers have much better tack than others partly due to the inherent strength of the uncross-linked polymer, but also due to the greater ease of molecular diffusion across the polymer interface.

Tack is tremendous practical importance. Composite rubber articles such as tires are built by use of this property. Surfaces, 'freshened' with suitable solvents, are merely stuck together and pressed into place.

Though contact lenses are as far a cry from automobile tires as hydrogels are from tire rubber, a valuable analogy may be drawn. Both rubber and gel are polymers with many entangled chains in constant molecular motion. This motion and the very properties that lead to the formation of the polymer from the polymer units lead to adherence of the more complex poly-network to other surfaces under the proper conditions.

Chen and Cyr (1970) describe this adherence and note that when a dry hydrocolloid is moistened with water, long chains of the polymer are hydrated and liberated to a freely moving state. When brought close to a substrate, the stretched, entangled or twisted molecules are now able to match their active sites to those on the hydrophylic substrate to form adhesive bonds or to match with each other to form cohesive bonds. Maximum adhesion is achieved in the presence of an optimum amount of water at or near the interface. If an insufficient amount of water is used, active wet adhesive sites are not completely liberated and exposed for interactions, while an excessive amount of

water causes overextension of hydrogen bonds and other adhesive forces leading to a weakening of the adhesion.

### The Hydrogel Environment and its Changes

All molecules undergo continuous random motion. In this manner, molecules are able to move from one region of a solution to another. In a solution, many molecular collisions may occur, each altering the direction of the molecule's movement. Over a period of time, these collisions establish a random walk or path for each molecule. A large number of these paths taken together can lead to a flux or diffusion of molecules in one direction, which, as Vander et al (1973) note always proceeds from a high to a low concentration, even in the absence of a specified force, such as pressure. The magnitude of the net flux is determined by the magnitude of the concentration gradient. When, as a result of these molecular migrations, the concentration is uniform throughout the solution, a state is reached where the net flux is zero. This is known as diffusion equilibrium and, once reached further changes in concentration do not occur.

A membrane which permits the free passage of selected molecules while restraining others is classified as a semipermeable membrane; only partially free to the passage of molecules. If a membrane which allows only water to pass through it were placed between two compartments of different concentrations, a new diffusion of water or osmosis will occur. Such an effect occurs as long as the concentration gradient exists. If both the water and the solute can cross the boundary, diffusion

proceeds in both directions; the solute concentration gradient promotes a flow of solute molecules to the lower osmolar concentration region, while the water concentration gradient prompts osmosis in the direction of lower water concentration. Such an exchange occurs until the concentration of both solute and water are equal in each compartment.

If a semipermeable membrane is placed at the boundary of the two sections and is permeable only to water, the equilibration process may only utilize water flow. Since the only way the solutions can become equilibrated is to have water from the more dilute compartment flow into the more concentrated compartment, a net volume change results. If the dilute solution is pure water, this volume change will continue until the column of liquid in the solution compartment exerts a force equal to the osmotic pressure.

In the case where both water and solute can pass through the membrane, no net change in volume will occur. When the membrane restricts the flow of solute molecules, a net change in volume must occur due to the dilution process.

#### Lens Reactions to Changes in the Environment

The SOFLENS contact lens may be regarded as a semi-permeable membrane and the mechanics of ion flow across it may be thought of as a combination of the two effects described above. It allows the passage of water and other small molecules and ions, but prevents the passage of larger ions and macromolecules such as protein. In the eye, there are two compartments with associated concentrations. The first compartment is the corneal surface consisting of a mucus layer and a tear layer made up of water and



solids. Adler (1965) reports that the solid phase (actually in solution with the tears) makes up about 2% of the total and consists primarily of protein (mostly urea at a concentration equal to that found in plasma) and sodium, potassium and chloride ions (at a concentration higher than that found in plasma). The second compartment is the interior of the lens made up of the polymer network and its aqueous phase. When the two compartments come in contact, a net exchange of ions or water will occur if their concentrations are not equal.

Refojo(1975) summarized the different osmotic effects associated with the hydrogel lens. He notes that the contact lens may be isotonic (of equal tonicity or osmotic pressure), hypertonic (of higher osmotic pressure) or hypotonic (of lower osmotic pressure) with respect to the tear layers in the eye. The tonicity of the gel aqueous phase may be controlled and manipulated by the solution the lens is stored in.

In general, the SOFLENS material is held in a solution whose salt concentration is roughly comparable to that which is found in the normal eye (0.85 to 0.90% saline). When a contact lens stored in this solution is placed in the eye, little net ionic migration will take place. The lens' aqueous phase and the eye's tear layer are isotonic with respect to each other. There will be a continual interchange of tear and lens fluid, yet Refojo notes that there will be no overall change in the tear tonicity and no changes in the optical or physical characteristics of the lens.

If the storage solution has a concentration sufficiently different from the tear layer, changes can be induced. If the lens is placed in

distilled water, it will become hypotonic with respect to the tear layer. When placed in the eye, a concentration gradient will exist, water will move from the aqueous phase of the lens to the tears (in an effort to dilute the tears), and K, Na, and Cl ions will tend to flow from the tears into the lens. These exchanges will continue to occur until equilibration, at which point a state of isotonicity is attained. The dominant transport of water out of the lens, however, leads to a net contraction of the lens and with this shrinkage, the lens adheres to the cornea. Further evidence to support this view is provided by a coincidental finding in the study of ionic flow by Refojo (1967) and others. It was noted that as the concentration of a solution containing certain ionic compounds increases, the percentage of water in the hydrogel decreases. These ions are, in fact, the primary ions found in the tears, potassium, sodium and chloride.

If the lens is bathed in a solution (such as an NaCl solution) with salt concentrations higher than the normal 0.85%, the lens can be made hypertonic to the tears. In the case, the reverse of the hypotonic reaction will occur. Placed in the eye, such a lens will osmotically draw water from the tears into the lens and the lens will swell. Again, salt will also move into the more dilute solution, from the lens into the tears, causing discomfort. Worse, however, the corneal epithelium is dried out from the osmotic effect and this may cause ocular irritation. Once more, these interchanges will continue until isotonicity is reached, at which time the normal interchanges will again take place.

It is this property or physical reaction of flow and contraction

which we believe to be one of the major contributors to the sticking of the lens to the eye. It is our experience that a lens soaked in distilled water adheres rather tenaciously to the cornea for a considerable period of time (15 minutes to 2 hours, observed). Such adherence is consistent with the osmotic processes detailed above, since the distilled water aqueous phase within the lens will flow out into the eye due to the difference in concentration. Salt will also tend to flow in and eventually equilibrium will be reached. However, at this equilibrium point, the lens will contain less volume of solution than its optimum amount and will consequently be smaller in size, thus adhering more tightly to the cornea. Eventually, the lens will rehydrate by absorption of tears and the adhesion will lessen.

It seems reasonable to postulate that a combination of these effects is taking place at the boundary between the two soft lenses. These would include in probable order of decreasing contribution, autoadhesion, covalent bonding, and hydrogen bonding.

Autoadhesion refers to the natural tack of the poly-HEMA material in contact with itself. The presence of partially unreacted monomer chains on the surface of the left lens further contributes to the soft-lens-soft-lens adhesion. In the presence of an aqueous phase, these chains obtain the mobility to attain the proper configuration for formation of covalent or hydrogen bonds. Hydrogen bonds between the two lenses would be a fairly minor effect, but given the presence of an aqueous phase at the boundary, a lens-water-lens hydrogen bond bridging effect is quite possible and would enhance the stability of

the adhesion. This effect would be lost in the presence of an excess of water, as would some of the covalent bonding. The covalent bonding would be of the same type responsible for the formation of the polymer from the monomer, but on a much smaller scale since only a small proportion of the available monomer chains would attain the proper configuration to form covalent bonds. Thus, these bonds would be relatively easily broken in a situation where the two large lens masses are being forced apart.

This drift of polymer fibrils and the constant movement of other entangled strands might be of some value in further explaining the strength of the observed adherence. In dry tack, one of the effects includes the extension of fibrils which contact and latch onto the other surface. Strands of material from this second surface are pulled toward the fibrils, forming a physical bond. If enough bonds are formed, adhesion may result. Wet adhesion is a dynamic phenomenon unlike the somewhat static occurrence in the dry state, yet it is not unlikely that the same kind of effect may occur. Fibrils from the polymer, constantly moving, extend from the network surface, and when they come in contact with another surface with similar fibrils, they might adhere to its strands.

In the case of a lens-lens sandwich, this is far from unreasonable. Two of the same materials with wandering fibrils touch. These same fibrils now extending from a polynetwork mass are the same basic material which was originally polymerized to form the mass. The same solvents and materials are present, and one may conclude that the same properties that led to polymerization may lead to a secondary effect.

This effect may be promoted by the equilibration process. Ions and water migrating out of the lens may carry polymer strands with them, causing further fibrils to extend from the network surfaces. Ilavsky and Prins (1970) note that when p-HEMA is subjected to a distortion, its original interchain correlation is partially destroyed. When the stress is relaxed, reorientation regions in the polymer network may be observed. It might also be possible that a reorganization occurs leading to interaction with external material.

As noted before, we had to rub the lens sandwich between the thumb and forefinger to separate it, perhaps shearing this adhesive bond. One must bear in mind, however, that this is a small secondary effect. It is, as proposed, quite possibly an interesting minor contributor to the adhesion and should be viewed accordingly.

### Summary

A number of interesting properties of the SOFLENS material became evident during this study. The SOFLENS contact lens sandwich adheres to the eye especially fast and for longer times than expected. based on previous work. It was noted that the heavier the lens, the quicker it stuck and the more prolonged its adherence.

This led to the belief that the added weight contributed additional pressure forcing the lens into closer contact with the cornea. In addition, it supported the view that many factors come into play in

contributing to the adherence of the lens to the eye or to another lens of the same material.

An attempt has been made to summarize the available material describing the nature of the contact lenses and their application in eye movement tracking. It has been shown that their optimum application involves the use of a sandwich of two soft contact lenses with almost any desired marker inserted between the two. These sandwiches, under the appropriate conditions, can be made to adhere to the cornea for considerable periods of time and provide a stable landmark for eye tracking.

One of the more challenging aspects of this work involved the investigation of the mechanism of adherence of the soft contact lens to the cornea. Diffusive forces die out after approximately 15 seconds, thus, other forces must play a role in the adherence. Several probable explanations were advanced, including osmotic shrinking and weight considerations. The manner in which the lenses stuck to each other was also investigated. Possible explanations for this were covalent bond formation and hydrogen bond formation stabilizing the natural tack-induced tenacity.

This is a summary of a more detailed explanation presented in my bachelor's thesis (Edelman, 1978).

## APPENDIX E

## VIDEO

Throughout this thesis, constant references have been made regarding terms describing various aspects of video technology. The next few pages will hopefully serve as an elementary guide and glossary for such information. Additional details regarding any of the video signals and their processing can be found in the suggested readings at the end of this appendix.

Scanning:

In the process of transmission known as scanning, a video picture is broken up into individual elements instead of being handled as an entire scene. In current systems, the picture is recorded in horizontal lines, or strips, which are transmitted one at a time.

The electron scanning beam begins at the upper left-hand corner of the screen or mosaic (point A in Figure E.1 below). Deflection coils create a magnetic field which causes the beam to sweep horizontally across the camera 'pickup' tube at a uniform speed. At the same time, a set of vertical deflection coils deflects the beam slightly downward. When the beam reaches the right-hand border of the picture, it is rapidly swept back to the left hand side in a motion known as horizontal retrace. Scanning from left to right, and slightly downward, the beam sweeps across the screen until it reaches the bottom (point B in Figure E.1). There, it is returned to the top of the screen by the vertical deflection coils. This

vertical retrace sets the beam at point C where it is ready to scan the horizontal picture sections that lie between the lines previously scanned. When the beam reaches point D, the entire two part scan of the picture is complete.

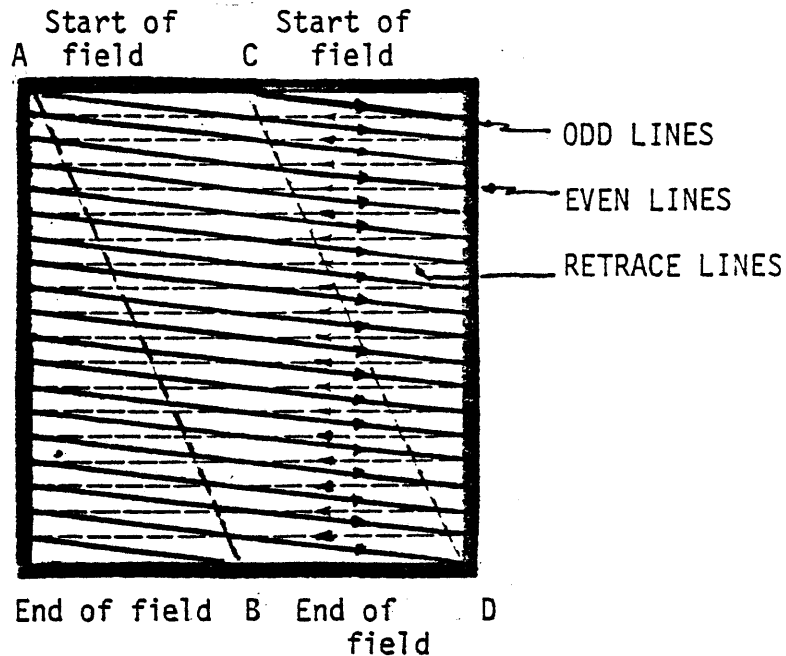


FIGURE E.1 The interlaced scanning pattern of a raster

This method of scanning is known as interlaced, referring to the fitting together of two picture halves to make a whole. The scanned halves are called fields; odd-numbered scanning lines appear in the odd field, even in the even field. These two fields combine their different information to produce a full picture or frame. Last, a third type of signal is transmitted to control the blanking of the screen. When horizontal or vertical retrace occurs, the beam may produce objectional interference if shown on the screen. Thus, blanking pulses are sent to black out this scan section. Horizontal blanking pulses appear, then, 15,750 times per second. A vertical counterpart occurs 60 times per second, at the end of every field.

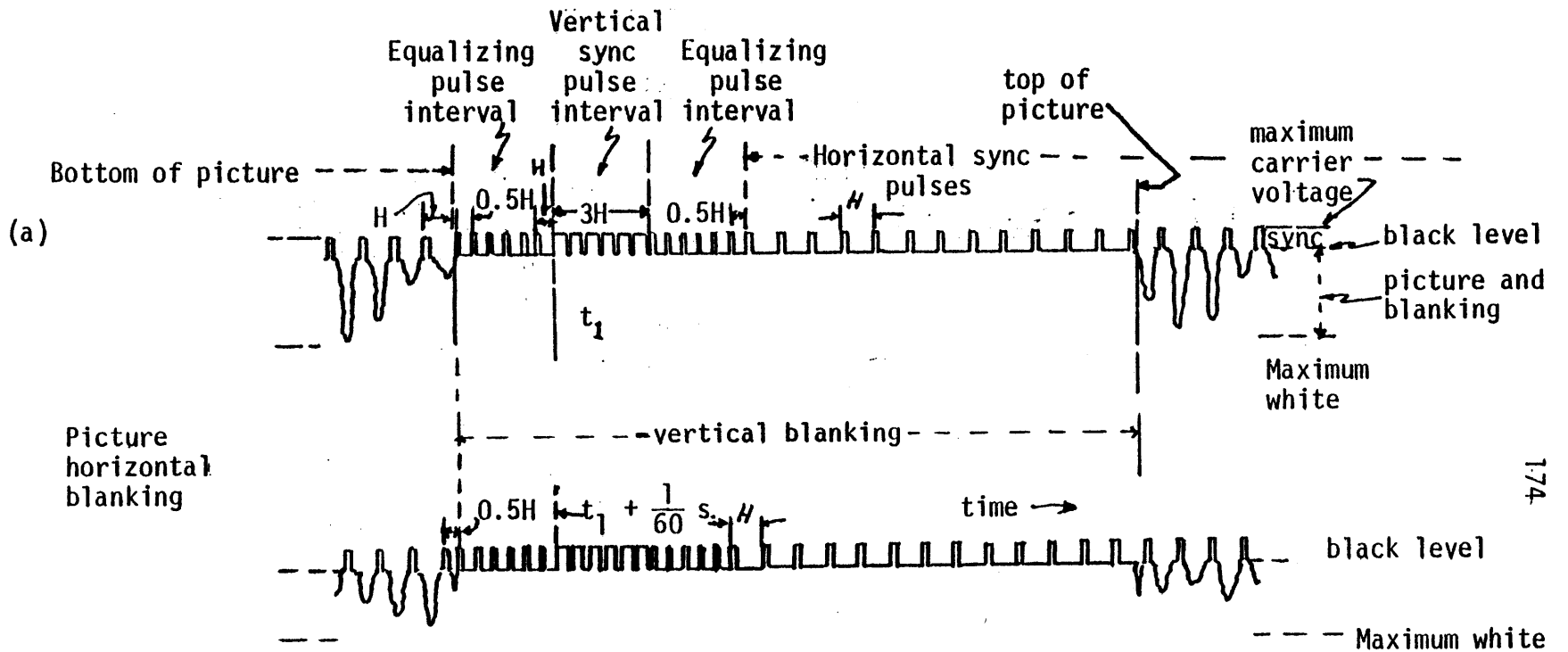


In standard American television systems, 525 lines are scanned per frame and thirty such frames, or 15,750 lines, are transmitted every second. These lines are split between the two fields 262 1/2 lines per field. This is shown in the above figure. Field 1 ends on a half line and field 2 starts on a half line.

Only 490 of the lines in a frame are active, the remainder occurring during the vertical retrace period when the viewing tube is blacked out. Complete synchronization must be maintained between scanning at the transmitter and the receiver. To effect this, synchronizing pulses are transmitted along with the video signal to lock the receiver oscillators, vertical and horizontal, into step with those at the transmitter.

The following figure provides a view of the sync pulses transmitted for one complete frame. The first waveform represents events that might occur in the first field, and the second waveform represents the second field of a picture.

There are many important features in the figure, but only a few are worthy of immediate notice. First, it should be noted that there is a horizontal half-line ( $0.5H$ ) difference between the two fields. Second, it should be noted that the vertical sync pulses are serrated and not presented as one continuous signal. This provides a means of locking the horizontal oscillation of the receiver in synchronization with the system during the transmission of vertical sync information, preventing drift which might otherwise occur. Finally, a group of six equalizing pulses precede and follow the vertical pulse. These pulses



are of a shorter duration than the square pulses and are transmitted to insure uniform spacing of the interlaced scanning lines and to prevent loss of synchronism during vertical retrace.

In summary, then, three types of information amplitude modulate the video transmitter: video, blanking and synchronizing. These signals are assigned different amplitudes and therefore offer varying degrees of modulation. The figure below illustrates these modulation levels in terms of relative amplitudes and approximate voltage values.

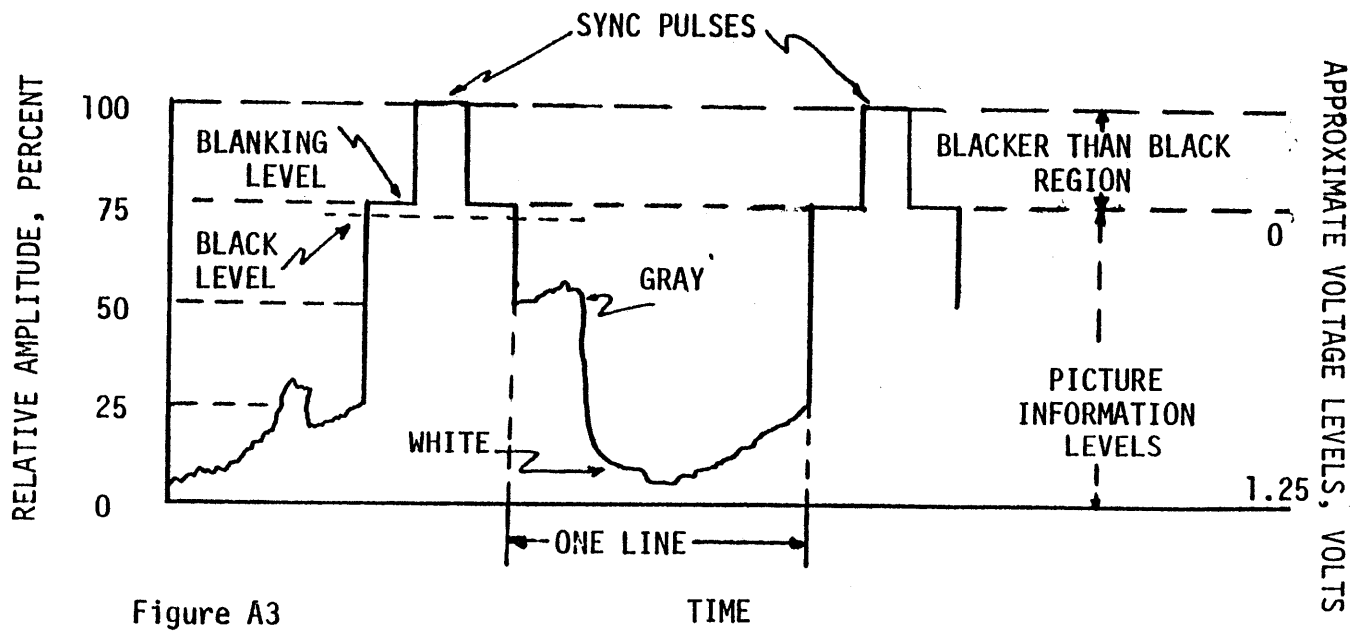


Figure A3

MODULATION LEVELS OF THE VIDEO, BLANKING AND SYNCHRONIZATION SIGNALS (after HELLER & SHULMAN)

177  
REFERENCES

- ADLER, F.H. Physiology of the Eye: Clinical Application, The C.V. Mosby Co. 1965.
- ANDERSON, E.P., Television Service Manual, T. Audel and Company, 1953, Chapters 1, 12, and 13.
- BEVINGTON, P.R. Data Reduction and Error Analysis for the Physical Sciences, McGraw Hill, Inc., 1969.
- BRANDT, T., WIST, E.R. and DICHGANS, J. "Foreground and Background in Dynamics Spatial Orientation", *Perception and Psychophysics*, 1975, Vol. 17(5).
- BROWN, B.W., HOLLANDER, M. Statistics, John Wiley and Sons, Inc., 1977.
- CHEN, J.L. and CYR, G.N., "Compositions producing adhesion through hydration" in: Adhesion in Biological Systems, R.S. Manley, Ed., Academic Press, New York, 1970.
- COLLEWIJN, H., VAN DER MARK, F., and JANSEN, T.C. "Precise recording of human eye movements", *Vision Research* 15:447-450, 1975.
- CORNSWEET, T.N. Visual Perception, Academic Press, Inc., 1970.
- DIAMOND, J.G., MARKHAM, C.H., SIMPSON, N.E., and CURTHOYS, I.S., "Binocular counterrolling in humans during dynamic rotation", *Acta Otolaryngol.* in press, 1979.
- DITCHBURN, R.W. Eye Movement and Visual Perception, Clarendon Press, Oxford, 1973.
- DICHGANS, J., HELD, R., YOUNG, L.R. and BRANDT, T. "Moving visual scenes influence the apparent direction of gravity", *Science*, Vol. 78:1217-1219, December 1972.
- DRAPER, N.R., and SMITH, H. Applied Regression Analysis, John Wiley and Sons, Inc., 1966.

- DUDA, R.O. and HART, P.E., Pattern Classification and Scene Analysis, John Wiley and Sons, 1973.
- DUKE-ELDER, S., WYBAR, K. System of Ophthalmology, Vol. VI: Ocular Motility and Strabismus, The C.V. Mosby Company, 1973.
- EDELMAN, E.R. Detection and tracking of eye movements using a video scanner, S.B. Thesis, MIT, Department of Electrical Engineering, May 1978.
- EIA Standard RS-170, Electrical Performance Standards for Monochrome Television Studio Facilities, November 1957.
- FINKE, R.A. and HELD, R., "State reversals of optically induced tilt and torsional eye movements", *Perception and Psychophysics*, 23:337-340, 1978.
- FLUUR, E., "A comparison between subjective and objective recording of ocular counterrolling as a result of tilting", *Acta Otolaryngologica* 79:111-114, 1975.
- FORGACS, P., JARFAS, K., and KUN, L. "Recording of Forgacs nystagmographic method", *J. Laryngol. and Otol.* 87:347-364, 1973.
- GALOYAN, U.R., ZENKIN, G.M., and PETROV, A.P. "Investigation of the torsional movements of the human eyes - II. Slow phase of torsion", *Biofizika* 21(6):1081-1086, 1976.
- HANNEN, R.A., KABRISKY, M., REPLOGLE, C.R., HARTZLER, V.L., and ROCCAFORTE, P.A., "Experimental determination of a portion of the human vestibular response through measurement of eyeball counterroll", *IEEE Transactions on Biomedical Engineering* BME-13:65-70, 1966.
- HANSEN, G.L. Introduction to Solid State Television Systems, Prentice Hall Publishing Co., 1969, Chapter 7.

- HELD, R., DICHGANS, J. and BAUER, J. "Characteristics of moving visual scenes influencing spatial orientation" *Vision Research*, Vol 15:357-365, 1975.
- HELLER, S. and SHULMAN, I. Television Servicing, McGraw Hill Book Company, Inc. 1950, Chapter 1 and 13.
- ILVASKY, M and PRINS, W. "Effects of diluents on poly-2-HEMA gels", *Macromolecules* 3:415, 1970.
- ISH-SHALOM, J. Measurement of Eye Movement with a Ferromagnetic Contact Ring , Master's Thesis, Technion-Israel Institute of Technology, Department of Electrical Engineering, July 1978.
- KAMADA, O., STA0, K., KITAMURA, S and NAKAMURA, H., "Two automatic methods of measuring the counterrolling of human eyes", *Digest of the 11th International Conference on Medical and Biomedical Engineering*, Ohawa, pp.510-511, 1976.
- KELLOGG, R.S. "Dynamic counterrolling of the eye in normal subjects and in persons with bilateral labyrinthine defects", In: The Role of the Vestibular Organs in Space Explorations, NASA SP-77, 1965.
- KHAW, B., RATNER, B.D, and HOFFMAN, A.S., "The thermodynamics of water sorption in radiation grafted hydrogels", in: Hydrogels for Medical and Related Applications, J.B. Andrade, Ed., American Chemical Society Symposium Series 31, Washington, DC pp. 295-304, 1976.
- KORNHUBER, H.H. et al, "Vestibular system part II; Psychophysics, applied aspects and general interpretations", Handbook of Sensory Physiology Vol. VI/2, 1974.
- LEDWITH, A. and NORTON, J. "Molecular behavior and the development of polymeric materials" 1975.

- MATIN, L and PEARCE, D.G. "Three dimensional recording of eye movements by a contact-lens technique", Biomedical Sc. Instrum. 2:79-95, 1964.
- MELVILL JONES, G "Ocular nystagmus recorded simultaneously in three orthogonal planes" Acta Otolaryng. 56, 1963.
- MELVILL JONES, G. "Vestibulo-ocular disorganization in the aerodynamic spin", Aerospace Medicine 36, 1965.
- MELVILL JONES, G. "From launch to space in a generation" an evolutionary challenge", Aerospace Medicine 39, 1968.
- MILLER, E.F., II. "Counterrolling of the human eyes produced by tilt with response to gravity", Acta Otolaryngologica 54:479-501, 1962.
- MILLER, E.F., II. and GRAYBIEL, A., "Otolith function as measured by ocular counterrolling", in: The Role of the Vestibular Organs in Space Exploration, NASA SP-77, 1965.
- MILLER, E.F., II. and GRAYBIEL, A "Effects of gravito-inertial force on ocular counterrolling" J. Applied Phys. 31:697-700, 1971.
- MILLER, E.F., II. and GRAYBIEL, A. "Ocular counterrolling measured during eight hours of sustained body tilt", NASA T-81633, 1972.
- MORTON, M. Rubber Technology 1973.
- NAKAYAMA, K. "Photographic determination of the rotational state of the eye using matrices", Am. J. Optometry and Physiological Optics, 51: 736-742, 1974.
- NAKAYAMA, K. and BALLIET, R., "Listing's law, eye position sense and perception of the vertical", Smith-Kettlewell Institute and Department of Visual Studies.
- PETROV, A.P. and ZENKIN, G.M., "Torsional eye movements and constancy of the visual field", Vision Res., 13:2465-77, 1973.



- RATNER, B.D. and HOFFMAN, A.S. "Synthetic hydrogels for biomedical applicatinos", in: Hydrogels for Medical and Related Applications, J.B. Andrade, ed., American Chemical Society Symposium Series 31, Washington, DC.
- REFOJO, M.F., "Hydrophobic interaction in poly(2-hydroxymethylmethacrylate) homogeneous hydrogel", *Journal of Polymer Science* 5:3103-3113, 1967.
- REFOJO, M.F., "A critical review of properties and applications of soft hydrogel lenses", *Survey of Ophthalmology*, 16:233-246, 1972.
- REFOJO, M.F. "Vapor pressure of hydrogels", in Hydrogels for Medical and Related Applications, J.D. Andrade, Ed., American Chemical Society Symposium Series 31, Washington, DC, 1973.
- ROBINSON, D.A., "A method of measuring eye movements using a scleral search coil in a magnetic field", *IEEE BME-10*:137-145, 1963.
- RUBEN, M. "Soft lenses", *Transactions of the Ophthalmological Society of the United Kingdom*, XCI:59-74, 1972.
- VANDER, A.J., SHERMAN, J.H. and LUCIANO, D. Human Physiology, the Mechanism of Body Function, McGraw Hill Book Co., New York, 1973.
- WESTHEIMER, G., and BLAIR, S.M. "The ocular tilt reaction - a brainstem oculomotor routine", *Investigative Ophthalmology*, 14, 1975.
- WOELLNER, G. and GRAYBIEL, A. "Counterrolling of the eyes and its dependence on the magnitude of gravitational or inertial force acting laterally on the body", *J. Appl. Physiol.* 14:632-634, 1959.
- YARBUS, A.L., Eye Movements and Vision, New York, Plenum Press, 1967.
- YOUNG, L.R. and SHEENA, D., "Methods and designs: Survey of eye Movement recording methods:", *Behavior Res. Methods and Instrumentation* 7:397-429, 1975.